KING FAHD UNIVERSITY OF PETROLEUM & MINERALS

DHAHRAN 31261, SAUDI ARABIA

DEANSHIP OF GRADUATE STUDIES

This thesis, written by **MD. ASHRAFUL ISLAM** under the supervision of his thesis Advisor and approved by his Thesis Committee, has been presented to and accepted by the Dean of Graduate Studies, in partial fulfillment of the requirements for the degree of **MASTER OF SCIENCE IN CHEMICAL ENGINEERING.**

Thesis Committee

Dr. Ibnelwaleed A. Hussein
(Chairman)

Dr. Basel F. Abu-Sharkh
(Co-Chairman)

Dr. Muhammad Atiqullah
(Member)

Dr. Mohamed B. Amin
Department Chairman

Dr. Ramazan Kahraman
(Member)

Dr. Mohammad Abdulaziz Al-Ohali
Dean of Graduate Studies

Dr. S. M. J. Zaidi
(Member)

عمادة الدراسات العليا
DEANSHIP OF GRADUATE STUDIES

Date: ١٤٢٦/٣/٢٤

3-5-2005

DEDICATION

Dedicated To My Parents

ACKNOWLEDGEMENT

In the name of Allah, Most Gracious, Most Merciful

First and foremost, all praise is to ALLAH *SUBHANAHU-WA-TA'ALA*, the Almighty, Who gave me an opportunity, patience and courage to carry out this work. I feel privileged to glorify His name in the sincerest way through this small accomplishment. I seek His mercy, favor and forgiveness. I ask Him to accept my little effort. May He, *SUBHANAHU-WA-TA'ALA,* guide us and the whole humanity to the right path (Ameen).

Acknowledgement is due to King Fahd University of Petroleum & Minerals for providing the research facilities and research assistantship to complete my M.S.

I wish to submit my sincere gratitude to my thesis advisor, Dr. Ibnelwaleed A. Hussein for his invaluable support, guidance, continuous encouragement and every possible way of cooperation through out the period of my research and in the preparation of this manuscript. His precious suggestion made this work interesting and learning for me. He was always kind, understanding and sympathetic to me.

I am also indebted to my thesis committee members Dr. Basel F. Abu-Sharkh, Dr. Muhammad Atiqullah, Dr. Ramazan Kahraman, and Dr. S. M. J. Zaidi for their sincere help, constructive suggestion, and cooperation.

I would like to thank Dr. M. B. Amin, Chairman, Department of Chemical Engineering, for providing me all the available facilities. I am also grateful to all the faculty members and staff of the department who has in one way or other enriched my academic and research experience at KFUPM. Special thanks are to Mr. Mafizul Islam Bhuiyan for his continuous help in arranging my experiment accessories.

I acknowledge the financial support provided by King Abdul Aziz City for Science and Technology (KACST) under Project # AT-22-16.

I also gratefully acknowledge the support of my fellow graduate students and to the members of the Bangladeshi community at KFUPM.

Last but not the least, I would like to pay my best gratitude to my beloved parents and my family members for their prayers, encouragement, and support that permitted me to indulge my passion for the long task to complete this work. Special thanks are to my dearest little daughter, Rida, whose face always keeps me alive in the pool of works.

Table of Contents

List of Figures

List of Tables

THESIS ABSTRACT

Name: MD. ASHRAFUL ISLAM

Title: Structure Property Relationships of Metallocene Linear Low Density Polyethylene (LLDPE).

Degree: Master of Science

Major Field: Chemical Engineering

Date of Degree: January, 2005

In this study, the structure-property relationships of metallocene linear low density polyethylene (m-LLDPE) are investigated. Particularly, the influence of the branch content (BC), composition distribution, and comonomer type on the thermal and mechanical properties of m-LLDPEs was studied. The mechanical properties were studied by means of stress/strain experiments. The increase in BC of m-LLDPEs lowered the crystallinity and the modulus. The ultimate mechanical properties of m-LLDPEs were weakly dependent on BC. The comonomer type had no significant effects on the mechanical properties of m-LLDPEs. The Ziegler-Natta LLDPEs (ZN-LLDPEs) were also studied for comparison purposes. However, ZN-LLDPEs showed higher small strain properties but lower ultimate properties than m-LLDPEs of similar Mw, branch type, and BC. In addition, the influence of strain rate on the mechanical properties of m-LLDPEs was examined. For low BC m-LLDPEs, there exists a very narrow strain rate window within which a maximum in modulus and ultimate properties was observed. The strain rate had no influence on the mechanical properties of the highly branched m-LLDPEs.

The nonisothermal crystallization kinetics parameters of m-LLDPEs were measured by modulated differential scanning calorimetry. It was found that BC causes a significant change in the crystallization behavior. Crystallization peak temperature shifts to lower region as BC increases. The secondary crystallization process strongly influenced the nonisothermal crystallization of all resins. The Avrami exponent, n, was in the range of 1.5 to 2.5, suggesting a rod-like growth. The comonomer type had almost no effect on the crystallization kinetics. A strong effect of composition distribution was observed on the crystallization peak and the enthalpy of crystallization. However, similar crystallization mechanism was observed for both m-LLDPEs and ZN-LLDPE. In addition, the effect of cooling rate on the nonisothermal crystallization mechanism of HDPE and LLDPE was examined.

Master of Science Degree

King Fahd University of Petroleum & Minerals

Dhahran, Saudi Arabia

ملخص البحث

الإســـم: محمد أشرف الإسلام
العنـــوان: تأثير التركيب الجزيئي على مواصفات البولي إيثلين الخطي قليل الكثافة.
الدرجـــة: ماجستير العلوم
المجـــال: هندسة كيميائية
تاريخ التخرج: يناير 2005م

تم في هذا البحث دراسة تأثير التركيب الجزيئي على مواصفات البولي إيثلين الخطي قليل الكثافة المصنّع بواسطة حفّاز الميتالوسين. تمت دراسة تأثير كمية ونوعية وتوزيع التفرع على الخواص الحرارية والميكانيكية للبولمر. وجد أن درجة البلورة تقل مع زيادة كمية التفرع مما يضعف من معامل قوة البولمر. وجد أن الخواص الميكانيكية النهائية لا تعتمد على كمية التفرع. وجد أن البولمرات المصنّعة بواسطة حفّاز زيقلر-ناتا لها خواص ميكانيكية أفضل من مثيلاتها المصنّعة بواسطة حفّاز الميتالوسين عند إستخدام قوة شد قليلة في حين أن البولمرات الميتالوسينية أحسن منها في حالة إستخدام قوة شد عالية.

أيضاً تمت دراسة حركية البلورة ومعاملاتها وتأثير الخواص الجزيئية في ذلك. وجد أن كمية التفرع تؤثر تأثيراً كبيراً في طريقة البلورة. كما أن البلورة الثانوية تتأثر بشدة بكمية التفرع. أما نوعية التفرع فليس لها تأثير كبير على الخواص الميكانيكية أو الحرارية. كذلك وجد أن توزيع التفرع له تأثير قوي على حركية البلورة، كذلك تمت دراسة درجة التبريد وسرعة الشد على الخواص الحرارية والميكانيكية.

ماجستير العلوم
جامعة الملك فهد للبترول والمعادن
الظهران – المملكة العربية السعودية

CHAPTER 1

INTRODUCTION

The development of polyethylene production technology did not proceed smoothly. It demanded untiring efforts before the utility of synthetic polymers was appreciated. Initially, polyethylene was a highly branched low density material with a limited range of physical properties. In the 1950s, new catalytic polymerization processes were developed that produced essentially linear polymers with higher densities. In the 1960s, the copolymerization of ethylene with small amounts of other α-olefins produced linear low density polyethylene (LLDPE). Metallocene catalysts have been known for several decades. However, their potential as commercial catalysts remained unrealized until 1980, when Kaminsky and coworkers [1983] discovered that the methylalumoxane co-catalyst improved their catalytic activity dramatically. Since that discovery, massive and intense research programs have been undertaken to bring metallocene products to commercial use. The most remarkable feature of these catalyst systems is the fact that all metallocene sites produce polymer chains with virtually the same architecture [Gupta, 1997]. It produces polymers with narrow molecular weight distribution, higher comonomer contents, and good compositional homogeneity [Horton, 1994]. Metallocene catalyzed elastomeric very low density polyethylene (VLDPE) resins became available commercially in 1993. The metallocene LLDPE (m-LLDPE) products followed in 1995 [Peacock, 2000].

Ziegler-Natta LLDPE resins consist of molecules with linear polyethylene (LPE) backbones to which are attached short alkyl groups at random intervals. These materials are produced by the copolymerization of ethylene with 1-alkene comonomers. These comonomers are typically α-olefins, principally 1-butene, 1-hexene, and 1-octene. LLDPE resins may also contain small levels of long chain branching as is found in low density polyethylene (LDPE). Chemically, these resins can be thought of as a compromise between LPE and LDPE, hence the name LLDPE [Peacock, 2000]. There are two types of LLDPE available in the market, conventional, Ziegler-Natta (ZN-LLDPE) and m-LLPDE. Metallocene-type ethylene-α-olefin copolymers are characterized by their narrow molecular weight distribution ($2.0 \leq$ polydispersity index ≤ 3.5) and almost homogeneous comonomer composition distribution. This is in contrast to Ziegler-Natta copolymers, which are broadly poly-dispersed in terms of molecular weight and composition. Here, the longer molecules incorporate a lower percentage of comonomers than the shorter ones [Stevens, 1996].

The mechanical properties of m-LLDPE resins are better than conventional resins in many respects, but there are also deficiencies in certain areas. On the positive side, the impact strength, puncture resistance and tensile strength of m-LLDPE films are all improved by a considerable level over those of conventional resins 300%, 50%, and 40%, respectively, according to one resin manufacturer [Vernyi, 1995]. On the other side, m-LLDPE films have lower tear strengths than the ZN counterparts. When tear strength is not a crucial factor, the use of m-LLDPE resins permits down gauging, which is always attractive to film producers [Peacock, 2000].

Metallocene-LLDPE has been targeted for film and packaging applications. Commercial applications of LLDPE are notably in the blown and cast film use, such as stretch film, as well as can liners and heavy duty sacks [Welch, 1995]. It has provided end users with many advantages such as: (1) increased packaging speeds due to lower seal initiation temperature, higher hot tack, and reduced blocking; (2) reduced package failures due to greater toughness and superior resistance to abuse; (3) improved package artistic due to lower haze and higher gloss; and (4) improved packaged product quality due to reduced package-product interactions, lower odor and extractability, etc [Gupta, 1997].

It is well known that the underlying microstructure of polymers plays a critical role in determining their physical and mechanical properties. For linear polyolefins such as poly (ethylene/α-olefin) copolymers, both the molecular weight distribution and comonomer distribution of the polymer chains influence the crystallinity and density of the samples [Xu et al., 2000]. Above a critical molecular weight, it is sometimes found that the crystallinity will decrease with increasing molecular weight, due to the inability of the longer chains to be incorporated in the crystalline structure [Hosoda & Uemura, 1992; Jordens et al., 2000]. More significantly, by increasing the number of short chain branches via incorporation of α-olefin comonomers such as 1-butene, 1-hexene, 1-octene etc., the polymer crystallinity and density can be reduced. The reason is that these side chains do not crystallize and are rejected into the amorphous or interfacial regions of the polymer [Kale et al., 1995; Simanke et al. 1999]. The interplay between molecular weight and comonomer composition distribution influences the proportions of crystalline and amorphous polymer that determine its crystalline microstructure. The crystallinity and

crystal structure are not only influenced by the microstructure of the polymer but also by the processing conditions that dictate the polymer thermal history [Mandelkern et al., 1997; Jordens et al., 2000]. In terms of mechanical properties, polymer crystallinity influences its stiffness and toughness. In general, as the polymer crystallinity decreases, its flexibility increases. By lowering the density with the incorporation of comonomer to promote short chain branching, the polymer ability to absorb and dissipate energy also increases [Kale et al., 1995; Bensason et al., 1996].

1.1 Objectives

From the above literature review it was observed that the influence of branch content, comonomer type on the crystallization and mechanical properties of m-LLDPEs needs to be studied. The objectives of this investigation are as follows:

1) Study the effect of branch content, branch type and the average comonomer composition on the mechanical properties of m-LLDPEs.

2) Examine the effect of strain rate on the mechanical properties of m-LLDPEs.

3) Study the effect of branch content, branch type, average composition, and crystallization temperature on crystallization kinetics of m-LLDPEs.

4) Investigate the influence of cooling rate on the crystallization of m-LLDPEs.

5) Correlate the molecular structure of m-LLDPEs to selective thermal and mechanical properties.

This study was part of a KACST funded project that aims at investigating the influence of molecular parameters on solution, melt and solid-state properties of m-LLDPEs.

NOTE: This thesis is written in paper format. Hence, the reader can skip the following two chapters and go directly to the results and discussion part given in Chapter 4. The first paper is entitled "Influence of Branch Content, Comonomer Type, and Strain Rate on the Mechanical Properties of metallocene LLDPEs". The second paper is entitled "Influence of Branch Content, Comonomer Type and Composition Distribution on non-isothermal Crystallization of Metallocene LLDPEs".

CHAPTER 2

LITERATURE REVIEW

2.1. Metallocene Catalyst

Metallocenes are a new generation of catalysts for the production of precisely designed polyolefins. The discovery of metallocene methylalumoxane catalysts has opened a frontier in the areas of organometallic chemistry, polymer synthesis, and processing (Sinn and Kaminsky, 1980; Brintzinger et al., 1995). Based on transition metals such as titanium and zirconium atoms sandwiched between ring structures with well defined single catalytic sites and well understood molecular structures (Thayer, 1995; Kaminsky et al., 1996a, Kaminsky, 1996b). It was found that changing the π-carboxylic ligands of the metallocene molecule can greatly affect the properties of the polymer (Kaminsky, 1998). Figure 2.1 shows some structures of Metallocenes that are used in the polymerization of olefins.

2.2. Mechanical Testing

The mechanical properties of a polyethylene specimen can be defined as those attributes that involve the physical rearrangement of its component molecules or distortion of its initial morphology in response to an applied force. The nature of a specimen's response to applied stress can be correlated to its morphological and molecular characteristics. These relationships are emphasized in this work. The mechanical properties of a specimen are controlled by its processing history within the

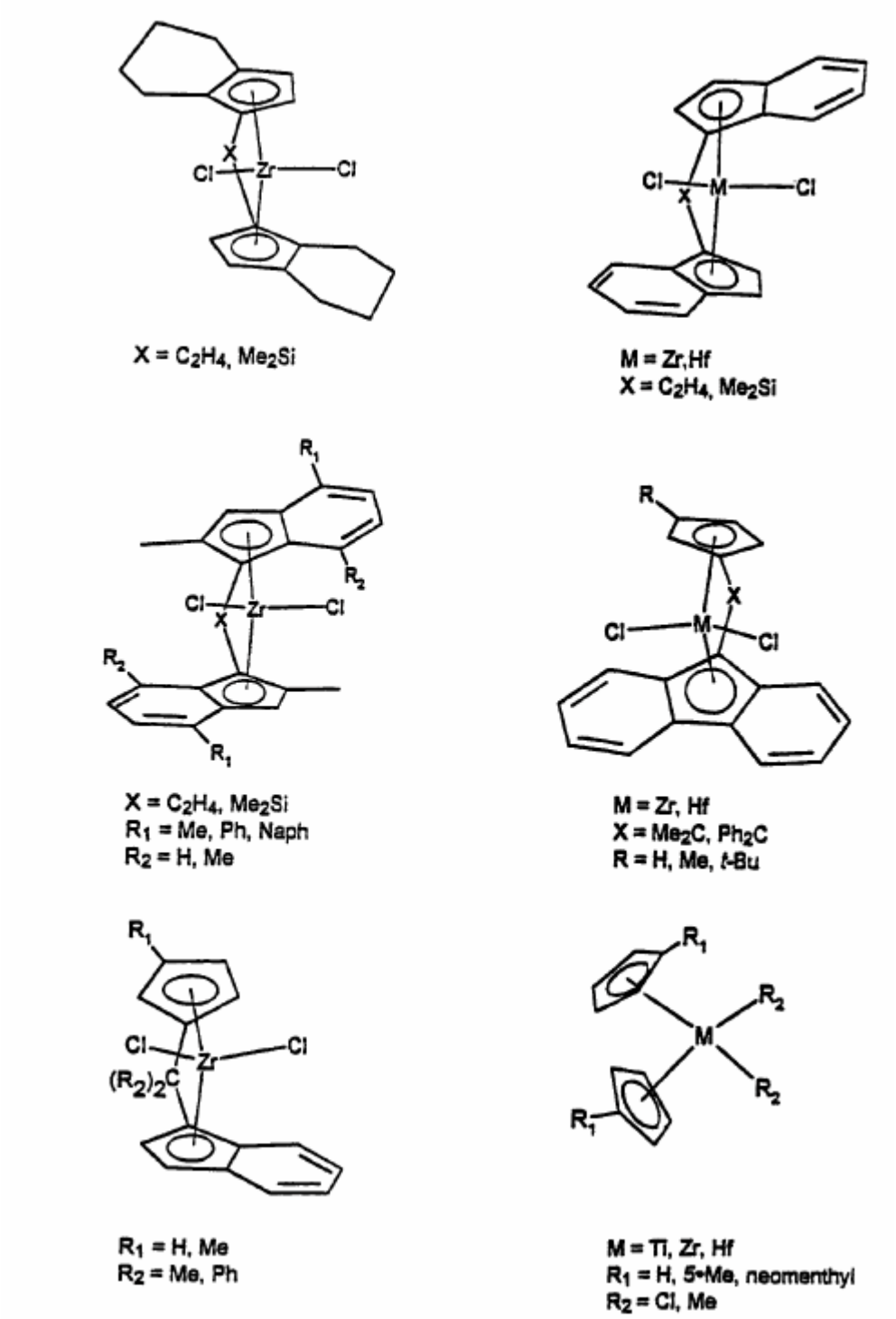

Figure 2.1: structures of Metallocenes that are used in the polymerization of olefins (Kaminsky, 1998)

limits imposed by its molecular characteristics. The typical mode of polyethylene deformation is one of yielding and necking followed by strain hardening (see Figure 2.2). Localized yielding is especially noticeable in samples with higher degrees of crystallinity.

The mechanical properties of polyethylene may be divided into two broad categories: (l) low strain properties such as yield stress and initial modulus and (2) high strain properties, characterized by ultimate tensile strength and elongation at break. To a first approximation, the low strain properties are controlled by sample morphological features and the high strain properties by its molecular characteristics.

2.2.1. Tensile Properties

Tensile properties of polymers are measured on instruments that record the force required to elongate a sample as a function of applied elongation. It is common to plot the load as "engineering stress", that is, the force per unit area based upon the original cross-section of the specimen as a function of the engineering strain calculated as the elongation divided by original gauge length. The polymer chain length and its distribution are important molecular parameters in controlling the physical, mechanical and processing characteristics of polymers. Tensile testing of the specimen is carried out following the ASTM D638 standard. Stress and strain are ‘sample’ dependent. The stress on any element of the sample is equal to the force experienced by the element divided by its effective cross-sectional area. If the cross-sectional area of the specimen varies along its length, the stress will vary accordingly, i.e., stress is not necessarily uniform along the length or across the width of the specimen.

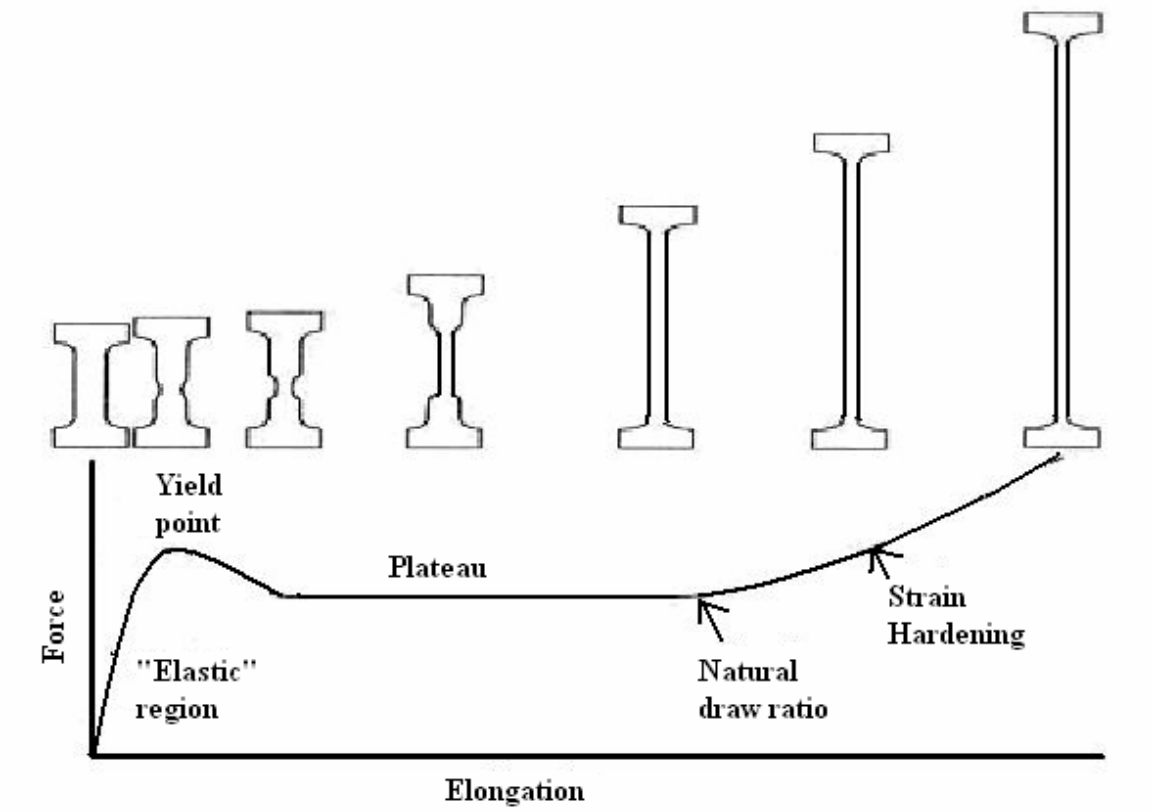

Figure 2.2: Generalized force versus elongation curve for polyethylene illustrating principal tensile phenomena [Peacock, 2000].

The strain and percent strain for any portion of a specimen are defined as

$$Strain = \frac{\text{current sample dimension} - \text{original dimension}}{\text{original dimension}} \quad (2.1)$$

$$\text{Percent } Strain = \frac{\text{current sample dimension} - \text{original dimension}}{\text{original dimension}} \times 100 \quad (2.2)$$

Most tensile samples start off as a "dog bone" (or dumbbell), the enlarged regions of which are gripped by the jaws of the tensile tester. Initially, the gauge region elongates homogenously until it reaches a point at which one cross-sectional slice yields independently of the rest of the specimen. The onset of heterogeneous elongation corresponds to the yield point. As elongation continues, the incipient neck becomes better established until it forms a sharply defined region. Upon further elongation, the neck propagates, growing to encompass the entire gauge length. The force required for neck propagation is essentially invariant, resulting in a "plateau" in the force versus elongation curve (Figure 2.2). Subsequent deformation, termed "strain hardening", is homogenous, with the necked region elongating uniformly until the sample breaks.

Depending on molecular weight (M_w) and its distribution (MWD), polyethylene can exist under a variety of formulations, each one with tailored properties for specific applications. The influence of M_w on mechanical properties is clearly depicted in the Figure 2.3. It is also important to note that some polymers may have different failure modes for different modes of deformation. In general, all polymers at temperatures significantly below their glass transition temperatures (T_g -T >100°C) undergo brittle fracture. In the region above the brittle fracture regime, but below T_g polymers usually

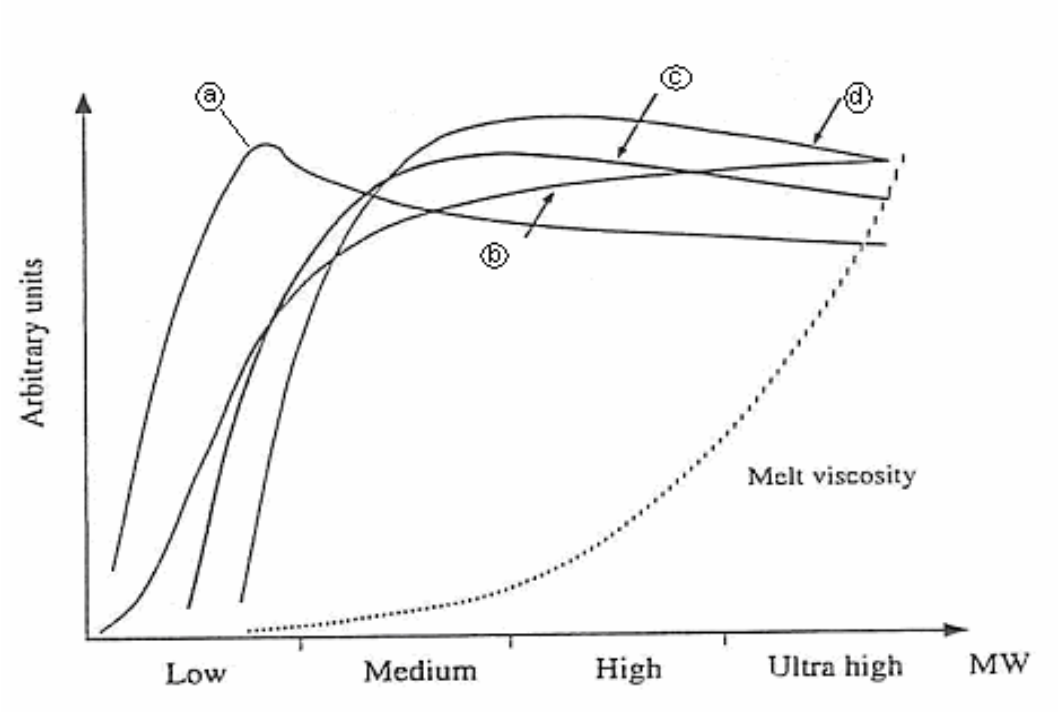

Figure 2.3: Effect of molecular weight on the mechanical properties of polymers. a) Tensile modulus curve, b) Tensile strength curve, c) Elongation at break curve, d) Impact strength curve [Ward & Hadley, 1993].

yield and undergo plastic deformation as the modulus decreases. This is illustrated in the bump that occurs in the stress-strain curves as shown in the Figure 2.4.

2.2.2. Elastic Modulus

When a polyethylene sample is subjected to external stress, there is an initial deformation prior to yield that is homogenous and is largely recoverable when the stress is removed. The value of elastic modulus is normally derived from the initial slope of the stress versus strain plot. The elastic modulus of a sample is a measure of its rigidity; the higher the modulus, the stiffer the sample. For the majority of isotropic samples, the increase of elastic modulus is approximately linear with the degree of crystallinity (Peacock, 2000). The two most commonly used units are pounds per square inch (psi) and mega Pascal (MPa).

2.2.3. Yield Phenomena

Yielding occurs in a polyethylene specimen when it ceases to deform homogenously and starts to deform heterogeneously. Up to the yield point, deformation is principally elastic, whereas afterwards the sample takes on a permanent set. The nature of yield point varies greatly with the type of polyethylene examined and the conditions under which it crystallized. In LLDPE and LDPE samples, two distinct maxima may occur in close succession. In other cases, an inflection may be followed by a diffuse maximum [Lucas et al, 1995]. The mechanisms associated with multiple yield-peaks are the subject of speculation but may correspond to the yielding of bimodal distributions of lamellar populations [Lucas et al, 1995].

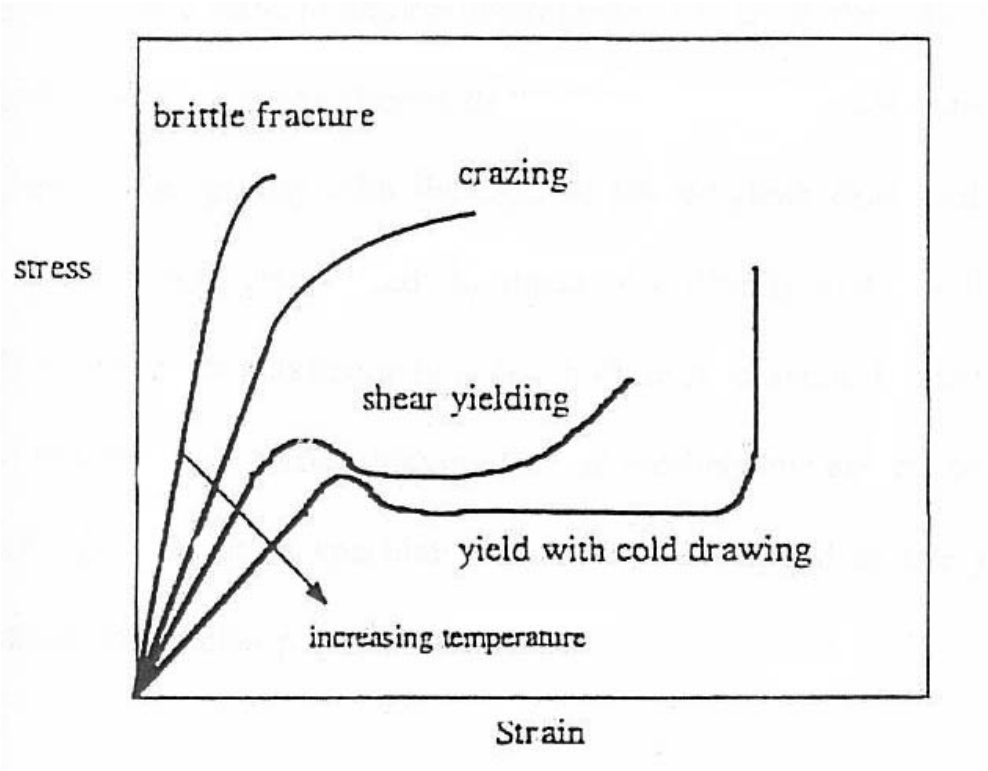

Figure 2.4: Schematic of some failure modes of glassy polymers [Swallowe, 1999]

The sharpness of the yield peak exhibited during stress versus strain measurements reflects the distinctness of usually observed neck. Samples with very low levels of crystallinity exhibit neither localized necking nor a distinct yield peak [Peacock, 1990]. For isotropic samples, the yield stress at room temperature is closely correlated to the degree of crystallinity and thus to the sample density [Peacock, 1990]. The yield stress of a specimen is of great interest from a practical point of view. In many cases it represents the maximum permissible load that a sample can withstand while still performing its assigned role. Once a sample has yielded, its dimensions are irrevocably changed, and it may no longer meet the requirements for continued service. In cases, where there is a distinct yield maximum in the stress-strain curve, the force required to propagate a neck along the length of a sample is lower than the yield stress. Once such a sample has yielded, it will continue to elongate unless the applied load is removed [Peacock, 2000].

2.2.4. Ultimate Tensile Stress

The ultimate tensile stress also known as the "tensile strength" of a sample is the force required to break it divided by its original cross-sectional area. The values of ultimate strength of LDPE samples are generally lower than that of LLDPE samples largely because of the higher percent elongation values obtained for the LLDPE samples. Actually, this is the property that gives LLDPE an advantage over LDPE in blown film packaging application.

2.2.5. Elongation at Break

This term refers to the strain of the sample at the point of tensile failure. The strain at break of the polyethylene sample is a function of its molecular nature and its initial orientation. The molecular characteristics that facilitate drawing are similar to those that promote the development of high degrees of crystallinity. Features that hinder the slippage of chains past one another during crystallization also inhibit the drawing process. The two principal inhibitors to chain movement are entanglements and branch points. Thus high molecular weight LPE resins and branched samples have lower strain at break values than low molecular weight unbranched samples. For ductile samples at a given M_w, the strains at break values fall as their comonomer content increases (Peacock, 2000). However, these observations were based on small strain data and low comonomer content PEs. Similarly, for a given comonomer content, the strain at break of ductile samples falls as the molecular weight increases. The molecular weight corresponding to the transition between brittle and ductile behavior increases as the comonomer content increases.

2.3. Modulated Differential Scanning Calorimetry

Several methods are available for the measurement of polymer crystallinity: dilatometry, microscopy, calorimetry, x-ray diffraction etc. With the exception of microscopy, all of the above techniques are very difficult to use when crystallinity must be evaluated as a function of time. DSC has made possible the much wider application of the calorimetric method to crystallinity studies [Barrall & Johnson, 1970]. The development of crystallinity in polymers is not instantaneous. Since the time for complete crystallization is somewhat indefinite, it is customary to define the rate of crystallization

at a given temperature as the inverse of the time needed to attain one-half of the total volume change [Billmeyer, 1984]. The rate of crystallization can be obtained using Avrami equation [Avrami, 1939-1941]

$$1-\phi(t)=\exp(-kt^{n}) \tag{2.3}$$

Where, $\phi(t)$ = fractional crystallinity at time t

k = rate of crystallization (temperature dependent)

n = nucleation index (temperature independent).

A plot of ln{-ln[1-ϕ(t)]} versus ln t will give 'n' as slope and 'lnk' as intercept. $\phi(t)$, the fractional crystallinity at time t can be determined from the heat evolved as follows:

$$\phi(t)=\Delta H_{t}/\Delta H_{\infty} \tag{2.4}$$

where, ΔH_t = heat evolved at time t

ΔH_∞ = heat evolved at the end of crystallization.

Conventional DSC involves dynamic calorimetric analysis of a sample whose temperature is being ramped at a controlled rate. This is achieved by measuring instantaneous heat capacity of a sample as a function of its temperature in a plot known as a thermogram. Endothermic and exothermic peaks respectively correspond to melting and crystallization processes, while step changes reflect material transitions, such as the glass transition. Quantitative information can be obtained with respect to both the temperature at which events occur and the associated heat flow. Differential scanning

calorimeters can also be used to measure transitions involving heat transfer that occur at fixed temperatures, such as isothermal crystallization.

Two varieties of differential scanning calorimeters exist, both of which are capable of making accurate measurements on samples in the range of 1-20 mg. Figure 2.5 illustrates the basic features of the two types.

In both cases, specimens are encapsulated in small aluminum sample pans, which are placed in a chamber for comparison against an empty reference pan. In the first type (Figure 2.5-a), the flow of heat into the sample chamber via the sample support is kept constant while the temperature of the sample pan with respect to the reference pan is recorded. In the second type (Figure 2.5-b), known as the power compensating type, the temperature of the sample and reference pans are determined to a precision of a few hundredths of a degree, while the flow of heat into the sample supports must be monitored and controlled to a similar precision. The net results of both methods are identical as far as the operator is concerned; each generates a precise plot of heat flow as a function of temperature.

An interesting recent modification to conventional thermal analysis is “Modulated DSC”, MDSC. This technique subjects a material to a linear heating method which has a superimposed sinusoidal temperature oscillation (modulation) resulting in a cyclic heating profile.

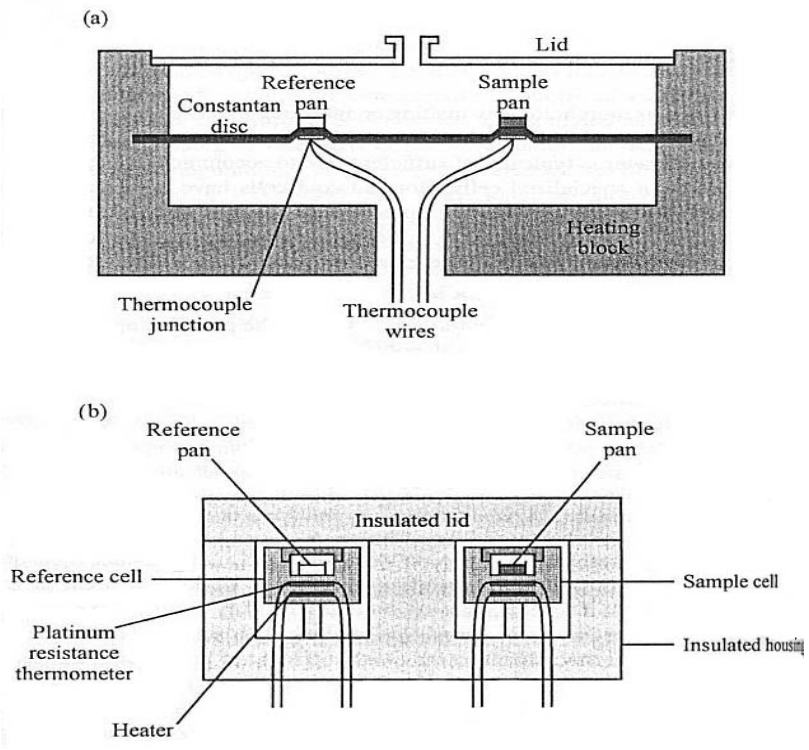

Figure 2.5: Schematic diagram of the two types of DSC sample chambers: (a) Constant heat flow into the chamber; (b) modulated heat flow to maintain specific temperature ramp [Peacock, 2000].

The equation, which describes heat flow in MDSC, is:

$$\frac{dQ}{dt} = Cp \frac{dT}{dt} + f(T, t) \qquad (2.5)$$

(Total) (Reversing) (Non-reversing)

where, $\frac{dQ}{dt}$ = total heat flow,

C_p = heat capacity,

$\frac{dT}{dt}$ = heating rate, and

$f(T, t)$ = heat flow dependent on absolute temperature and time.

The concept involves the imposition of a sine wave on the normally linear heating ramp so that portions of each cycle are at different heating and cooling rates, although the general overall trend is a linear change in average temperature.

The amplitude and period of the modulation, along with the average heating rate, are set by the operator. A wide range of instantaneous heating and cooling rates are established within each experiment by such a process. The typical range of operating parameters would be heating rates of less than $5^oC\ min^{-1}$, using a period of 10 to 100 seconds, and amplitude of 0.01 ^oC to 2.0^oC. It is important that there be several, i.e., at least five, complete cycles of the program over the temperature range of any feature under investigation, in order for the subsequent deconvolution scheme to function properly. Higher frequencies can be achieved through radiant heating, but with reduced amplitudes in the temperature cycle [Wishikawa and Saruyama, 1995].

The major contribution of this technique is that the total heat flow rate can be separated into two additional signals. Deconvolution of the resultant heat flow profile provides not only the "total" heat flow obtained from conventional DSC, but also separates that "total" heat flow into its heat capacity-related (reversing) and kinetic (non-reversing) components [Thomas, TA Instruments Publication]. A typical "raw" curve of the heat flow rate for MDSC is shown in Figure 2.6(b). Subsequent deconvolution of this "raw" data using a discrete Fourier transform yields several pieces of information besides a curve equivalent to the conventional DSC curve; Figure 2.6(c). One of these is a curve, which represents the component of total rate of heat flow that is heating rate dependent, i.e., that which is in phase with the modulated heating. The second curve corresponds to the rate of heat flow that is dependent on only the absolute temperature, i.e., that which is out of phase with the modulated heating. These two components of the heat flow are designated as "reversing" and "non-reversing", respectively. The second major advantage of MDSC is that, once the instrument has been calibrated at the same amplitude and period, the heat capacity data can be determined in a single run and with somewhat greater precision and accuracy [Turi, 1997].

2.4. Literature Review

Amarasinghe et al. [2003] used MDSC to study the melting and crystallization behavior of various PEs. It was found that all samples of highly branched LDPE, LLDPE, and VLDPE showed a broad exotherm before the main melting peak in the non-reversing curve, suggesting crystallization and annealing of crystals to be more stable forms. Other samples of HDPE, except quickly cooled HDPE, did not show any significant crystallization and annealing before melting. The crystallinity indicated that dynamically

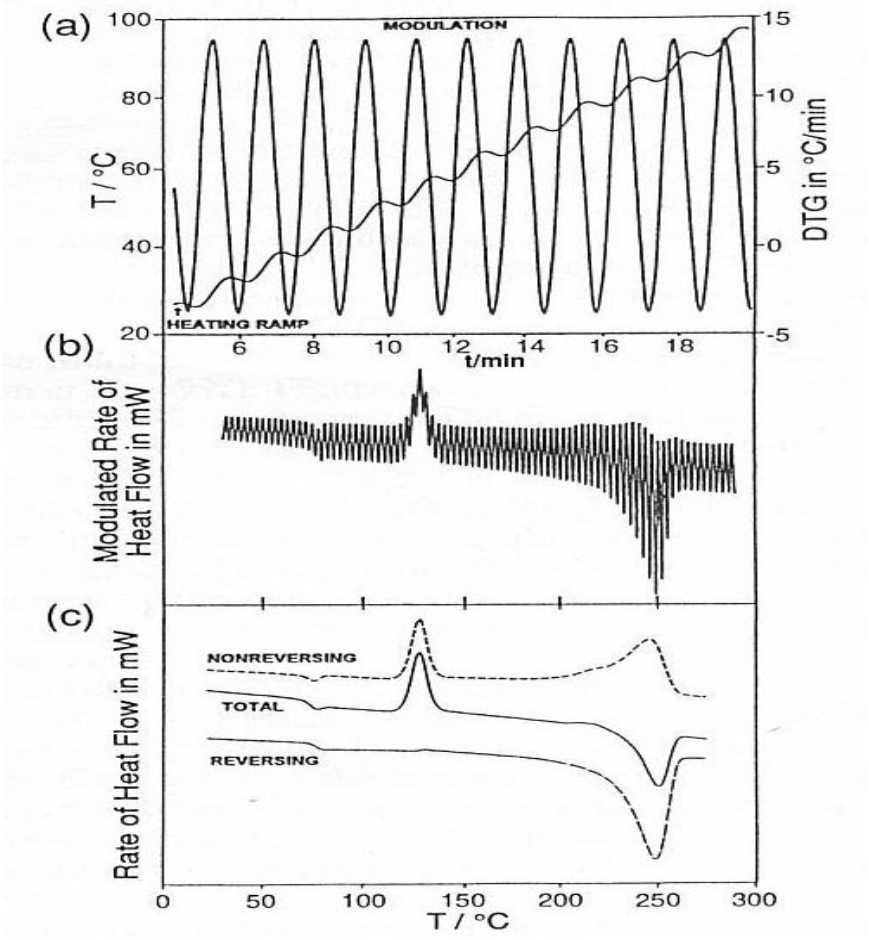

Figure 2.6: Example of MDSC: (a) Typical temperature-time profile, (b) Raw data for an MDSC scan of quenched PET, (c) Deconvolution and analysis of the curve in (b) [Reprint from TA Instruments, Inc.].

cooled polymers were much more crystalline, which can be attributed to crystal perfection at the lamellar surface.

Walker et al [2003a] prepared a range of metallocene and Ziegler-Natta catalyzed LLDPEs by injection moulding to determine the effect of density, molecular weight, MFI and polydispersity on their mechanical performance. In their work, DSC analysis showed a progressive increase in melt temperature with increasing density. In this case, hexene m-LLDPEs exhibited higher elongation at break than the octene m-LLDPEs at similar densities. The cooling rate had a more pronounced effect on the hexene m-LLDPEs, illustrated by larger differences in the melting temperature. The results also showed that the conventional materials have higher melting temperature than the metallocene. They also found that the tensile modulus was dependent on both density and overall crystallinity. Dynamic Mechanical Thermal Analysis (DMTA) of the various polymers showed that both the phase transitions and storage modulus were dependent on comonomer type and density. The results also tend to suggest that the 1-hexene α-olefin comonomer m-PE types exhibited a lower storage modulus than the octene α-olefin comonomer m-PE type for similar density materials.

Walker et al. [2003b] in a similar work discussed the dynamic mechanical properties. The intensity of tan δ peak increased with the decrease in density. It was suggested that this increase in the damping of tan δ is associated with increased side chain branching.

Miller et al. [2002] investigated the effect of quenching conditions in the cast film extrusion process on the mechanical performance and crystalline development of a range of commercially available 1-hexene and 1-octene based metallocene PEs. In that

investigation, DSC analysis showed increase in crystallinity with increasing quench temperature and decreasing MFI. The results of tensile test showed an overall increase in Young's modulus with increase in quench temperature 30^{o} - 60^{o}C.

Kontou et al [2002] studied a set of commercial m-LLDPEs. The results were compared with those of traditional ZN-LLDPEs. They found that the type and amount of comonomer strongly affected the degree of crystallinity and branching, resulting in different material morphology and macroscopic thermo-mechanical behavior. Furthermore, the polymers present a gradual decrease in the percentage crystallinity, position and intensity of β and γ transition, as a function of the comonomer content.

Lovisi et al [2001] synthesized copolymers of propylene/1-hexene and propylene/1-octene using a highly isospecific metallocene catalyst system. In the study, it was observed that properties such as enthalpy of crystallization (ΔH_c), crystallization temperature (T_c), melting temperature (T_m), glass transition temperature (T_g), storage modulus (E′), and density decreased in a linear pattern with increasing comonomer content in the copolymer. From the study, it was also observed that the longer the alkyl branch, the less comonomer was necessary to separate the polymer chains and disrupt the crystalline structure. It, therefore, increased the free volume and the amorphous phase and reduced the size of crystallites, which then translated into lower densities and rubbery copolymers.

Bensason et al. [1996] studied ethylene-octene copolymers prepared by Dow's INSITE^{TM} technology. They found that with the increase of comonomer content, the accompanying tensile behavior changes from necking and cold drawing typical of a semi-crystalline thermoplastic to uniform drawing and high recovery characteristic of an

elastomer. Although changes in morphological features and tensile properties occur gradually with increasing comonomer content, the observations related to melting behavior, morphology, dynamic mechanical response, yielding and large scale deformation have suggested a classification of scheme with four distinct categories. Materials with densities higher than 0.93 g/cc exhibit a lamellar morphology with well developed spherulitic superstructure. Polymers with densities between 0.93 and 0.91 g/cc have thinner lamellae and smaller spherulities. Materials with densities between 0.91 and 0.89 g/cc have a mixed morphology of small lamellae and bundled crystals. These materials can form very small spherulities. Copolymers with densities less than 0.89 g/cc have no lamellae or spherulities.

Kontou and Spathis [2003] examined two types of metallocene ethylene-α-olefin copolymers with some essential differences in their micro morphology that affected their macroscopic behavior. They studied the viscoelastic behavior of the materials in a wide temperature range (from -170^{o}C up to the melting temperature) at four different frequencies (0.2, 1, 10 and 50 Hz) in terms of DMA, and obtained the experimental curves of E (t). They concluded that using this method, values of E(t) at extremely low values of time were available. Hereafter, this function satisfactorily predicted the stress-strain response of the material in the initially linear viscoelastic region in terms of a single integral constitutive equation without the requirement for any model parameters. For higher values of deformation, where plastic strain was enhanced, a plasticity theory of separating the plastic and viscoelastic part of strain was applied, to completely describe the stress-strain behavior.

Soares et al. [2002] synthesized a series of poly (ethylene-co-1-hexene) resins with very distinct, and in some cases bimodal crystalline distributions. These resins possess narrow and similar molecular weight distributions (as expected from metallocene catalysts) but different short chain branch distribution. They found that the tensile properties of a copolymer could be controlled by regulating the ratio of the crystalline species present in the sample.

Nitta and Tanaka [2001] examined dynamic mechanical properties of metallocene Linear PEs with various M_w varying from 20×10^3 to 260×10^3 and branched linear polyethylenes (BPEs) having various degrees of short chain branching. It was found that the positions of α (crystal) relaxation and melting temperature had similar functional dependence of the inverse of the lamellar thickness 1/Lc. The β relaxation appeared around 250 K in the dynamic mechanical spectra for higher molecular weight PEs having more than about 200×10^3 of M_w. The molecular mechanism underlying β relaxation for Linear PEs was different from that for BPEs.

Razavi-Nouri and Hay [2001] made a comprehensive study on a metallocene polyethylene characterizing the isothermal crystallization kinetics, melting and crystallization behavior, crystal growth and dynamic mechanical properties to understand the relationship between molecular structure and mechanical properties of this new class of polyethylene. The melting behavior after step-wise crystallization showed that m-PE consisted of molecular fractions with different molecular weight and branch distribution. Dynamic mechanical property studies showed that three transitions existed in m-PE with the α-transition increasing in intensity and shifting to higher temperatures in samples crystallized at higher temperature compared to the rapidly cooled samples.

Mauler et al. [2001] studied the influence of comonomer content and type on the dynamic mechanical behavior of some ethylene/α-olefin (1-hexene, 1-octene, 1-decene, 1-octadecene and 4-methyl-1-pentene) copolymers. It was observed that the comonomer content greatly influenced α and β transitions, but hardly influenced γ transition. Thus the α transition intensity decreased and β transition intensity increased as the comonomer content increased. Only 1-octadecene showed a different behavior. At higher comonomer content, ethylene/1-octadecene comonomer showed two defined transitions in the α transition region, suggesting the presence of crystals of different sizes.

Strack and LÖfgren [2002] did similar work using α-olefins such as 1-octene, 1-tetradecene and 1-octadecene. Their DMA measurements showed the loss modulus maximum to be a more sensitive value than the loss tangent maximum for the characterization of the comonomer distribution. The intensity of the β transition of 1-octadecene did not increase with increasing branching in contrast to the situation for 1-octene and 1-tetradecene copolymers.

Jordens et al. [2000] synthesized several linear polyethylene homopolymers of various molecular weights using a metallocene catalyst. They examined the thermal, morphological, and mechanical behaviors as a function of molecular weight and thermal treatment. They found that the Young's modulus, yield stress, and yield strain were directly related to percent crystallinity and independent of molecular weight. However, increasing molecular weight suppressed the peak in the stress-strain curves at the yield point. They also found that thermal treatment had a large influence on the shape of the mechanical α-relaxation, while the crystal content affected the strength of γ and β relaxations.

Keating and Lee [1999] studied over 20 commercially available PEs of Ziegler-Natta and Metallocene types. ZN PEs presented a prominent α transition in addition to the β transition in the tan δ curves. The metallocene PEs did not show the α transition. The tan δ peak intensities of m-C_4 and m-C_8 were higher than their ZN counterparts. Moreover, the β transitions of the m-C_4 PEs were 7^o - 8^oC higher than those of the ZN-C_4 PEs at equivalent compositions.

Sacristan et al. [1999] synthesized a series of HDPE via homogeneous polymerization with metallocene catalyst in two different reactors (glass and stainless steel). No marked influence was found for the reaction parameters on the mechanical behavior of the polymers. Their mechanical and dynamic mechanical properties were close to those of Ziegler-Natta polyethylenes.

Starck [1997] investigated commercial LLDPE and VLDPE produced using traditional high activity ZN and metallocene catalysts, respectively, using dynamic mechanical thermal analysis and reported that the intensity of the tan δ maximum peak increased with the incorporation of more comonomer. Starck did not provide explanations for these observations. The metallocene polymers, with the exception of the metallocene LLDPE studied, gave the highest tan δ intensity values which demonstrated the ease of incorporating higher comonomer amounts in the case of single site polymers. The studied m-LLDPEs showed a behavior very close to that of LDPE. In many cases, the study of the maxima of the loss modulus curves gave still more exact information of the smaller amounts of branching present in the polymer.

Woo et al. [1996] performed dynamic mechanical analysis on a series of m-PEs and results were compared with LDPE and ZN-LLDPE. It was found that the measurement was in good agreement with the calculated response.

From the above literature review, it can be concluded that most of the researchers

1) compared the mechanical and thermal properties of traditional ZN-LLDPE with those of m-LLDPE.
2) compared the mechanical and thermal properties of different grades of mPEs such as HDPE, LDPE, LLDPE, VLDPE, etc.
3) studied the effect of molecular weight and thermal treatment on the various thermal transitions.
4) examined the effect of comonomer type and branch content on the different thermal transitions.
5) investigated the effect of quenching condition of the film on the final properties.

However, the previous work did not isolate the interactions between the different molecular parameters such as branch content and composition distribution. Also, the influence of molecular parameters on crystallization kinetics of m-LLDPEs was not studied before. In this research work, the influence of different molecular parameters such as branch type and branch content on thermal and mechanical properties of m-LLDPEs will be studied.

Note: More literature update is available in the actual papers in Chapter 4.

CHAPTER 3

EXPERIMENTAL

3.1. Materials

Currently the widest range of m-LLDPE is produced by ExxonMobil Chemical Corporation. Twelve samples of m-LLDPEs, three ZN-LLDPEs, one ZN high density polyethylene (ZN-HDPE) and one metallocene high density polyethylene (m-HDPE) of various densities were selected for this research work. The details of branch types, melt index, and density of these samples are given in Table 3.1. The density and melt index were supplied by the manufacturer. The m-LLDPEs set contains 4 ethylene-butene copolymers (m-EB), 6 ethylene-hexene LLDPE (m-EH) and 2 ethylene-octene copolymers (m-EO). The m-LLDPE resins were selected to include low and high density LLDPEs (0.880 – 0.918). The MI is directly related to M_w where high MI implies low M_w. On the other hand, density correlates with branch content (BC) where high branch content results in low density. Three ZN-LLDPEs were selected from each branch type to examine the influence of composition distribution. ZN-HDPE and m-HDPE were included for comparison purpose.

GPC characterization of all these resins was performed to obtained M_n, M_w, M_z, and MWD of these polymers. GPC data was collected using 1,2,4 trichlorobenzene as solvent at 150 ^oC in a WATERS GPC2000 instrument. Polystyrene standards were used for calibration. Also, ^{13}C NMR was performed to obtain branch content. A sample of about 50-60 mg was dissolved in 0.4 ml Trichlorobenzene (TCB) solvent. 0.1 mg

Table 3.1**:** Branch type, melt index and density of selected samples

SAMPLE CODE	**SAMPLE TYPE**	**COMMERCIAL NAME**	**DENSITY**
ZN-HDPE	HDPE	HMA-014	0.9600
m-HDPE	HDPE	N/A	N/A
m-EB15	**B**-LLDPE	EXACT-3125	0.9100
m-EB19	**B**-LLDPE	EXACT-3128	0.9000
m-EB37	**B**-LLDPE	EXACT-4011	0.8880
m-EB42	**B**-LLDPE	EXACT-4033	0.8800
ZN- EB13	**B**-LLDPE	LL-1001 X 72	0.9180
m-EH12	**H**-LLDPE	EXCEED-2518CB	0.9180
m-EH15	**H**-LLDPE	EXACT-9107	0.9120
m-EH18	**H**-LLDPE	EXACT-3132	0.9000
m-EH20	**H**-LLDPE	EXACT-9106	0.9020
m-EH24	**H**-LLDPE	EXACT-4151	0.8950
m-EH32	**H**-LLDPE	EXACT-4056	0.8830
m-EO16	**O**-LLDPE	EXACT-0201	0.9020
m-EO33	**O**-LLDPE	EXACT-8201	0.8820

deteriorated Benzene (C_6D_6) was added to get the lock signal from NMR. 2-3 mg Feric acetile acetate (FAcAc) was added as relaxation agent. The solution then transferred into a 5 mm NMR tube. Data were collected at 135^oC for 2 hours with 2000 scan. Results are given in Table 3.2.

Polymers were selected to study the influence of molecular parameters one at a time. For example, comparison of m-EB15 and m-EH15 revealed the influence of comonomer type (butene vs. hexene) since the two have similar M_w, MWD and BC. The influence of composition distribution was examined by comparing resins of similar MI, density and comonomer types such as m-EB15 and ZN-EB13. Further, the influence of branch density is revealed by comparing resins of similar Mw, branch type and composition distribution such as m-EO16 vs. m-EO33.

3.2. Experimental Procedure

3.2.1. Mechanical Testing

Sample Preparation: A rectangular plate was prepared by compression molding from the "as-received" resins in a Carver press. To produce a controlled thermo-mechanical history, the following procedure was followed. At 170^oC, a load of 1 metric ton (MT) was applied for 2 min., followed by a load of 3 MTs for 3 min., then a load of 5 MTs for 1 min., and a load of 7 MTs for 3 min., and finally the mold was water-cooled for 7 min. A Pneumatic punch cutter was used to cut 'dog-bone' specimens from this plate according to ASTM D638 (type V). Figure 3.1 shows the photographs of the Carver press and the Pneumatic Punch Cutter.

Table 3.2**:** Selected properties of the experimental LLDPEs

SAMPLE CODE	**SAMPLE TYPE**	**M_n**	**M_w**	**M_Z**	**MWD**	**BC CH_3/1000C**
ZN-HDPE	HDPE	24217	82733	225054	3.42	0.0
m-HDPE	HDPE	51200	121800	N/A	2.34	0.0
m-EB15	**B**-LLDPE	55386	107958	178554	1.95	14.5
m-EB19	**B**-LLDPE	62106	110466	177163	1.78	18.5
m-EB37	**B**-LLDPE	41349	86832	148381	2.10	36.6
m-EB42	**B**-LLDPE	69403	125471	193010	1.80	42.0
ZN- EB13	**B**-LLDPE	38601	118347	298895	3.07	13.2
m-EH12	**H**-LLDPE	67387	94417	122565	1.40	12.02
m-EH15	**H**-LLDPE	47883	102388	192375	2.14	14.4
m-EH18	**H**-LLDPE	57256	107787	174314	1.83	18.02
m-EH20	**H**-LLDPE	45971	94725	164267	2.06	19.74
m-EH24	**H**-LLDPE	49802	91990	149062	1.85	23.6
m-EH32	**H**-LLDPE	47812	96736	161771	2.02	32.17
m-EO16	**O**-LLDPE	44363	90441	159083	2.04	16.32
m-EO33	**O**-LLDPE	47621	94672	167453	1.99	32.67

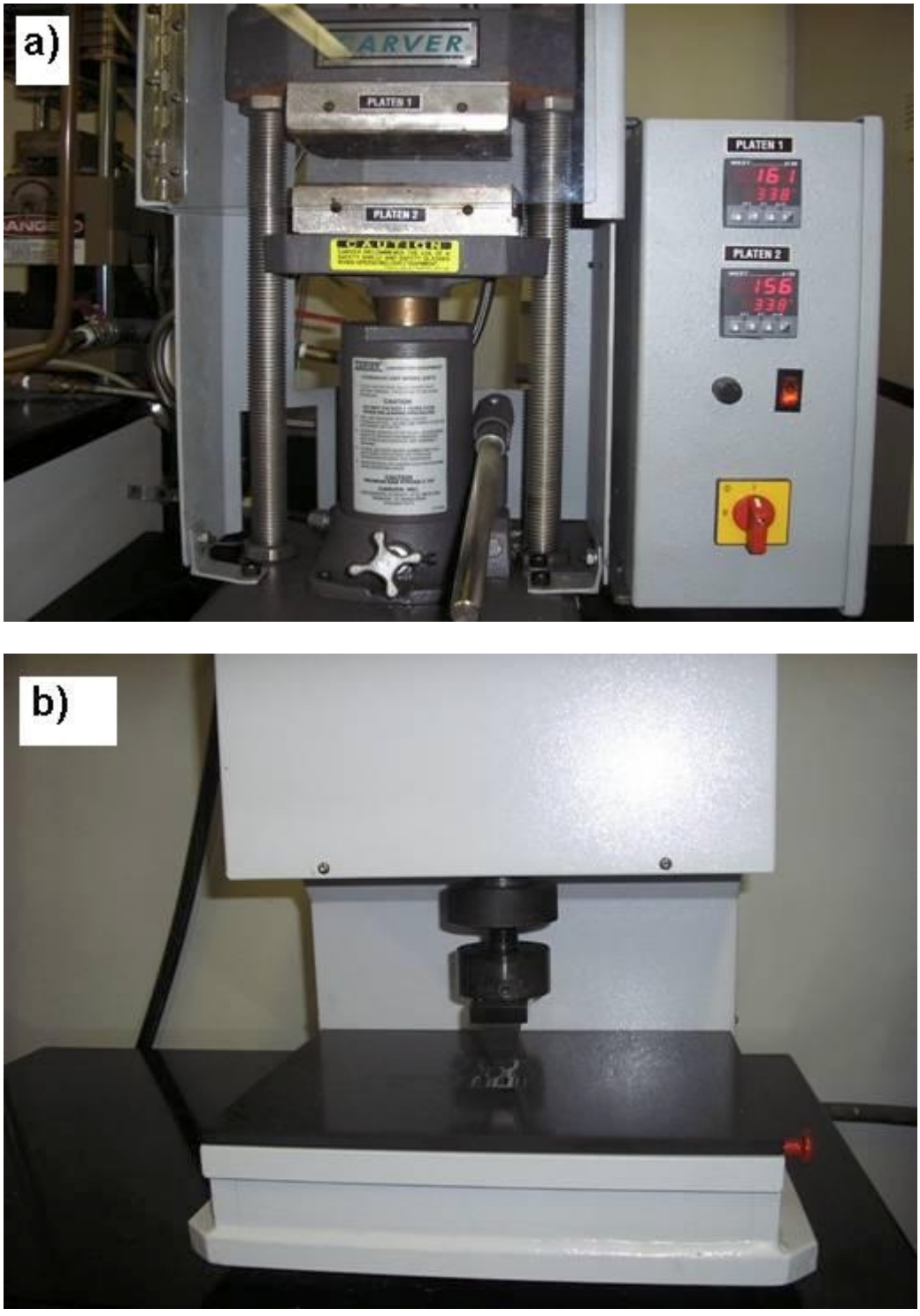

Figure 3.1: a) Hydraulic Carver Press; b) Pneumatic Punch Cutter.

Mechanical Testing: The stress-strain tests were carried out using an Instron Tensile testing machine model 5567 at room temperature (24^{o}C). The controlling limits were viewed on the digital control panel at any time during the test along with other test variables (e.g. start and stop of the test, gauge length adjustment etc.). Any preloading induced during clamping was adjusted to zero prior to testing by the recalibration of the load cell after clamping. Due to the slippage of samples between grips, the instrument was facilitated with pneumatic side action grips of 100 kN capacity. The Instron Series Merlin^{TM} software (Version 4.42) was used for data acquisition, and control and analysis of the samples.

The software provided position and corresponding load of the test with a constant position increment till fracture at the ultimate tensile strength, which is logged along the final position before fracture. All the samples were tested at a crosshead speed of 125 mm/min with a gauge length of 25.40 mm. Also, m-EB15, m-EB42, and ZN-HDPE were tested at crosshead speeds of 10, 50, 125, 250 and 500 mm/min to examine the influence of strain rate on the mechanical properties. The reported results were based on an average of a minimum of five samples. Figure 3.2 shows the picture of Instron Universal Electromechanical load frames (Model 5567) with Pneumatic side action grips.

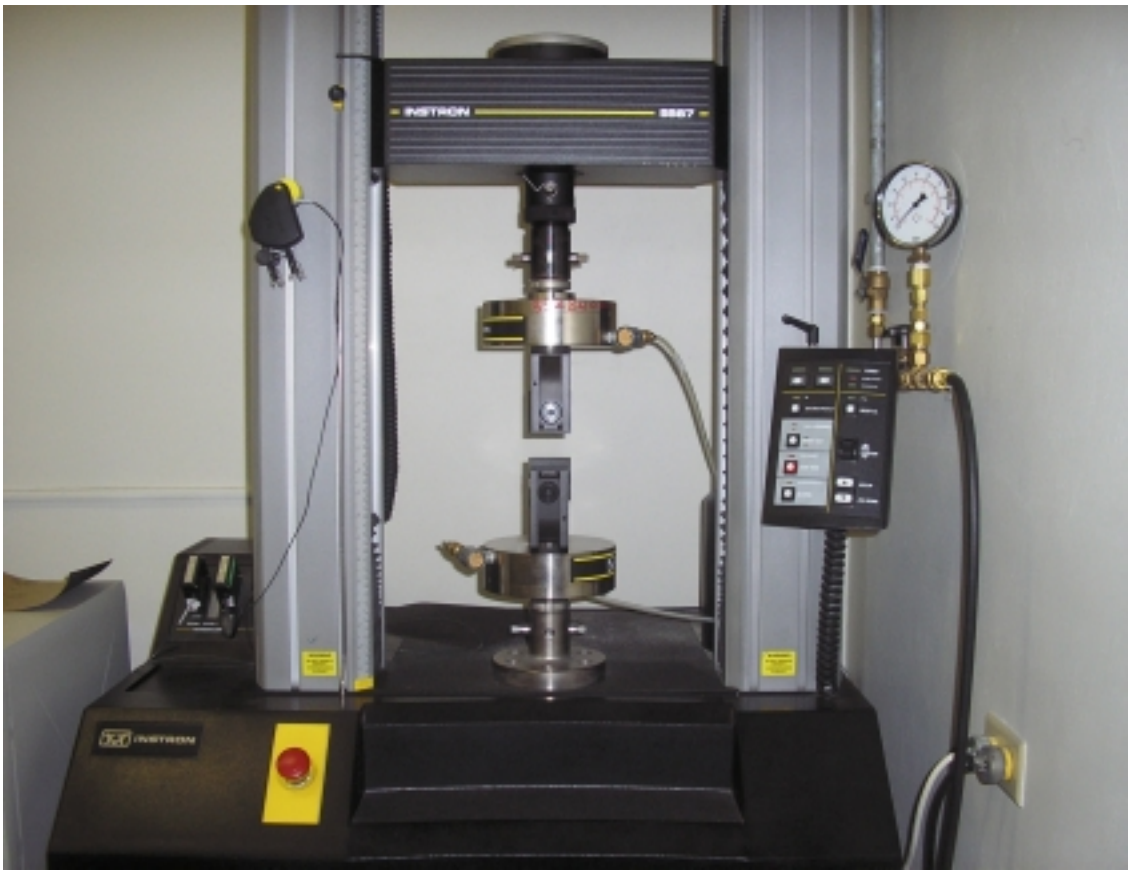

Figure 3.2: Instron 5567 equipped with Pneumatic side action grips.

3.2.2. Modulated Differential Scanning Calorimetry (MDSC)

Samples of 6-10 mg were sliced from the as-received pellets, and then they were compressed into non-hermetic aluminum sample pans for testing in a TA Instruments DSC (Model # Q1000) with modulated option. The instrument was blanketed with nitrogen gas to protect the samples from oxidation. A modulation period of 40 seconds, a heating rate of 2^{o}C/min and amplitude of $\pm$ 0.2^{o}C were used. Temperature scan rates were varied, in the range of 2^{o} - 20^{o}C/min to study the influence of cooling rate on crystallization. Each sample was heated to 160^{o}C to remove the thermal history, and then was cooled at a fixed cooling rate to 5^{o}C. Figure 3.3 shows the Q1000 DSC, which is equipped with auto sampler.

Figure 3.3: a) Modulated DSC Q1000, TA Instrument Inc. equipped with Auto sampler b) Liquid Nitrogen Cooling System (LNCS).

CHAPTER 4

RESULTS AND DISCUSSION

4.1. Influence of Branch Content, Comonomer Type, and Strain Rate on the mechanical properties of metallocene LLDPEs

4.1.1. Abstract

The influence of branch content (BC) and comonomer type on the mechanical properties of metallocene linear low density polyethylene (m-LLDPEs) was studied by means of stress/strain experiment at room temperature. A total of 14 samples of different BC and comonomer types were used. In addition, the influence of strain rate on the mechanical properties of m-LLDPEs with different BCs was examined. The degree of crystallinity of these copolymers was determined by differential scanning calorimetry. In addition, one Ziegler-Natta LLDPE (ZN-LLDPE) having comonomer type of butene (ZN-EB) and one Ziegler-Natta HDPE (ZN-HDPE) were also studied for comparison purposes. The increase in BC of m-LLDPEs lowered the crystallinity and the modulus. However, having close Mw and BC, ZN-EB13 showed higher small strain properties but lower ultimate properties than m-EB15. In comparison with low BC resins, m-LLDPEs with high BC exhibited a stronger strain hardening during stress/strain experiments. The strain hardening was modeled by a modified Avrami equation, and the order of the mechanically induced crystal growth is in the range of 1-2 suggesting athermal nucleation. The strain rate was varied from 10 to 500 mm/min. For low BC m-LLDPEs, a very narrow strain rate window existed within which a maximum in modulus and

ultimate properties was observed. The location of the maximum was independent of BC. The influence of the strain rate on the mechanical properties of m-LLDPEs is a strong function of BC. The strain rate did not influence the mechanical properties of highly branched m-LLDPEs.

4.1.2. Introduction

Metallocene-catalyzed polyethylenes (m-PEs) have attracted great attention from film manufacturers since their commercial development. Metallocene linear low density polyethylenes (m-LLDPEs) are now widely used in packaging film applications [1]. The major advantage of m-LLDPEs over conventional (Ziegler-Natta type) LLDPEs is the possibility of the synthesis of ethylene copolymers with a narrow molecular weight distribution (MWD) and homogeneous composition distribution. The lack of high and low molecular weight tails in these copolymers has significant effects on their processing characteristics and physical properties [2].

Microstructure of polymers plays an important role in determining their mechanical properties. A number of structural and morphological factors such as type, concentration, and distribution of branching; degree of crystallinity; average molecular weight (M_w); and MWD directly influence the mechanical properties of polyethylenes [3-10]. Many studies have investigated the effect of branch content and branch type on the crystallization behavior and mechanical properties of ethylene/α-olefin copolymers [11-21]. The authors have reported either the small strain behavior or the properties of low BC ZN-LLDPEs.

Simanke et al. [11] studied the effect of branching on the mechanical properties of 1-hexene, 1-octene, 1-decene, 1-octadecene and 4-methyl-1-pentene and their results

were limited to the small strain behavior. They failed to obtain the full stress/strain curves of these copolymers due to slippage in the grips. The branch distribution and comonomer type at similar crystallinity had only small effects on the modulus but considerable variations were found in modulus with increasing branch content [13,22]. The initial modulus decreased monotonically with the increase in branching, irrespective of the crystallization mode [22]. Sehanobish et al. [13] also observed similar results and suggested that the modulus of branched polyethylene was primarily dominated by crystallinity. On detailed examination, Mandelkern and his coworkers [4,5] clarified that the influence of crystallinity on modulus was complex.

By increasing the number of short chain branches via incorporation of α-olefin comonomers such as 1-butene, 1-hexene, 1-octene, etc., the polymer crystallinity and density can be reduced. These side chains do not crystallize and are rejected into the amorphous or interfacial regions [11,12]. m-LLDPEs are generally believed to have homogeneous composition distribution and a narrow MWD. So, m-LLDPEs provide an opportunity to investigate the roles of short chain branching on the mechanical properties of these copolymers. So, mechanical properties of LLDPEs are influenced by BC, comonomer type, as well as other molecular parameters such as M_w and MWD. However, the previous work that studied the influence of BC and comonomer type on the mechanical properties was limited to small strain properties. Here, large strain properties have been investigated.

In addition, mechanical properties of polymers can be influenced by the test parameters. During mechanical testing, the effect of increasing deformation rate or strain rate on the low strain portions of the stress-strain curve was suggested to be similar to the

effect of increasing a sample's degree of crystallinity or decreasing the test temperature [2]. Generally, for polymers, the flow stress (stress needed for plastic flow) increases with temperature. The sensitive nature of flow stress on strain rate and temperature can be described by Eyring's equation [23]. According to Eyring's equation, the slope of the linear dependence of yield stress on strain rate is related to materials elemental motion unit and the testing temperature.

Understanding of the strain rate dependence on the deformation behavior of polyethylene is important for the end-users. The effect of strain rate on the deformation of polymers has received wide attention by many researchers [24-30]. In LDPE, till now no attention has been given to the influence of strain rate on the polymers with different branch content (BC). The strain rate has a strong effect on the deformation process of polymers because the energy used during plastic deformation is largely dissipated as heat. This effect was observed to be more prominent at high strain rates associated with adiabatic drawing rather than during small strain rates where isothermal drawing occurred [26,28]. Termonia et al. [29] reported that each molecular weight exhibited a different temperature or elongation window within which optimum drawing occurred. Within these windows, the rate of slippage of chains through entanglements reached a maximum value. Again, the previous work did not study the influence of BC on the strain rate dependency of the mechanical properties of m-LLDPE.

In the present work, metallocene copolymers of ethylene and 1-butene (m-EB), 1-hexene (m-EH) and 1-octene (m-EO) were used. The selected m-LLDPEs had similar Mw and MWD. The objective was to investigate the influence of BC and comonomer type on the mechanical properties of m-LLDPEs at small and large strains. For the first

time, the effect of BC on the large strain properties of m-LLDPEs is measured and modeled using a modified form of Avrami equation. Some conventional LLDPEs (ZN-LLDPEs) were examined for comparison with m-LLDPEs of similar BC, comonomer type, and Mw. The influence of BC was studied using m-LLDPE with BC in the range 14-42 branches/1000 C. To explore the consequences of varying the comonomer type, butene; hexene; and octene ethylene copolymers of selected BCs were used. In addition, the impact of strain rate on the mechanical properties of m-LLDPEs of different BCs was determined.

4.1.3. Experimental

Materials and Sample Preparation

Twelve commercial samples of m-LLDPEs, three ZN-LLDPEs and one high density polyethylene (HDPE) were used. The types of m-LLDPEs are as follows: four 1-butene, six 1-hexene and two 1-octene ethylene copolymers. The three ZN-LLDPEs, one from each comonomer type, were selected for comparison with m-LLDPEs and a ZN-HDPE was used as a reference. The ZN-HDPE represents a limiting case for LLDPEs with low BC since it has zero BC. All samples were ExxonMobil products. Weight average molecular weights (Mw) of all LLDPEs (both metallocene and ZN) are close to 100 kg/mol and the MWD of m-LLDPEs is (≅ 2). Hence, the only primary micro structural variable is BC. Table 4.1.1 provides characterization data for all of the samples. Density and Melt Index (MI) values were provided by ExxonMobil. In addition, information about Mw and BC was determined by gel permeation chromatography (GPC) and 13C NMR, respectively. Details about the GPC and the NMR characterizations were given in a previous publication [31]. Resins were named according

Table 4.1.1**:** Polyethylene properties

Resin	Density, g/cm^3	MI, g/10min	$M_{w,}$ kg/mol	M_w/M_n	BC *
m-EB15	0.910	1.20	108	1.95	14.50
m-EB19	0.900	1.20	110	1.78	18.50
m-EB37	0.888	2.20	87	2.10	36.62
m-EB42	0.880	0.80	126	1.81	42.00
ZN-EB13	0.918	1.0	118	3.07	13.20
m-EH12	0.918	2.50	94	1.40	12.02
m-EH15	0.912	1.20	102	2.14	14.50
m-EH18	0.900	1.20	108	1.83	18.02
m-EH20	0.902	2.0	95	2.06	19.74
m-EH24	0.895	2.20	92	1.85	23.60
m-EH32	0.883	2.20	97	2.02	32.17
m-EO16	0.902	1.10	90	2.04	16.32
m-EO33	0.882	1.10	95	1.99	32.67
ZN-HDPE	0.961	0.70	102	6.7	0.0

* (CH_3/1000C)

to their branch type and content. For example, a metallocene ethylene-butene copolymer with a BC of 14.5 CH_3/1000C is named as m-EB15.

Mechanical Testing

Compression molding was used to obtain sheets (about 3 mm thick) in a Carver press by applying the following thermal history: At 170^{o}C, a load of 1 metric ton (MT) was applied for 2 min., followed by a load of 3 MTs for 3 min., then a load of 5 MTs for 1 min., and a load of 7 MTs for 3 min., and finally the mold was water-cooled for 7 min. Pneumatic punch cutter was used to cut 'dog-bone' specimens from this plate according to ASTM D638 (type V). The tensile tests were performed using an Instron 5567 tensile testing machine at room temperature (24^{o}C). To prevent slippage between regular grips at higher strains, pneumatic side action grips were used. It should be noted that the previous work of Simanke et al. [11] faced slippage problem; hence, large strain mechanical properties were not obtained. All samples were tested at a crosshead speed of 125 mm/min with a gauge length of 25.40 mm. Also, m-EB15, m-EB42 and linear HDPE were tested at crosshead speeds of 10, 50, 125, 250 and 500 mm/min to examine the impact of strain rate on mechanical properties. The results reported in this study are based on an average of a minimum of five samples.

Differential Scanning Calorimetry (DSC)

DSC measurements were performed on a TA Q1000 instrument under nitrogen atmosphere. The nitrogen flow rate was 50 ml/min. The samples obtained from the Carver press were used to obtain the crystallinity. Also, the samples of PEs were collected from the fractured surface of the strained specimens. Samples of 5-10 mg were sliced and then compressed into non-hermetic aluminum pans. Then, heating from 0 to

150^{o}C was carried out at a rate of 10 ^{o}C/min. Calculations of the stress-induced crystallinity were based on a heat of fusion of 290 J/g for a perfect polyethylene crystal [32].

4.1.4. Results and Discussion

Influence of Branch Content

Figures 4.1.1, 4.1.2 and 4.1.3 show the stress-strain behavior of 1-butene, 1-hexene -and 1-octene m-LLDPEs with different BC obtained at a crosshead speed of 125 mm/min. In general, the yield stress decreases with increasing BC. At large strains, the situation is quite different. Strain hardening was observed for almost all samples and it was more pronounced in high BC resins.

Crystallinity: The crystallinity values were obtained from DSC for all samples before and after the stress/strain experiments. Results are given in Table 4.1.2. DSC testing of PE samples before the stress/strain experiment will reveal the initial crystallinity, which influences the Young's modulus. On the other hand, the testing of the strained samples will disclose the influence of strain hardening behavior on final crystallinity. The objective of testing strained samples is to check for induced crystallization due to the application of stress. The DSC thermograms of EB before (solid line) and after (dashed line) mechanical testing are given in Figure 4.1.4. It was found that the crystallinity changes slightly after deformation for copolymers with high initial crystallinity (low BC). However, copolymers with BC higher than 30 CH_3/1000C exhibit an appreciable increase in final crystallinity after deformation (see Table 4.1.2). Figure 4.1.4 shows a clear shift in the melting peak of m-EB15 and m-EB19 resins.

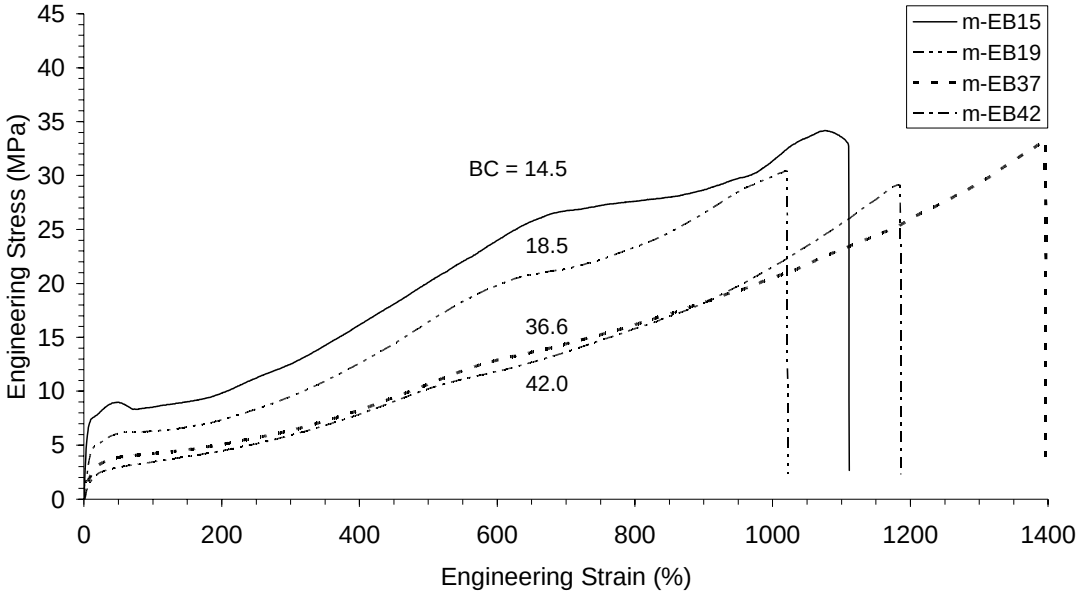

Figure 4.1.1: Stress/strain curves for EB m-LLDPEs with different BCs.

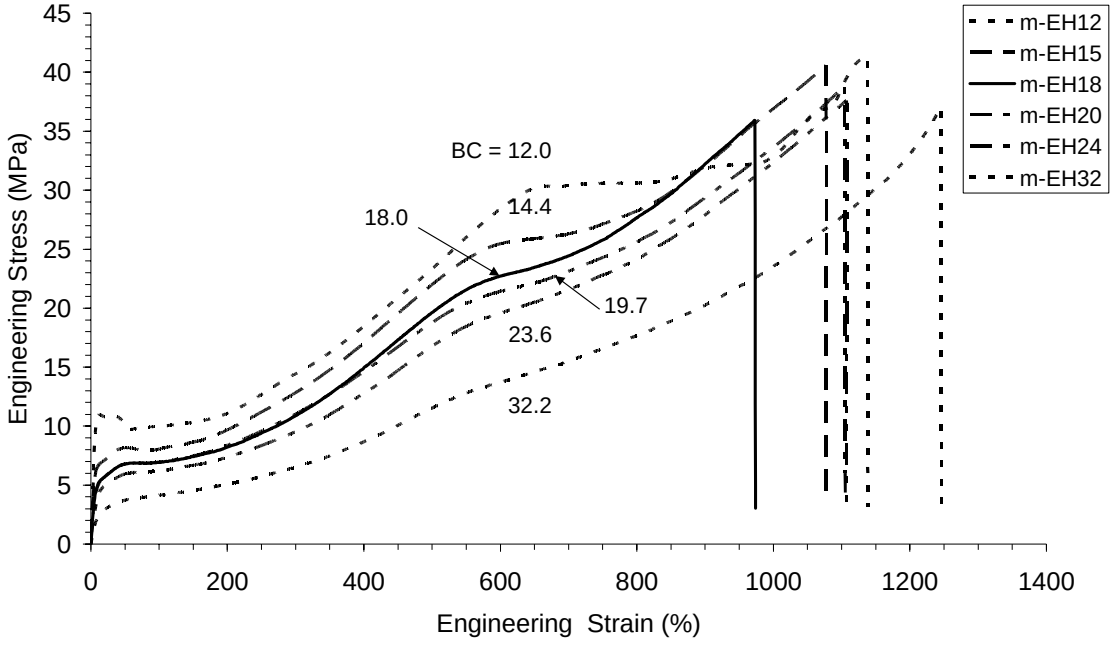

Figure 4.1.2: Stress/strain curves for EH m-LLDPEs with different BCs.

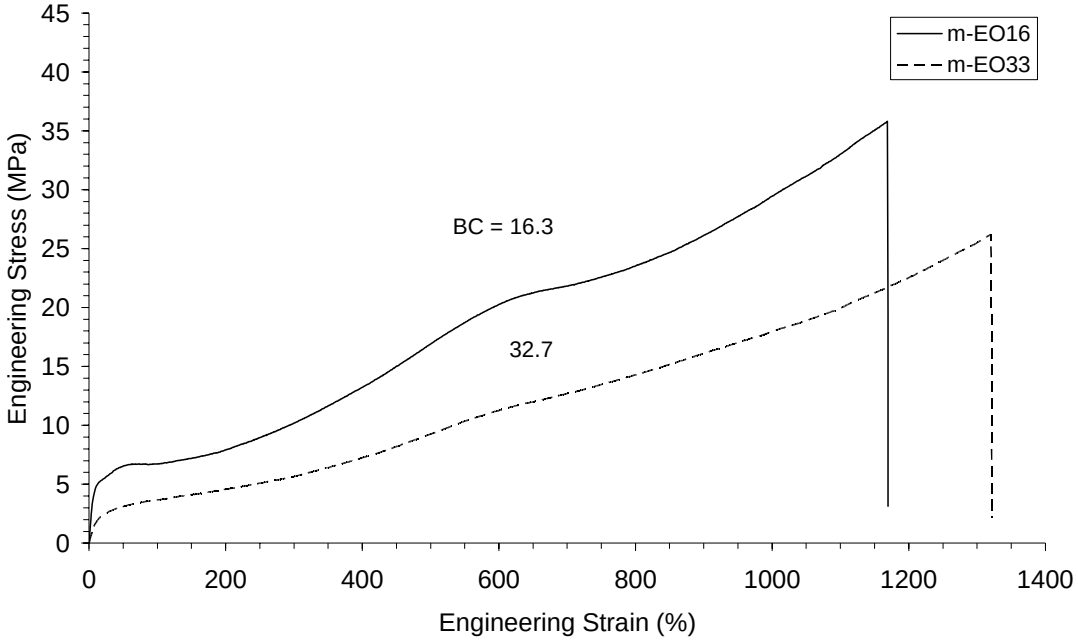

Figure 4.1.3: Stress/strain curves for EO m-LLDPEs with different BCs.

Table 4.1.2**:** Selected thermal properties of ethylene/α-olefins copolymers.

Resin	BC (CH_3/1000C)	Melting Peak (^oC)		Stress-induced crystallinity (%)	
		Before	After	Before	After
m-EB15	14.50	104.7	108.4	39.3	39.9
m-EB19	18.50	92.8	97.0	29.6	29.4
m-EB37	36.62	48.1, 71.0	43.2, 73.8	21.8	26.9
m-EB42	42.00	43.0, 63.2	46.4, 64.5	16.0	20.4
m-EH12	12.02	115.2	114.7	40.3	41.6
m-EH15	14.50	105.7	103.0	34.9	36.0
m-EH18	18.02	95.7	99.6	28.9	29.0
m-EH20	19.74	45.1, 88.3	45.4, 94.7	31.1	31.5
m-EH24	23.60	47.2, 90.3	43.2, 92.6	28.4	29.6
m-EH32	32.17	46.4, 73.2	44.7, 80.0	22.6	25.2
m-EO16	16.32	95.2	97.2	29.6	29.5
m-EO33	32.67	42.5, 72.2	44.9, 75.9	20.5	24.4

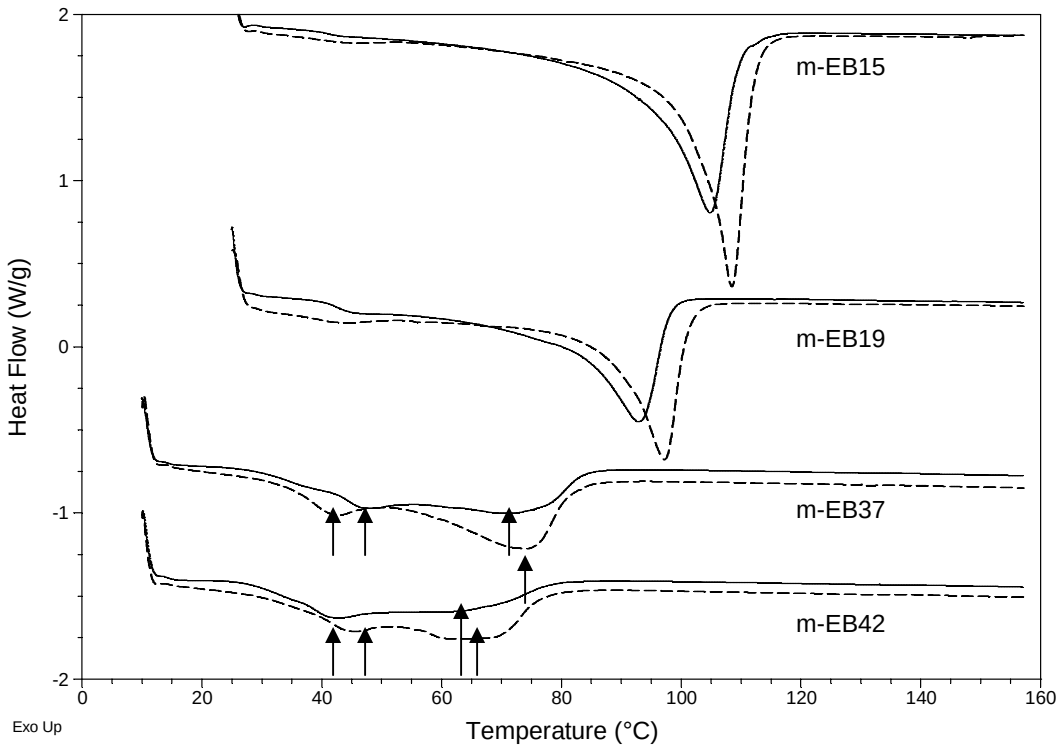

Figure 4.1.4: DSC thermograms of EBs before (solid line) and after (dashed line) mechanical testing at crosshead speed of 125 mm/min. (the arrows show the appearance of the peaks.)

Sumita et al. [33] showed that the increases in both the heat of fusion and melting temperature of polyethylene were attributed to orientation of the amorphous phase as a result of drawing (induced crystallization). They proposed that the excess free energy of the amorphous phase resulting from orientation increases the melting temperature. This is a direct result of the decrease in ΔS due to orientation; hence, ΔG is more positive ($\Delta G=\Delta H-T\Delta S$). Results in Table 4.1.2 show that samples with low BC displayed increase in T_m without any significant change in total crystallinity. So, it is likely that crystal perfection rather than induced crystallization might have taken place. The low BC m-LLDPEs have a high initial crystallinity. So, it is reasonable to assume that most of the applied stress is used to perfect the crystals. Crystal perfection due to the application of stress was previously observed for ZN-LLDPE [34]. It was suggested that the more defective crystals of LLDPEs were destroyed during tensile testing and rebuilt into more perfect crystals [34]. This assumption is reinforced in our current observation that the strain hardening for low BC resins was lower than that for the high BC m-LLDPEs.

The stress on samples with high BC (more amorphous) resulted in increased total crystallinity and a shift in T_m. However, for high BC resins, the peaks are very broad and more than one melting peak was observed. Both melting peaks in m-EB37 and m-EB42 were shifted to the right. In addition, the applied stress has improved the sharpness of the peak in high BC resins. This suggests that part of the applied stress was used to perfect the weak crystal of highly branched m-LLDPEs as well as increase the depth of the peaks (increase crystallinity) as a result of induced crystallization. For high crystallinity resins (m-EB15 and m-EB19), the shift in T_m is easy to detect.

Now, the presence of two melting peaks in m-LLDPEs with high BC will be discussed. This is likely due to the poor branch distribution of m-LLDPE with high BC, which will lead to linear portions and branched parts in the same molecule. Hence, crystallization of the different parts of the same molecule will take place at different temperatures with branches being excluded from the crystalline lattice. Similar observation and explanations were reported by Tanem and Stori [35] for copolymers with high BC. The interfacial region may have some ordering retained from the crystalline phase [16]. The DSC results show that stress-induced crystallization is more pronounced in the more amorphous resins (high BC samples). So, it is likely that high stresses result in perfection of crystals of low BC samples and induced crystallization in high BC resins.

The stress-induced crystallization has resulted in an increase in stress with time. The increase in stress beyond the yield point is believed to be a result of orientation or induced crystallization. The point at which the stress/time curve starts to show increase in stress is taken as (σ_o, 0). With time, the polymer crystallinity will increase and the stress needed to maintain a constant strain rate will increase, too. This increase in stress will continue till the sample failure at (σ_f, t_f). At any time on the stress/time curve (obtained from stress/strain curve) the increase in stress (σ-σ_o) will induce the formation of crystals. In thermally induced crystallization, ΔT is the driving force for crystallization. On the other hand, $\Delta\sigma$ is the driving force for mechanically induced crystallization. Sumita et al. [33] obtained a linear relationship between the heat of fusion (proportional to crystallinity) and the melting point. Therefore, it is assumed that the increase in stress is proportional to the increase in crystallinity [$\Delta\sigma \alpha X$].

Hence, the fractional increase in stress [$(\sigma-\sigma_o)/(\sigma_f-\sigma_o)$] is equal to the fractional increase in crystallinity, X_t. The physics of the mechanically and the thermally induced crystallizations are similar. So, it was found attractive to model the mechanically induced crystallization by a modified Avrami equation that is widely used in studying the kinetics of crystallization [36]. The authors are not aware of any previous work that attempted to use Avrami type equation to model the mechanically induced crystallization.

The well known Avrami equation is defined as [37, 38]:

$$1 - X_t = \exp(-kt^n) \tag{4.1.1}$$

Where n is the Avrami crystallization exponent dependent on the mechanism of nucleation, t is the time taken during the crystallization process, k is the growth rate constant, and X_t is relative crystallinity of polymers. Both k and n are constants which denote a given crystalline morphology and type of nucleation at a particular crystallization condition [39]. The relative crystallinity, X_t is defined as follows:

$$X_t = \frac{\int_{t_o}^{t} (dH_c/dT)dT}{\int_{t_o}^{t_\infty} (dH_c/dT)dT} \tag{4.1.2}$$

where dH_c/dT is the rate of heat evolution and t_o and t_∞ are the times at which crystallization starts and ends, respectively. Eq. (1) was further modified by several authors to describe non-isothermal crystallization [40-43] for non-isothermal crystallization at a chosen cooling rate; X_t is a function of the crystallization temperature (T). That is, Eq. 2 can be rewritten as follows:

$$X_t = \frac{\int_{T_o}^{T} (dH_c/dT)dT}{\int_{T_o}^{T_\infty} (dH_c/dT)dT} \tag{4.1.3}$$

Where T_o and T_∞ represent the onset and final temperature of crystallization, respectively.

Crystallization time, t can be converted from temperature using the following equation [40].

$$t = \frac{T_O - T}{R} \tag{4.1.4}$$

where R is the cooling rate (^oC/min). Using Eq. (1) in double-logarithmic form

$$\ln[-\ln[1 - X_t]] = \ln k + n \ln t \tag{4.1.5}$$

and plotting ln[-ln[1-X_t]] versus ln t for each cooling rate, a straight line is obtained. From the slope and intercept of the lines, one can determine the Avrami exponent n and the crystallization rate k. Here, the crystallization rate depends on the cooling rate. Thus, the crystallization rate constant k should be corrected adequately. At a constant cooling rate, k can be corrected as follows [40]:

$$\ln k' = \ln k \ / R \tag{4.1.6}$$

In the present work, the idea of non-isothermal crystallization was borrowed to model the crystallization induced by the applied stress during stress/strain experiments. This method was applied only for EH samples due to availability of a good number of samples of the same branch type. Therefore, X_t, can be defined as follows:

$$X_t = \frac{\int_{\varepsilon_o}^{\varepsilon} (d\sigma_c / d\varepsilon) d\varepsilon}{\int_{\varepsilon_o}^{\varepsilon_f} (d\sigma_c / d\varepsilon) d\varepsilon} \tag{4.1.7}$$

where ε_o and ε_f represent the onset and final point of engineering strain (mm/mm) in stress/strain curve where increase in stress observed due to strain hardening. From Figure 4.1.2 the beginning of strain hardening was observed for all EH samples about to 150%

engineering strain. So, ε_o was taken at 150%. The final strain, ε_f, was taken 15 second before the sample failure, except for m-EH12. For m-EH12, ε_f was taken up to 650% because beyond this point the stress/time curve is flat. Crystallization time, t was converted from the engineering strain by the following equation:

$$t = \frac{\varepsilon_O - \varepsilon}{D} \tag{4.1.8}$$

where D is the strain rate (min^{-1}). Strain rate was calculated in the following way:

$$Strain\ Rate = \frac{Crosshead\ Speed\,(mm/\min)}{Initial\ \ Specimen\ Length\,(mm)} = \frac{125\,(mm/\min)}{25.4\,(mm)} = 4.92(\min^{-1}) \tag{4.1.9}$$

At a constant strain rate, k can be corrected as follows:

$$\ln k' = \ln k \ \ / D \tag{4.1.10}$$

Figure 4.1.5 shows a plot of ln[-ln[1-X_t]] versus lnt for EH m-LLDPEs resins. Avrami parameters estimated from Figure 4.1.5 are listed in Table 4.1.3. It was found that the Avrami exponent (n) is in the range of 1- 2, which suggests athermal nucleation (see p. 147 of Wunderlich [39]).

Table 4.1.3: Avrami parameters for EH m-LLDPEs.

Resin	Avrami Exponent (n)	Crystallization Rate Constant (k′)
m-EH12	0.65	1.010666
m-EH15	1.34	0.948392
m-EH18	1.31	0.909502
m-EH20	1.44	0.959755
m-EH24	1.35	0.889249
m-EH32	1.34	0.808478

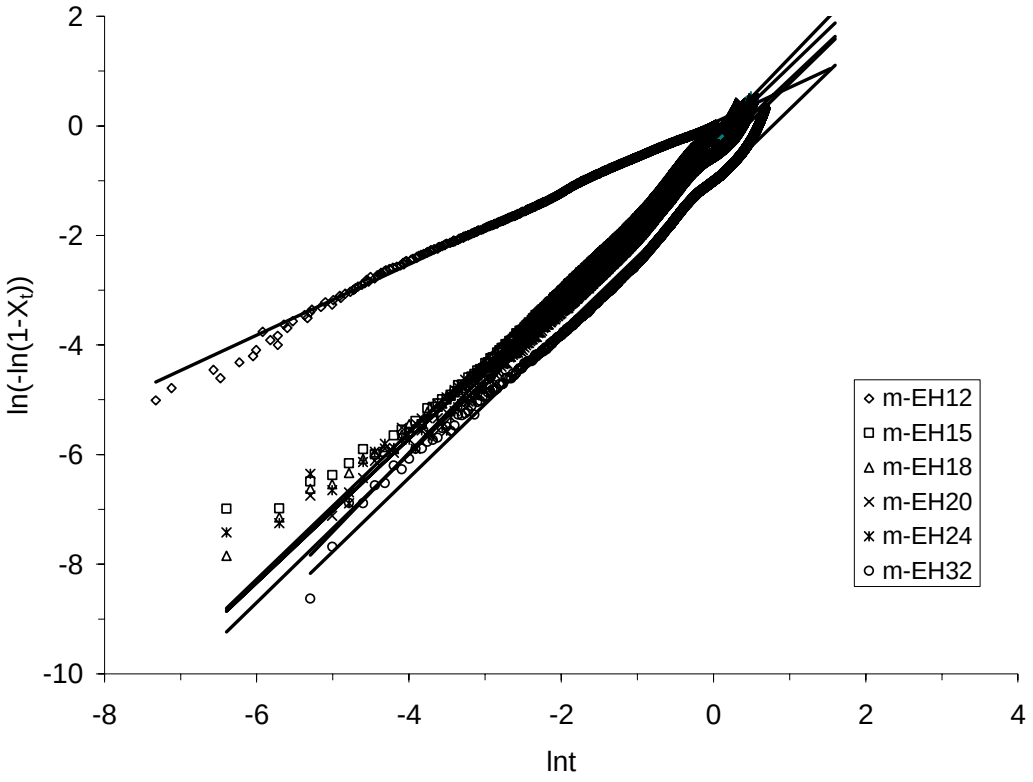

Figure 4.1.5: Avrami plot for EH m-LLDPEs (strain rate 4.92 min^{-1}).

Young's Modulus and Yield Stress: Figure 4.1.6 shows an expanded view of stress-strain curves in the vicinity of yielding. It was observed that the yield peak becomes less distinct with increasing BC regardless of the comonomer type. Also, the yielding region broadens with an increase in BC. Similar observations were reported by Bensason et al. [14]. A double yield phenomenon is also observed for samples with BC < 20. At the first yield point, temporary plastic deformation was assumed, followed by a recoverable re-crystallization of the lamellae. The second point is the onset of permanent plastic deformation in which the lamellae are destroyed [44]. It was postulated that the double yielding phenomena is due to a partial melting re-crystallization process. With deformation the melted species will re-crystallize in the draw direction with a simultaneous reduction in stress [45, 46].

In general, the copolymers with lower α-olefin contents showed higher yield stress and Young's modulus. Our results suggest that the yield stress does not depend on the branch type but rather on BC. This result agrees with the observations of Simanke et al. [11]. Results of Young's modulus as a function of BC for all m-LLDPEs are presented in Figure 4.1.7. The error bars indicate the range of these results for a minimum of 5 samples. In Figure 4.1.7, a relationship (modulus = 15279 $BC^{-1.748}$) is introduced to fit all data points. It is clear from Figure 4.1.7 that the modulus decreases with the increase in BC but the relationship is not linear. For HDPE, the modulus is about 1100 MPa, whereas m-LLDPEs show a modulus in the range of 30 to 240 MPa depending on BC. The influence of crystallinity on modulus was suggested to be complex [4]. The modulus is not a linear function of the degree of crystallinity. Popli and Mandelkern [4] have tried to describe the plot by an "S" shaped curve. Branched polymers with Young's modulus

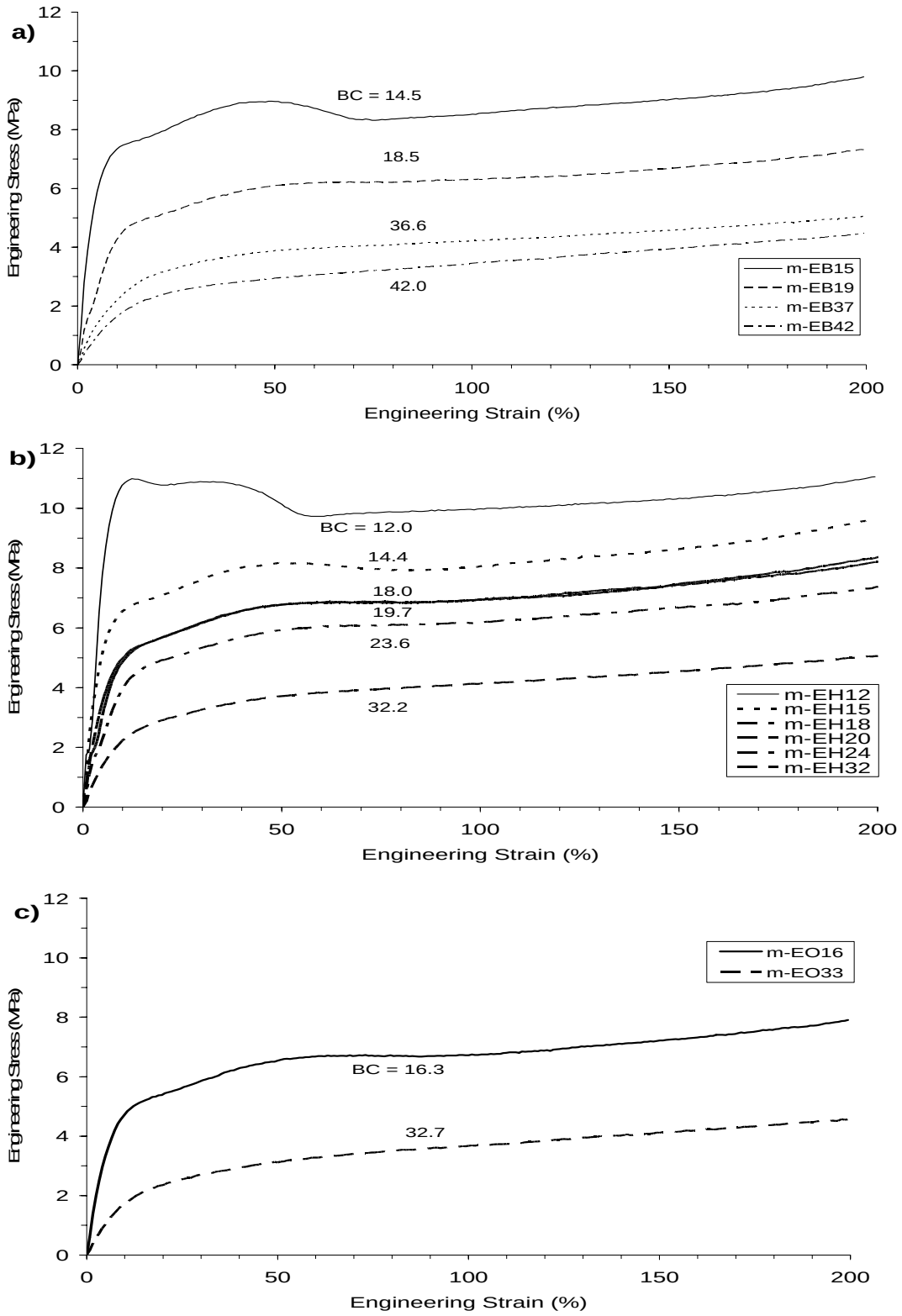

Figure 4.1.6: Effect of BC and branch type on yielding behavior (crosshead speed of 125 mm/min).

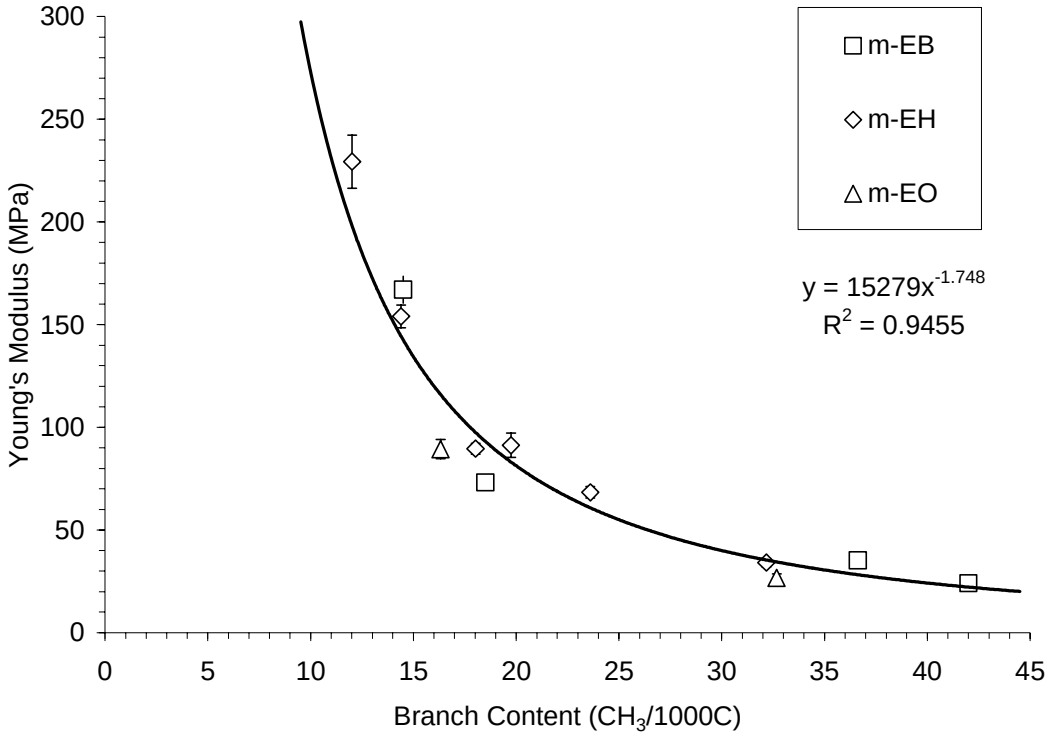

Figure 4.1.7: Young's modulus as a function of BC (crosshead speed 125 mm/min)

in the range of 100 to 200 MPa fall in the lower part of the "S" shaped curve, which agrees very well with the present results. Comparison between m-EB15 and ZN-EB13 reveals that the ZN-EB13 possesses higher modulus than m-EB15 of the same branch type and of similar average BC. It is likely that the presence of linear molecules as a result of the structural and size heterogeneity of ZN-LLDPE are behind this observation [20,47]. As indicated by our results on the linear HDPE, the linear molecules show a higher modulus. So, branch or composition distribution is another factor that influences the mechanical properties of LLDPEs.

Ultimate properties: The major ultimate properties to be discussed here are elongation at break (%) and ultimate tensile strength. In addition, another property named 'Ultimate Modulus, UM', was introduced to measure the degree of strain hardening. It is the slope of stress/strain curve near the ultimate values. Figure 4.1.8 shows estimated UM as a function of BC. It is clear from Figure 4.1.8 that the relationship between UM and BC is complex. In general, EB and EH resins showed similar strain hardening behavior. For most of the samples, the UM lie in the range of 3 to 11 MPa, while the Young's modulus (initial slope of stress/strain curve) was in the range of 30 to 240 MPa. ZN-EB13 showed less strain hardening than m-EB15, which may be a direct consequence of composition distribution.

Elongation at break (%) as a function of BC is shown in Figure 4.1.9. Our results on m-LLDPEs suggest that the elongation at break (%) is not a strong function of BC as well as comonomer type. These results agree with previous observations reported on ZN-LLDPEs [4,34]. The ultimate properties are reported to be independent of the

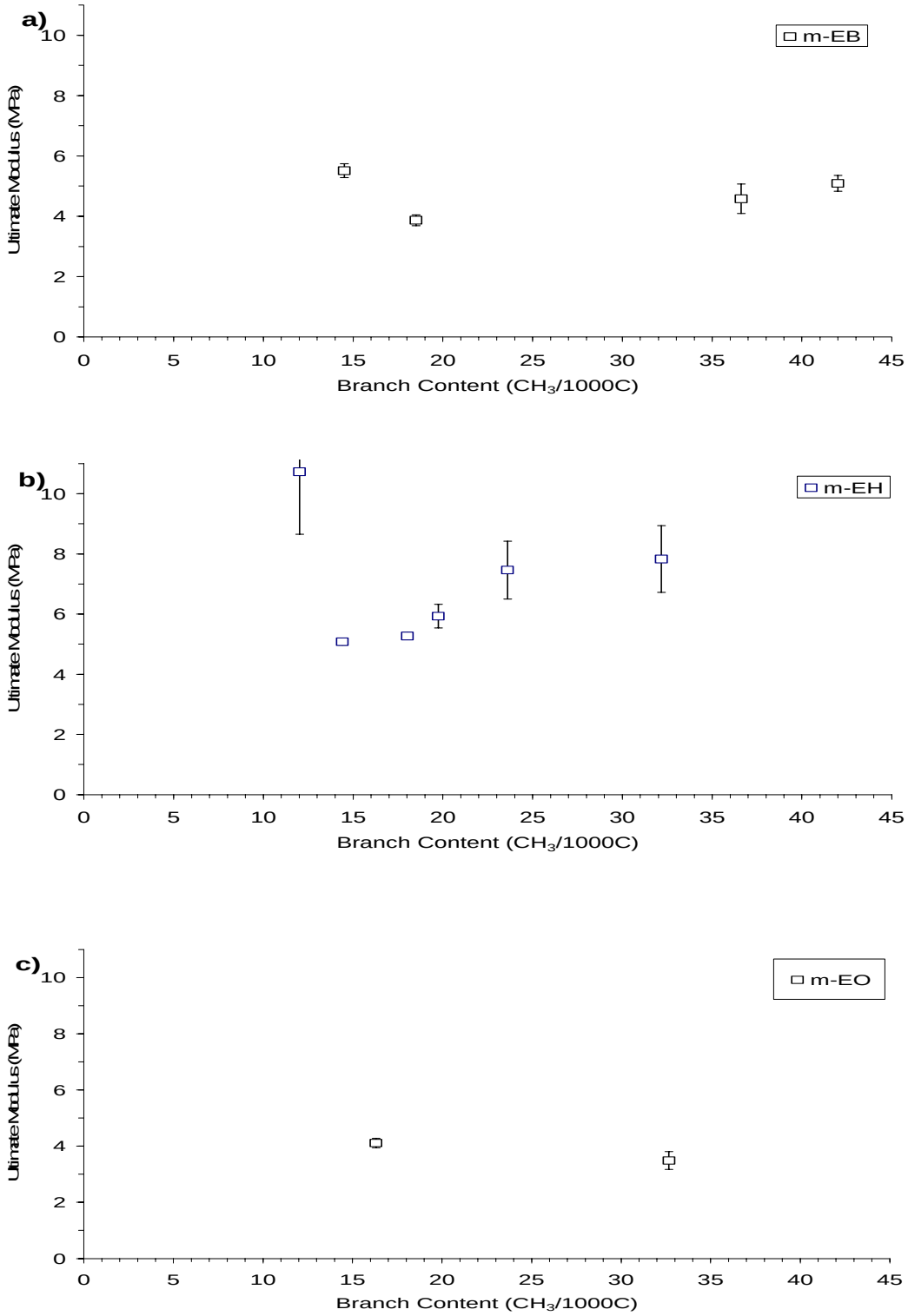

Figure 4.1.8: Ultimate Modulus as a function of BC and branch type (crosshead Speed 125 mm/min).

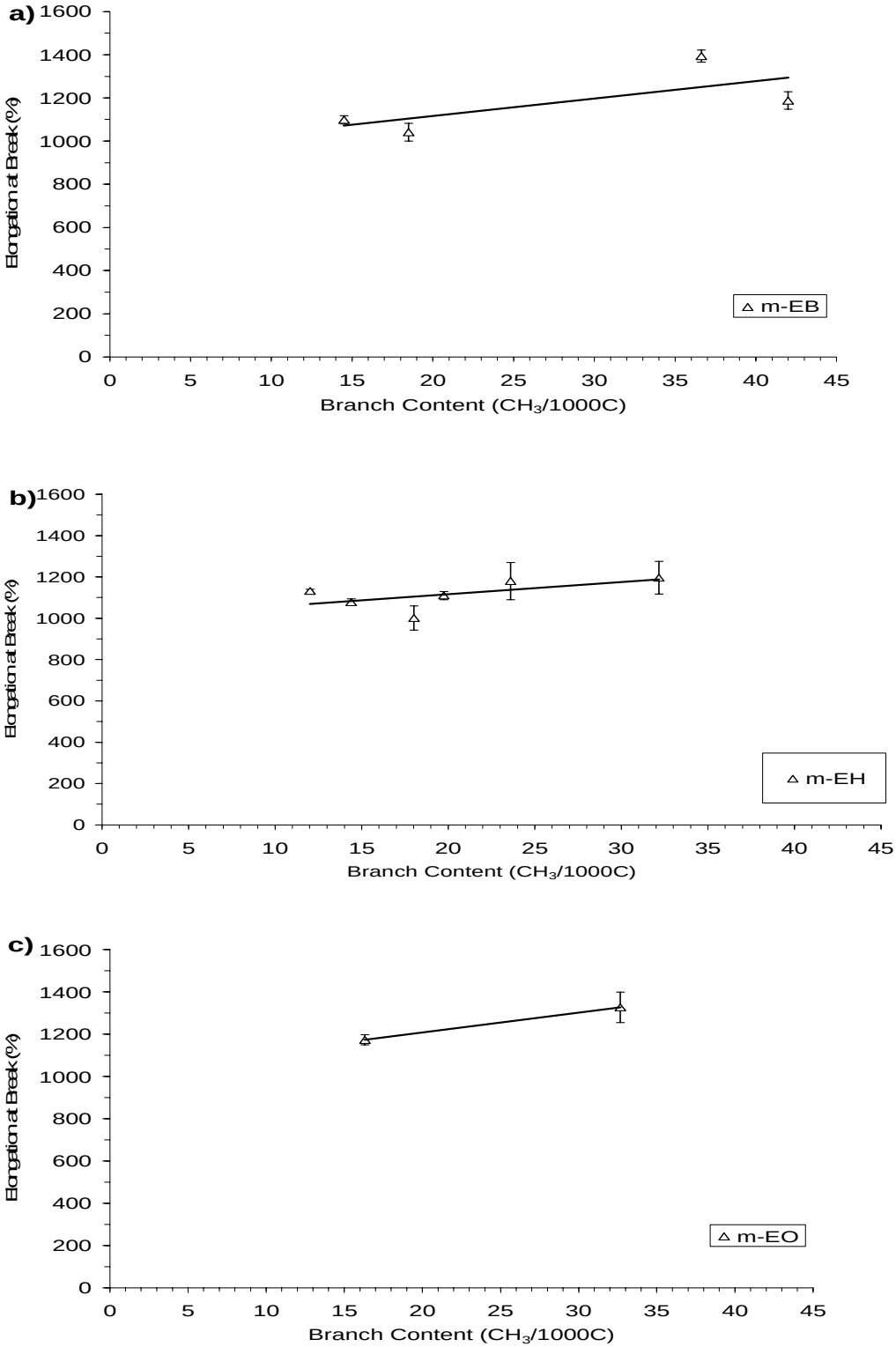

Figure 4.1.9: Elongation at break as function of BC and branch type (crosshead speed 125 mm/min).

morphological and structural variables and do not depend on the M_w, MWD or comonomer concentration [4].

The influence of BC on the ultimate tensile strength is shown in Figure 4.1.10. For EB, the BC showed no influence on ultimate tensile strength. For EH and EO resins, the ultimate tensile strength showed a weak dependency on BC. In general, BC has weak influence on the ultimate tensile strength. Our current results on the influence of BC of m-LLDPEs on ultimate properties are in agreement with previous observations on ZN-LLDPEs [4]. For the influence of comonomer type, ultimate tensile strength decreases slightly with the increase in BC for EH resins. Also, m-EH resins exhibited higher stress at break compared to EB. From Figures 4.1.9 and 4.1.10, ZN-LLDPEs displayed lower elongation at break and tensile strength in comparison to m-LLDPEs. So, comonomer type and content of m-LLDPEs have weak influence on the ultimate tensile strength and strain at break. However, there exists a complex relationship with ultimate modulus (strain hardening behavior).

Influence of Strain Rate

In general, higher strain rates are observed to increase elastic modulus, higher yield stresses, lower elongation at break, and a better defined neck [2,48]. Figure 4.1.11 shows Young's modulus as a function of crosshead speed for three resins of different BCs. Figures 11a-c correspond to PEs with BC of 0 (linear HDPE), 15 (m-EB15) and 42 (m-EB42), respectively. An interesting phenomenon was observed. For all three resins, it seems that there exists a critical value (near the crosshead speed of 125 mm/min) after which Young's modulus was not much influenced by the crosshead speed. It should be noted that the location of the maximum is independent of BC.

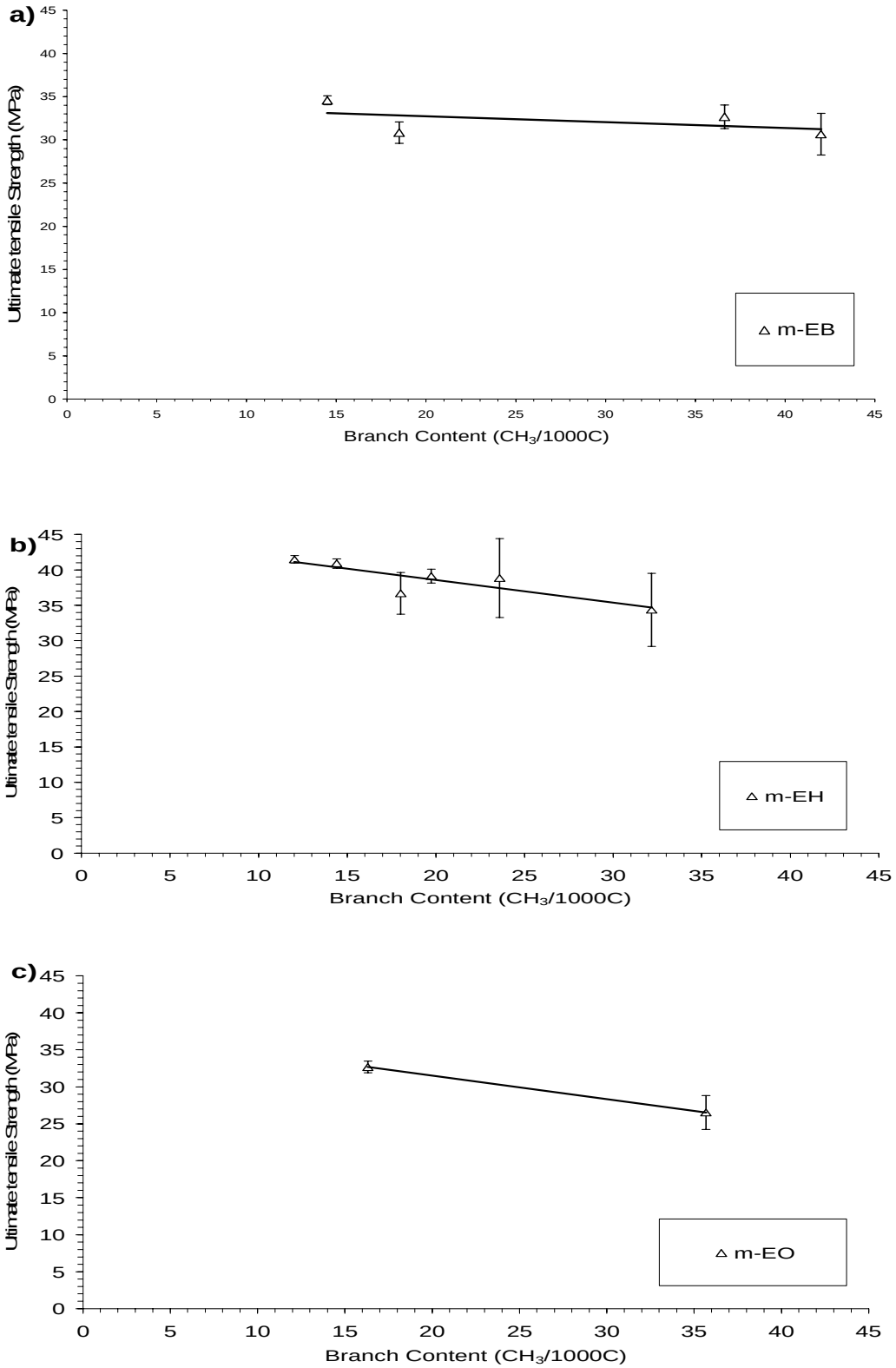

Figure 4.1.10: Ultimate tensile strength as a function of BC and branch type (crosshead speed 125 mm/min).

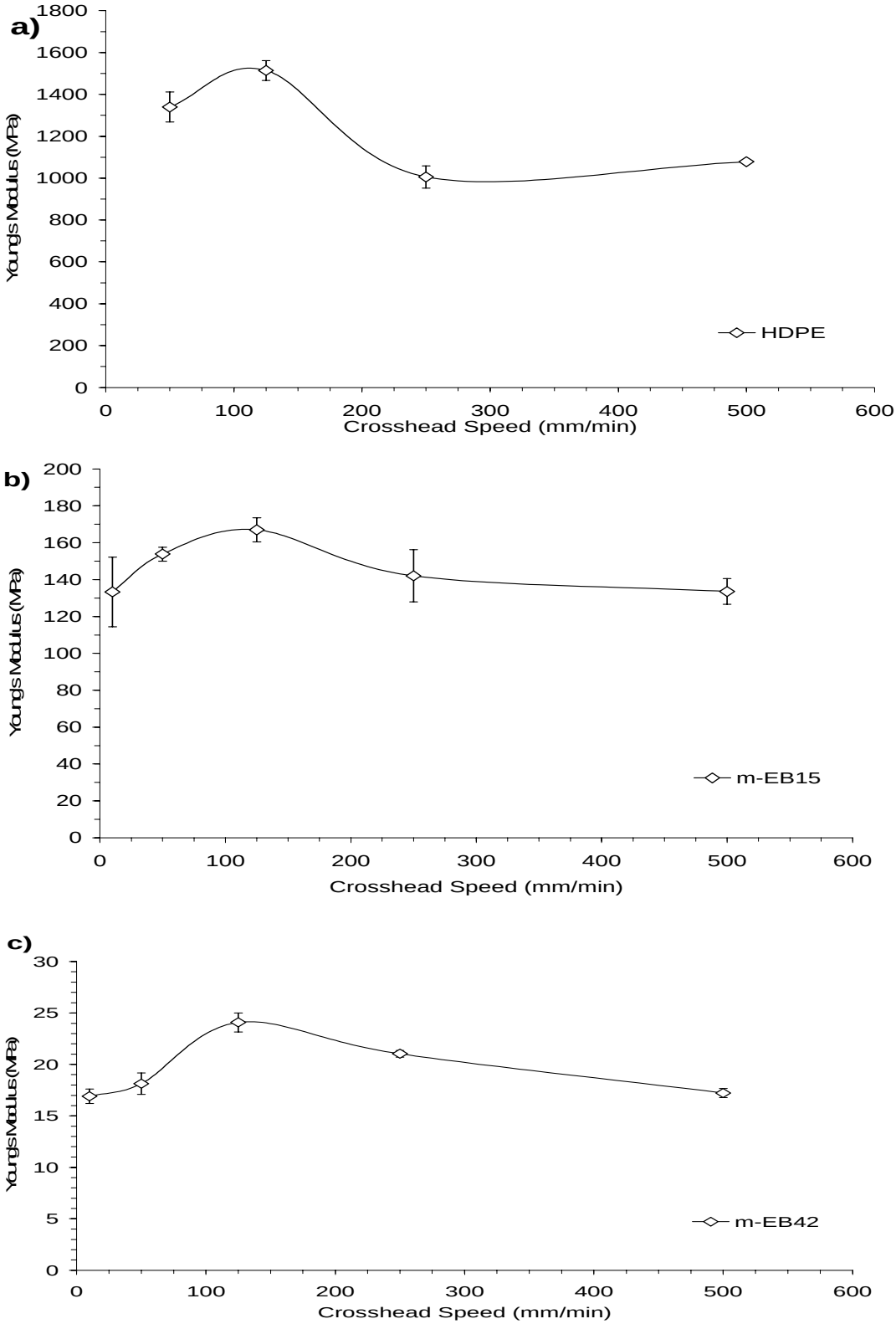

Figure 4.1.11: Young's Modulus as function of crosshead speed and BC.

For HDPE, Young's modulus, yield stress and other parameters associated with the strain response were reported to decrease rapidly with the increase in strain rate, when strain rate is larger than a critical value [25]. Liu and Harrison [25] reported this critical value for polyethylene near a strain rate 100 mm/min (see Figure 14 ref. 25) which is also close to our critical value (125 mm/min). The normal time-temperature superposition principle does not appear to hold in this case. It was suggested that this decrease in modulus and yield stress is not caused by a temperature rise during strain. May be it is caused by void formation and crazing, which are relatively uniform throughout the sample. They provided optical microscopic picture of polypropylene (see Figure 7 ref. 25) to support their assumption.

Elongation at break and ultimate tensile strength as a function of strain rate for m-LLDPEs with different BC are shown in Figures 4.1.12 and 4.1.13, respectively. The percent elongation at break of linear HDPE decreased immediately with the increase in strain rate as shown in Figure 4.1.12. The ultimate tensile strength of HDPE was not included as it was broken immediately after reaching its yield point. Again a critical value is observed in Figures 4.1.12 and 4.1.13 (a) for m-EB15 at a strain rate of 125 mm/min. Termonia et al. [29] reported that for each Mw of melt-crystallized monodispersed PE, there exists a very narrow temperature or elongation rate window within which maximum drawability occurs. Though it was true for m-EB15 but it does not hold for m-EB42, where a minimum was observed. Also, increasing the rate from 125 to 250 mm/min did not influence the ultimate tensile strength. These results show that elongation at break and tensile strength for m-EB42 was almost independent of strain rates (Figures 4.1.12 and 4.1.13b) over a wide range.

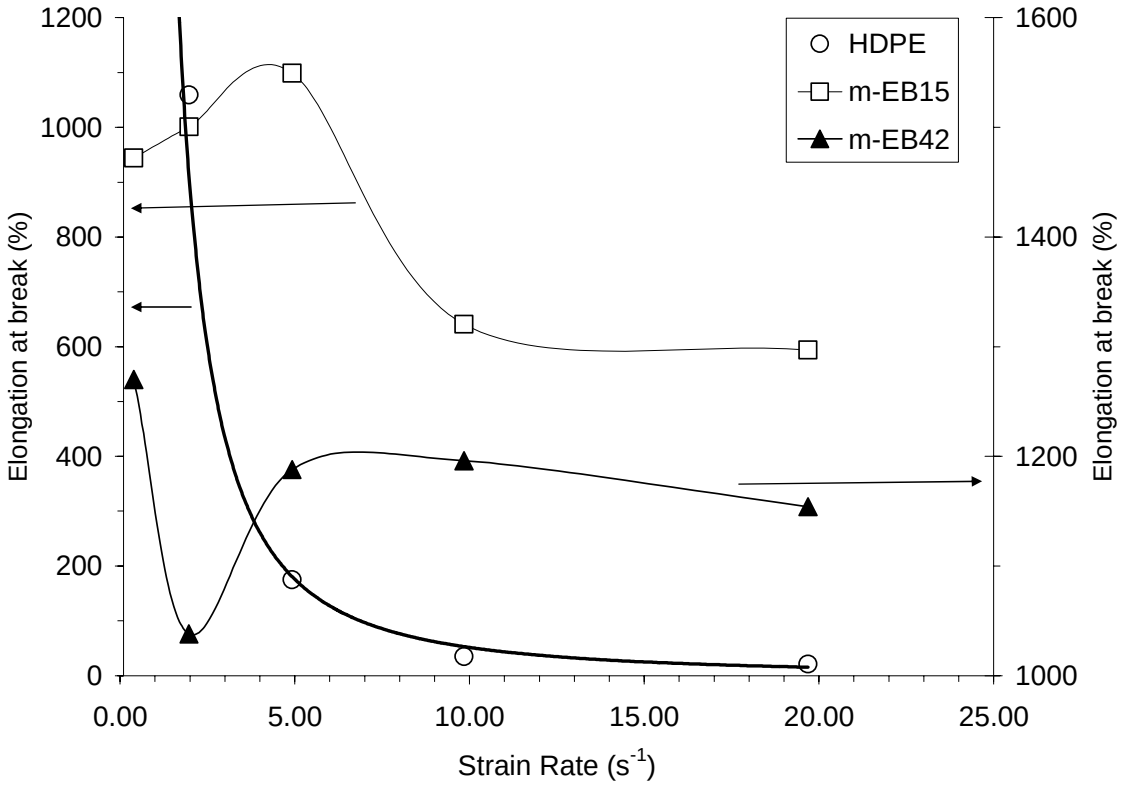

Figure 4.1.12: Elongation at break (%) as a function of crosshead speed and BC.

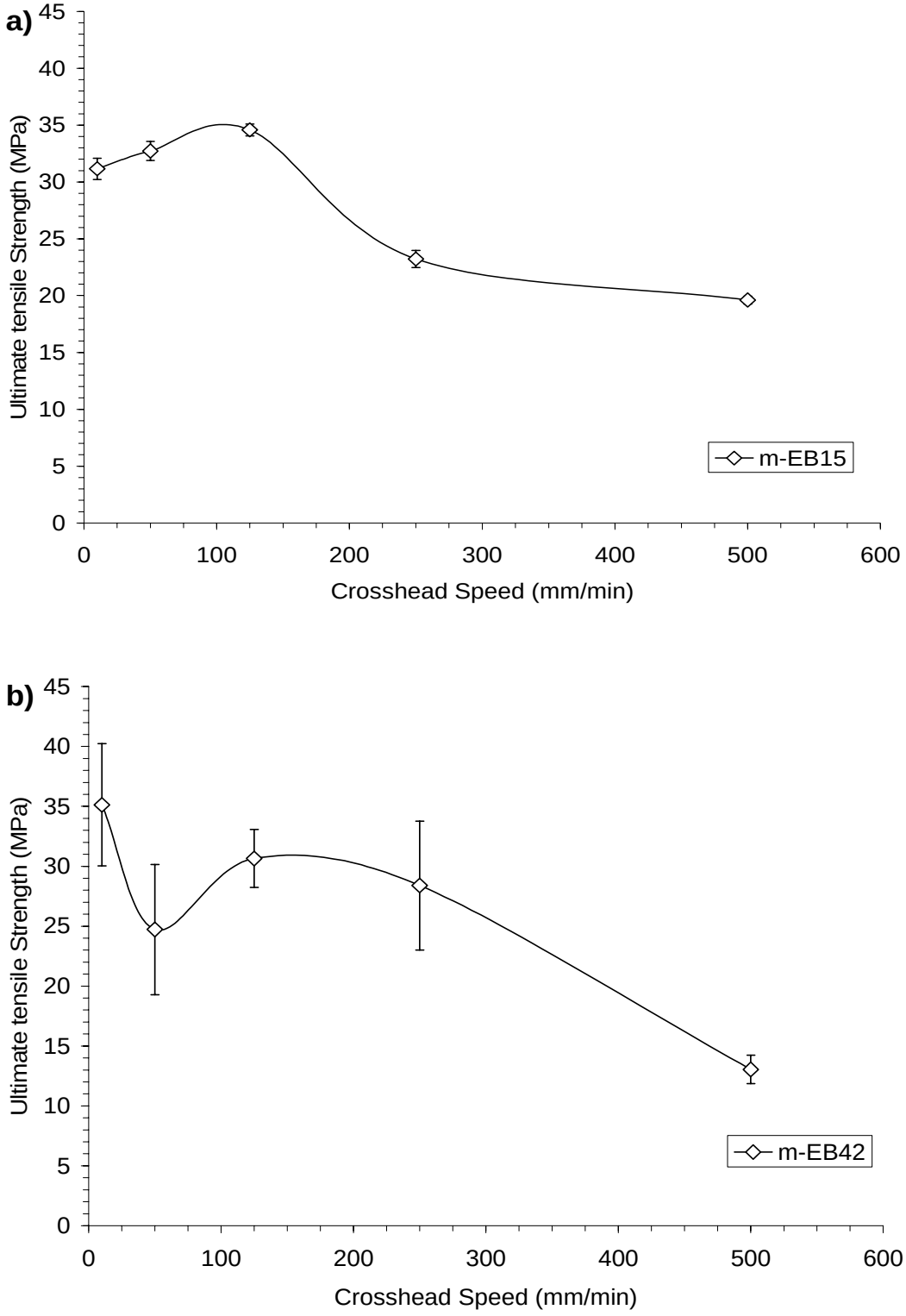

Figure 4.1.13: Tensile Strength (MPa) as function of crosshead speed and BC.

However, at very high strain rates (500mm/min) ultimate properties drop very fast. This may be due to the high amorphous portion in m-EB42 which enhances the possibility of void formation and crazing [25].

Examination of Figures 4.1.11-4.1.13 for the combined influence of strain rate and BC on the mechanical properties shows some interesting observations. The properties obtained at very low (10 mm/min) rates were compared with those measured at very high (500 mm/min) rates. The modulus of linear HDPE showed a decrease of ~30%. However, the modulus of branched m-LLDPEs at 500 mm/min has almost retained the same values obtained at 10 mm/min. Hence, the strain rate had no or little effect on the modulus of m-LLDPEs regardless of their BC. However, it has influenced the modulus of linear HDPE. It is likely that the high strains have lead to immediate destruction of crystals. For large strain properties, such as elongation at break, the influence of strain rate is BC-dependent. The linear HDPE has suffered the highest difference (>500 times) between the low and high rates due to its high crystallinity. On the other hand, the elongation at break of m-EB15 was reduced by ~50% and that of the highly branched m-EB42 was lowered by ~15%. This is likely a result of the rubbery nature of highly branched (more amorphous) m-LLDPEs. The elongation at break at high strain rates (short process time; more solid-like behavior) was lower than that obtained at low rate (long process time; liquid-like behavior). The overall behavior could be explained by a Deborah number effect.

4.1.5. Conclusion

The following conclusions can be drawn from the above discussion:

1. Samples with low BC displayed an increase in melting temperature (T_m) without any significant change in total crystallinity. An increase in T_m and a significant increase in total crystallinity were observed for high BC samples. For high BC samples the peaks were broad and multiple melting peaks were observed.
2. Young's modulus is directly influenced by the BC and a power relationship ($E = 15279BC^{-1.748}$) is obtained. Young's modulus is independent of branch type. ZN-EB13 show higher values compared to m-EB15, due to the contribution of the linear components.
3. Yield stress becomes less distinct and broader with the increase of BC regardless of comonomer type.
4. Ultimate properties of m-LLDPEs have shown weak dependency on BC as well as comonomer type.
5. An interesting phenomenon is observed due to the influence of strain rate. There exists a critical value (near the crosshead speed of 125 mm/min) after which Young's modulus was not much influenced by the crosshead speed. The position of the maximum is independent of BC.
6. Elongation at break of linear HDPE decreased immediately with the increase in strain rate.
7. For low BC m-LLDPE, a maximum value is observed both for elongation at break and ultimate tensile strength at a crosshead speed of 125 mm/min. However, a minimum in elongation at break was obtained for high BC m-LLDPE at a

crosshead speed of 125 mm/min. At low strain rates (<125 mm/min), a wide range of ultimate tensile strength behavior was observed for high BC m-LLDPEs a function of the crosshead speed. However, at higher strain rates ultimate tensile strength of high BC m-LLDPEs drops very fast.

8. Modified Avrami equation can describe and fits very well the stress-induced crystallization. The kinetics of the stress-induced crystallization can be fitted by an order of 1-2 suggesting athermal nucleation.

Acknowledgement

Authors are grateful to King Abdul Aziz City for Science and Technology (KASCT) for providing financial support for this research under research Grant # AT-22-16. Authors also acknowledge the support of KFUPM.

4.1.6. References

[1] Miller BG, Nally GM, Murphy WR. ANTEC 2002, 2415.

[2] Peacock AJ. Handbook of Polyethylene: Structures, Properties, and Applications, 1st Ed., New York: Marcel Dekker, Inc.; 2000. p. 516

[3] Mandelkern L. Polym J 1985; 17:337.

[4] Popli R, Mandelkern L. J Polym Sci, Part B: Polym Phys 1987; 25:441.

[5] Kennedy MA, Peacock AJ, Mandelkern L. Macromolecules 1994; 27: 5297.

[6] Kontou E, Niaounakis M, Spathis G, Eur Polym J 2002 ; 38:2477.

[7] Graham JT, Alamo RG, Mandelkern L. J Polym Sci, Part B: Polym Phys 1997;35:213.

[8] Sacristan J, Benavente R, Perena JM, Perez E, Bello A, Rojas R, Quijada R, Rabagliati FM. J Thermal Analysis and Calorimetry 1999;58: 559.

[9] Jordens K, Wilkes GL, Janzen J, Rohlfing DC, Welch MB. Polymer 2000; 41: 7175.

[10] Li Pi Shan C, Soares JBP, Pendelis A. Polymer 2002; 43: 767.

[11] Simanke AG, Galland GB, Baumhardt NR, Quijada R, Mauler RS. J Appl Polym Sci 1999;74:1194.

[12] Kale L, Plumley T, Patel R, Redwine O, Jain P. J Plas Film and Sheeting 1995;12:27.

[13] Sehanobish K, Patel RM, Croft BA, Chum SP, Kao CI. J Appl Polym Sci 1994;51:887.

[14] Bensason S, Minick J, Moet A, Chum S, Hiltner A, Baer E. J Polym Sci, Part B: Polym Phys 1996;34:1301.

[15] Alamo RG, Viers BD, Mandelkern L. Macromolecules 1993;26:5740.

[16] Alamo R, Domszy R, Mandelkern L. J Phys Chem 1984;88:6587.

[17] Minick J, Moel A, Hiltner A, Baer E, Chum SP. J Appl Polym Sci 1995;58:1371.

[18] Seguela R, Rietsch F. Polymer 1986;27:703.

[19] Xu X, Xu J, Feng L, Chen W. J Appl Polym Sci 2000;77:1709.

[20] Hussein IA. Polym Int 2004;53:1327; Polym. Int., submitted.

[21] Hussein IA, Hameed T. Macromol Mater Eng 2004;289:198.

[22] Peacock AJ, Mandelkern L. J Polym Sci, Part B: Polym Phys 1990;28:1917.

[23] Ward IM, Hadley DW. An Introduction to the Mechanical Properties of Solid Polymers, 3rd Ed., John Wiley & Sons, New York, 2000. p. 237.

[24] Andrew JM, Ward IM. J Mater Sci 1970;5:411.

[25] Liu T, Harrison IR. Polymer 1988 ;29:233.

[26] Dasari A, Duncan SJ, Misra RDK. Mater Sci Tech 2002;18:1227.

[27] Dasari A, Misra RDK. Mater Sci Eng 2003;A358:356.

[28] Van der Wal A, Mulder JJ, Gaymans R.J. Polymer 1998;39:5477.

[29] Termonia Y, Allen SR, Smith P. Macromolecules 1988;21:3485.

[30] Brooks NW, Unwin AP, Duckett RA, Ward IM. J Polym Sci, Part B: Polym Phys 1997;35:545.

[31] Hameed T, Hussein IA. Polymer 2002 ;43:6911.

[32] Mark HF, Bikales NM, Overberger CG, Menges G. Encyclopedia of Polymer Science and Engineering, 2nd Ed., vol 6, John Wiely & Sons; 1986, p. 477.

[33] Sumita M, Miyasaka K, Ishikawa K. J Polym Sci, Part B: Polym Phys 1977;15:837.

[34] Seguela R., Rietsch F. Polymer 1986 ;27:532.

[35] Tanem BS, Stori A. Polymer 2001;42:5389.

[36] Wunderlich B, In: Turi EA, editor. Thermal characterization of Polymeric Materials, vol. 1, New York: Academic Press; 1997, p. 252.

[37] Avrami M. J Chem Phys 1939;7:1103.

[38] Avrami M. J Chem Phys 1940;8:212.

[39] B. Wunderlich, Macromolecular Physics, Vol 2, New York: Academic Press; 1976, p. 147.

[40] Jeziorny A. Polymer 1978;19:1142.

[41] Tobin MC. J Polym Sci, Part B: Polym Phys 1974;12:399.

[42] Juana RD, Jauregui A, Calahora E, Cortazar M. Polymer 1996 ;37:3339.

[43] Herrero CH, Acosta JL. Polymer J 1994;26:786.

[44] Brooks NWJ, Duckett RA, Ward IM. Polymer 1999;40:7367.

[45] Flory PJ, Yoon DY. Nature 1978;272:226.

[46] Lucas JC, Failla MD, Smith FL, Mandelkern L. Polym Eng Sci 1995;35:1117.

[47] Usami T, Gotoh Y, Takayama S. Macromolecules 1986;19:2722.

[48] Freid JR. Polymer Science and Technology, vol 2, New Jersey: Prentice Hall, Inc.; 2003,

4.2. Influence of Branch Content, Comonomer Type and Comonomer Composition Distribution on non-isothermal Crystallization of Metallocene LLDPEs

4.2.1. Abstract

The effect of branch content (BC), comonomer type and comonomer composition distribution on the non-isothermal crystallization kinetics of metallocene LLDPEs was studied. The crystallization kinetics parameters were measured by modulated differential scanning calorimetry. It was found that BC causes a significant change in the crystallization behavior. Crystallization peak temperature shifts to lower region as BC increases. Also, the enthalpy of crystallization decreased as BC increased. The secondary crystallization process strongly influenced the nonisothermal crystallization of all the experimental resins. The Avrami exponent, n, was in the range of 1.5 to 2.5, suggesting a rod-like growth. The comonomer type had almost no effect on the crystallization kinetics. A strong effect of composition distribution was observed on the crystallization peak and the enthalpy of crystallization. However, similar crystallization mechanism was observed for both m-LLDPEs and ZN-LLDPE.

4.2.2. Introduction

Study of polymer crystallization kinetics is significant both from theoretical and practical points of view (Evans, 1945; Ozawa, 1971; Jeziorny, 1978; Hay, 1982; McHugh, 1986; Parasnis, 1999; Jayakannan, 1999; Sajkiewicz, 2001; Qui, 2003). The relationship between structure and properties of polymer requires, among other factors, analysis of melting and crystallization behavior. A number of studies were devoted to the

crystallization of ethylene α-olefin copolymers (Kao, 1986; Phillips, 1986; Nordmeier, 1990; Sutton, 1996; Wagner, 1999; Wagner, 2001).

The microstructure of polymers plays an important role in determining their thermal properties. The influence of molecular weight (M_w), molecular weight distribution (MWD), the branch type, the branch content (BC), and various crystallization conditions on the crystallization of ethylene-α-olefin copolymers were investigated for long time (Mandelkern, 1979; Strobl, 1983; Maderek, 1983; Alamo, 1984; Mandelkern, 1985; Usami, 1986; Alamo, 1989; Fatou, 1990; Alamo, 1993; Shanks, 2000; Zhang, 2001; Rabiej, 2004; Jiao, 2005). Most of the previous studies used ZN-LLDPEs. Due to the random comonomer sequence distribution of conventional LLDPEs, separation of effects of the individual factors on the crystallization is difficult. For example, for a given short chain BC, the super molecular structure becomes more poorly developed with an increase in the content of high Mw species (Mandelkern, 1979). On the other hand, with the increase in BC the lamellae first become shorter, then segmented, and eventually deteriorate into small crystallites (Bensason, 1996). So, previously systematic studies of ethylene copolymers relied primarily on fractions of conventional heterogeneous LLDPEs with respect to short chain branch content and/or Mw (Mandelkern, 1979; Maderek, 1983; Usami, 1986; Voigt-Martin, 1986; Shanks, 2000).

m-LLDPEs are generally believed to have homogeneous composition distribution and a narrow MWD. The lack of high and low Mw tails in these copolymers opens the possibility of more controlled structure of m-LLDPEs. Some studies on the thermal properties and molecular structure of m-LLDPEs were reported by different authors (Bensason, 1996; Keating, 1999; Starck, 1999; Xu, 1999; Janimak, 1999; Razavi-Nouri,

2001; Fu, 2001; Wang, 2001; Zhang, 2001; Chiu, 2002; Starck, 2002; Teng, 2002). Most of the authors focused on the influence of short chain branch distribution (Keating, 1999; Starck, 1999; Xu, 1999; Wang, 2001; Zhang, 2001; Teng, 2002), on melting and crystallization kinetics of a single polymer and its fractions using different fractionation techniques (Fu, 2001; Razavi-Nouri, 2001; Chiu, 2002; Teng, 2002; Starck, 2002). Bensason et al. (1996) classified homogeneous ethylene/1-octene copolymers based on comonomer content and reported the melting phenomena, crystal morphology relating their results to the tensile and dynamic mechanical properties. However, the influence of BC and branch type on the crystallization kinetics of m-LLDPEs is yet to be studied.

Modulated Differential Scanning Calorimetry (MDSC) is a relatively new thermal analysis technique, which applies a sinusoidal temperature oscillation (modulation) on a linear heating/cooling rate in a conventional DSC and makes the total heat flow (such as that from conventional DSC) to be separated into the heat capacity-related (reversible) and kinetic (nonreversible) component (Gill 1993). This makes MDSC a very powerful technique for the separation of exotherms (including crystallization and re-crystallization) from glass transitions, reversible melting or other heat capacity-related events (Reading, 1993; Okazaki, 1997; Janimak, 1999; Yuan, 2000; Höhne, 2001; Qui, 2003).

In the present work, 12 metallocene copolymers of ethylene and 1-butene (m-EB), 1-hexene (m-EH) and 1-octene (m-EO) were used. One metallocene high density polyethylene (m-HDPE), one Ziegler-Natta HDPE (ZN-HDPE) and one Ziegler-Natta ethylene 1-butene copolymer (ZN-EB) were selected for comparison purposes. The objective was to study the relationship between BC and comonomer type and the non-isothermal crystallization kinetics of m-LLDPEs by using MDSC. All of the resins had

similar Mw and MWD and BC ranges from 0-42 branches/1000C. ZN-EB of the same average BC and M_w as m-EB were used to examine the influence of comonomer composition distribution on the kinetics of nonisothermal crystallization.

4.2.3. Experimental

Materials and Sample Preparation

Twelve commercial samples of m-LLDPEs, one ZN-LLDPE, one conventional high density polyethylene (ZN-HDPE) and one metallocene HDPE (m-HDPE) were used in this study. The types of m-LLDPEs are as follows: four 1-butene, six 1-hexene and two 1-octene ethylene copolymers. Ziegler-Natta 1-butene ethylene copolymer was selected for comparison purposes. Both ZN-HDPE and m-HDPE were used as reference. Weight average molecular weights (M_w) of all LLDPEs (Both metallocene and ZN) are close to 100 kg/mol and the MWD of m-LLDPEs is ≅ 2. Table 4.2.1 provides selected properties of the experimental LLDPEs. Density values were provided by ExxonMobil. In addition, information about M_w and BC was determined (see Table 4.2.1) by gel permeation chromatography (GPC) and ^{13}C NMR, respectively. Details about the GPC and NMR characterizations were given in a previous publication (Hameed 2002). Resins were named according to their branch type and content. For example, a metallocene ethylene-butene copolymer with a BC of 18.5 CH_3/1000C is named as m-EB19.

Modulated Differential Scanning Calorimetry (MDSC)

Instrumentation: MDSC measurements were performed in a TA Q1000 instrument equipped with a liquid nitrogen cooling system (LNCS). Nitrogen gas (purity 99.99%) was used as a purge gas and the flow rate was 50 ml/min. Samples of 7.5-9.8 mg were sliced and then compressed into non-hermetic aluminum pans. To minimize the thermal

lag between the sample and pan, samples with flat surface were used. An empty aluminium pan was used as reference. Previous thermal effects were removed by heating the samples to 140^{o}C and holding at this temperature for 5 minutes. It was reported that PEs, at these density ranges, are partially melted at room temperature. So, it is necessary to choose subambient temperatures for complete evaluation of crystallization (Shanks 2000). The samples were cooled from 140 ^{o}C to 5 ^{o}C at a rate of 2^{o}C/min. Standard modulation conditions of oscillation period of 40 seconds and amplitude of 0.2^{o}C were used. First, the baseline was calibrated using empty crimped aluminum pans, and the melting temperature and heat of fusion was calibrated using a high purity Indium standard (156.6^{o}C and 28.45 J/g). A sapphire disc was also used to check heat capacity measurement in the range of interest. Calculations of absolute crystallinity were based on a heat of fusion of 290 J/g for a polyethylene crystal (Mark 1986). Another set of experiments were performed on m-HDPE, HDPE, m-EB15 and ZN-EB13. Conventional DSC program was used at a rate of 5, 10 and 20 ^{o}C/ min to investigate the influence of cooling rate on the crystallization.

Data analysis: Two approaches are presently available for data analysis. The first is the reversing and non-reversing heat capacity approach (Gill 1993); the second is the complex heat capacity, which can be separated into in-phase and out of phase signals using the phase angle (Schawe 1995). However, the problem associated with complex heat capacity approach is the lack of interpretation of the out of phase component that is significantly influenced by the phase angle and thereby by heat transfer effects (Righetti 1999). So, in this work the results are presented and discussed using reversing and non-reversing curves. Figure 4.2.1 is a typical MDSC thermogram of sample m-EB15

Table 4.2.1: Selected properties of the experimental LLDPEs.

Resin	Density, g/cm^3	$M_{w,}$ kg/mol	M_w/M_n	BC *
m-HDPE	N/A	122	2.34	0.0
ZN-HDPE	0.961	102	6.7	0.0
m-EB15	0.910	108	1.95	14.50
m-EB19	0.900	110	1.78	18.50
m-EB37	0.888	87	2.10	36.62
m-EB42	0.880	126	1.81	42.00
ZN-EB13	0.918	118	3.07	13.20
m-EH12	0.918	94	1.40	12.02
m-EH15	0.912	102	2.14	14.50
m-EH18	0.900	108	1.83	18.02
m-EH20	0.902	95	2.06	19.74
m-EH24	0.895	92	1.85	23.60
m-EH32	0.883	97	2.02	32.17
m-EO16	0.902	90	2.04	16.32
m-EO33	0.882	95	1.99	32.67

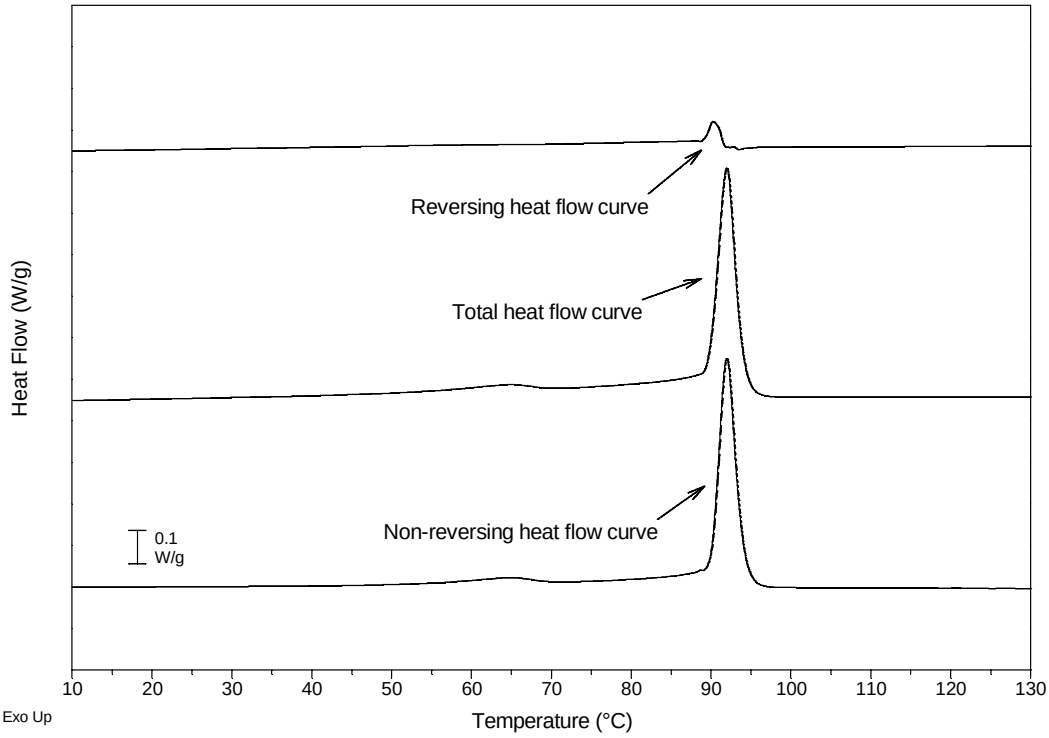

Figure 4.2.1: MDSC thermograms of m-EB15, the three curves from top to the bottom are reversing hear flow, total heat flow and non-reversing heat flow, respectively.

showing total (middle curve), reversing (top curve) and non-reversing (bottom curve) heat flow curves. Kinetics data were collected from the non-reversing curve and were processed using Universal analysis software provided by TA Instruments, Inc.

Theoretical Background

Several analytical methods were developed to describe the nonisothermal crystallization kinetics of polymers: (1) the modified Avrami analysis (Jeziorny, 1978; Tobin, 1974; Rychly, 1993; Herrero, 1994); (2) the Ozawa analysis (Ozawa, 1971); (3) Ziabicki analysis (Ziabicki, 1974; Ziabicki, 1967); and others (Liu, 1997; Caze, 1997; Nakamura, 1973; Chan, 1994). In this article, the modified Avrami analysis (Jeziorny, 1978) is used to describe the nonisothermal crystallization kinetics of m-LLDPEs since other approaches require collection of data at different cooling rates.

The well known Avrami equation is defined as follows [Avrami, 1939; 1940; 1941]:

$$1 - X_t = \exp(-k_t t^n) \tag{4.2.1}$$

where n is the Avrami crystallization exponent dependent on the nucleation mechanism and growth dimension, t is the time taken during the crystallization process, k_t is the growth rate constant, which is dependent on nucleation and crystal growth and X_t is relative crystallinity of polymers (Wunderlich, 1976). Relative crystallinity, X_t is defined as follows:

$$X_t = \frac{\int_{t_o}^{t} (dH_c / dt)dt}{\int_{t_o}^{t_\infty} (dH_c / dt)dt} \tag{4.2.2}$$

where dH_c/dt is the rate of heat evolution and t_o and t_∞ are the times at which crystallization starts and ends, respectively. Equation (1) was further modified to describe

non-isothermal crystallization (Jeziorny, 1978; Tobin, 1974). For non-isothermal crystallization at a chosen cooling rate, relative crystallinity is a function of the crystallization temperature (T). That is, Equation. 2 can be formulated as:

$$X_T = \frac{\int_{T_o}^{T_c} (dH_c / dT) dT}{\int_{T_o}^{T_\infty} (dH_c / dT) dT} \tag{4.2.3}$$

where T_o denotes the initial crystallization temperature and T_c and T_∞ represent the crystallization temperature at time t and after the completion of the crystallization process, respectively. Crystallization time, t, can be converted from crystallization temperature, T_c, with the well known relationship for nonisothermal crystallization processes that is strictly valid when the sample experiences the same thermal history by the following equation (Ziabicki, 1967; Jeziorny, 1978).

$$t = \frac{T_o - T}{R} \tag{4.2.4}$$

where R is the cooling rate (^oC/min). Using Equation. (1) in double-logarithmic form

$$\ln[-\ln[1 - X_t]] = \ln k_t + n \ln t \tag{4.2.5}$$

and plotting ln[-ln[1-X_t]] versus lnt, a straight line is obtained. From the slope and intercept of the lines, one can determine the Avrami exponent n and the crystallization rate k_t. Although the physical meanings of k_t and n cannot be related to the nonisothermal case in a simple way, their use provides further insight into the kinetics of nonisothermal crystallization. Because the rate of nonisothermal crystallization depends on the cooling rate, the crystallization rate constant, k_t, can be properly corrected to obtain the corresponding rate constant at a unit cooling rate, k_R [Jeziorny 1978]:

$$\ln k_R = \ln k_t \ / R \tag{4.2.6}$$

4.2.4. Results and Discussion

Nonisothermal Crystallization Kinetics

Figures 4.2.2, 4.2.3, 4.2.4 and 4.2.5 are the MDSC nonreversing curves (crystallization exotherm) for EB, EH and EO LLDPEs and HDPEs, respectively. These crystallization exotherms are quite similar in appearance. Table 4.2.2 lists the initial crystallization temperature, T_o, which is the temperature at the crossing point of the tangents of the baseline and the higher temperature side of the exotherm, the peak temperature (T_p), the enthalpy of crystallization (ΔH_c) and absolute crystallinity of nonisothermal crystallization of all the resins. T_o and T_p both show a strong shift to lower temperature region as BC increases, indicating that BC influences the crystallization of LLDPEs. This phenomenon is observed for all of the three comonomer types. Having similar M_w and BC ZN-EB13 has shown high crystallization temperature than m-EB15. A decrease in the crystallization enthalpy with increasing BC is also observed.

From the crystallization exotherm, raw data for the relative crystallinity as a function of temperature can be calculated using Equation 4.2.3. A plot of relative crystallinity (X_T, relative crystallinity calculated based on temperature) versus temperature is shown in Figure 4.2.6. Figure 4.2.6(a) and 4.2.6(b) represent EB and EH LLDPE, respectively. EO-LLDPE along with ZN-HDPE and m-HDPE are shown in Figure 4.2.6(c). All of the curves exhibit a common sigmoid like shape. This indicates that the principal nonisothermal crystallization goes through two crystallization processes. After the maximum in the heat flow curves (see Figures 4.2.2, 4.2.3, 4.2.4 and 4.2.5) has passed, a large fraction of crystallinity develops by slower, secondary kinetic process. In Figure 4.2.6(b) sample m-EH20 did not show the same sharp increase

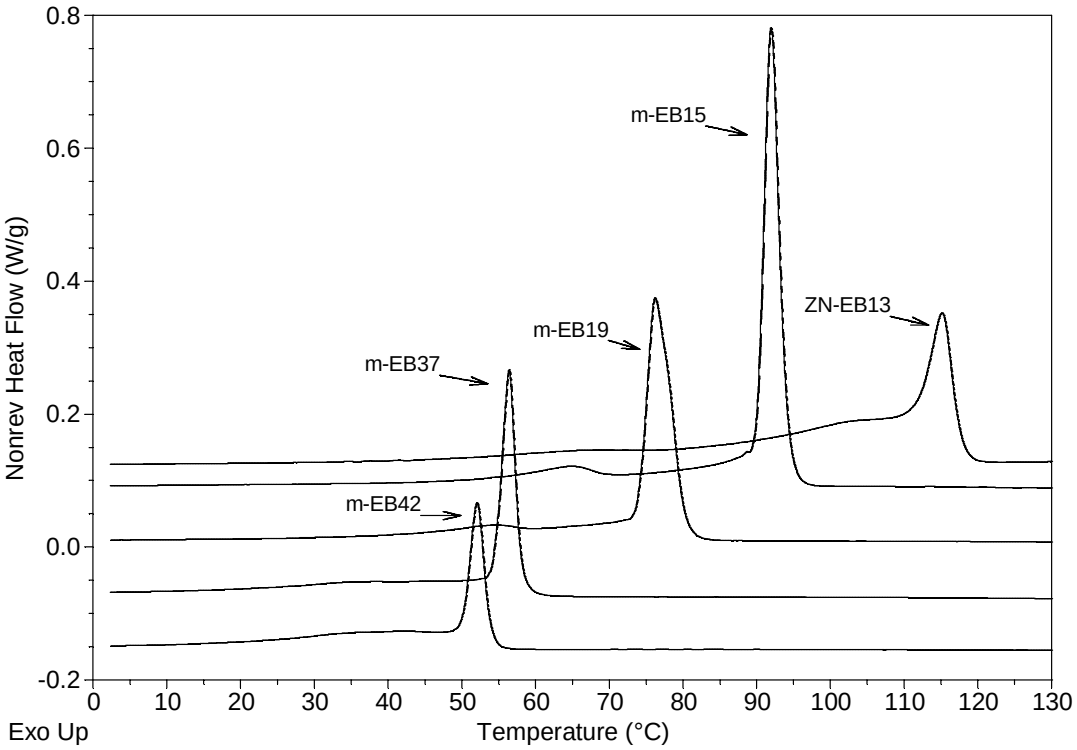

Figure 4.2.2: MDSC crystallization exotherms of EB m-LLDPEs and ZN-LLDPE.

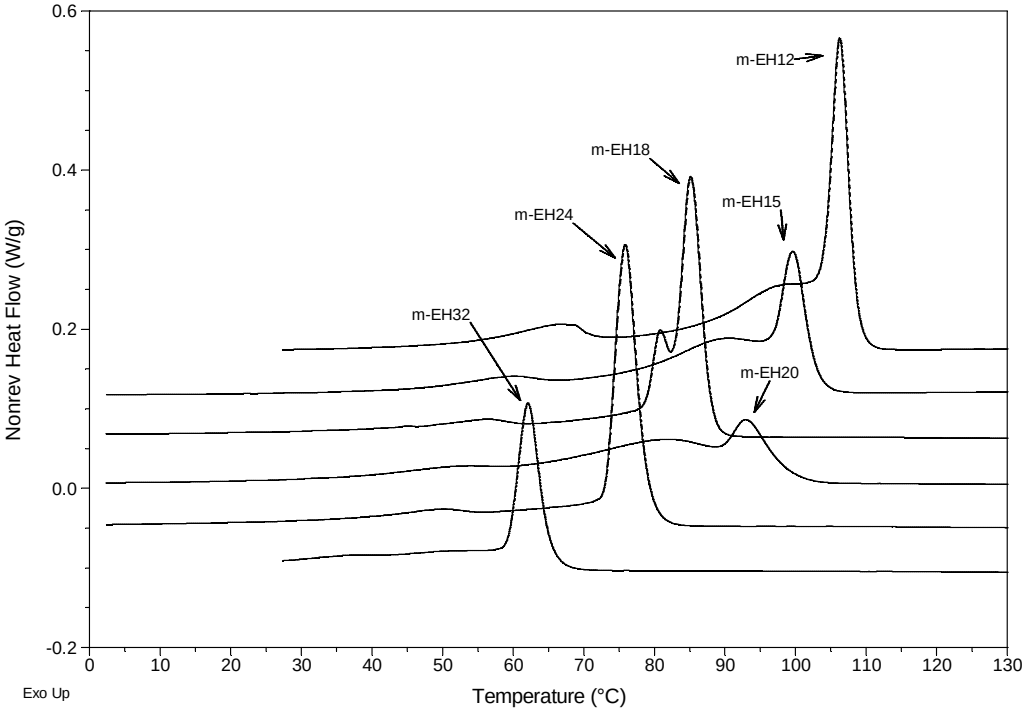

Figure 4.2.3: MDSC crystallization exotherms of EH m-LLDPEs.

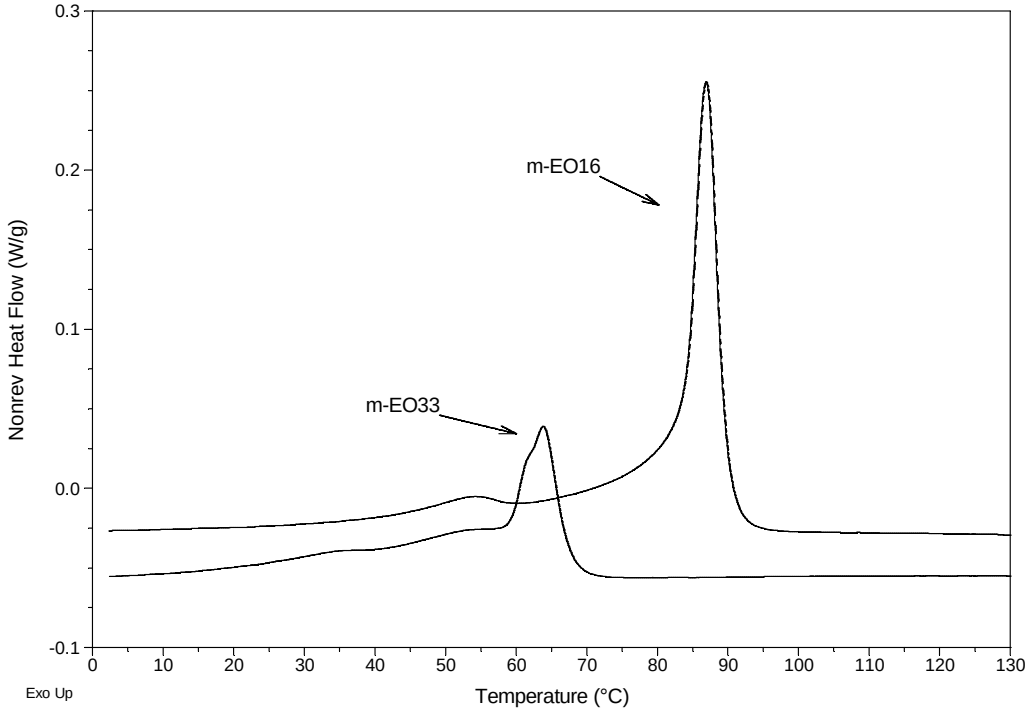

Figure 4.2.4: MDSC crystallization exotherms of EO m-LLDPEs.

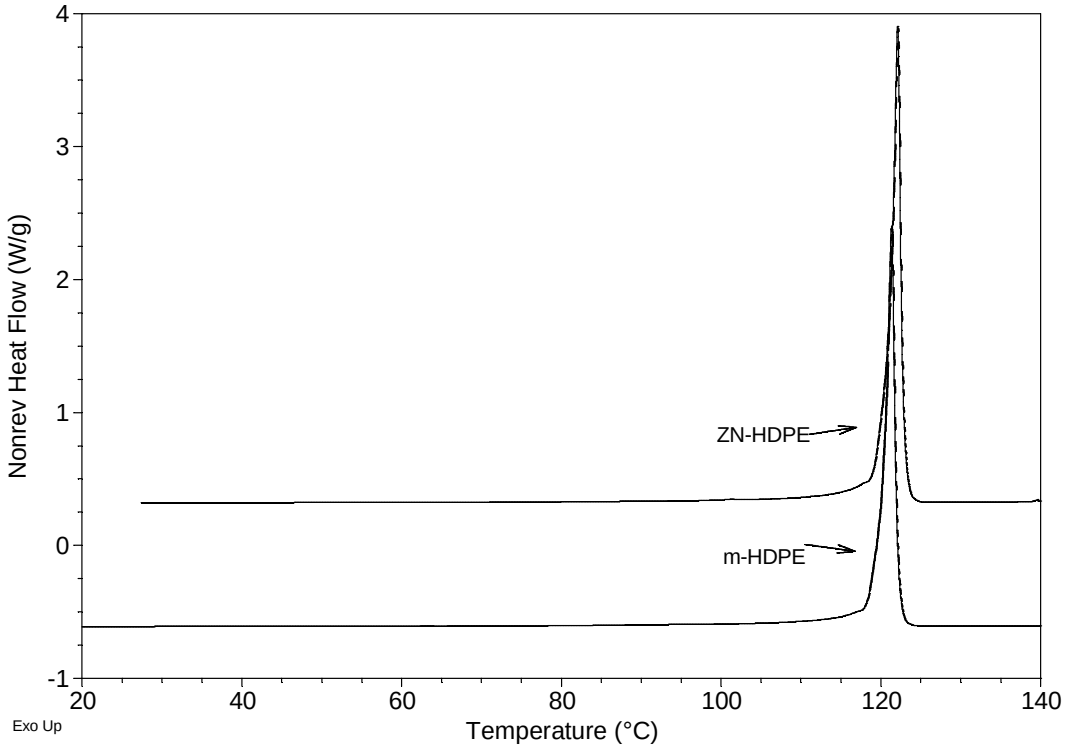

Figure 4.2.5: MDSC crystallization exotherms of m-HDPE and ZN-HDPE.

Table 4.2.2: Thermodynamic Properties of Ethylene/α-Olefins Copolymers.

Resin	To (^{o}C)	Tp (^{o}C)	ΔHc (J/g)	Crystallinity (%)
ZN-HDPE	122.79	122.11	239.3	82.52
m-HDPE	122.05	121.34	198.6	68.48
m-EB15	94.04	91.93	86.51	29.83
m-EB19	80.22	76.22	65.25	22.5
m-EB37	58.06	56.40	43.78	15.10
m-EB42	53.88	52.04	36.19	12.48
ZN-EB13	117.77	115.16	89.83	30.98
m-EH12	108.70	106.26	99.33	34.25
m-EH15	102.95	99.56	74.12	25.56
m-EH18	87.95	85.09	69.83	24.08
m-EH20	99.43	92.95	66.78	23.03
m-EH24	78.93	75.82	63.66	21.95
m-EH32	64.95	61.86	45.23	15.60
m-EO16	89.86	86.88	71.48	24.65
m-EO33	67.62	63.80	40.38	13.92

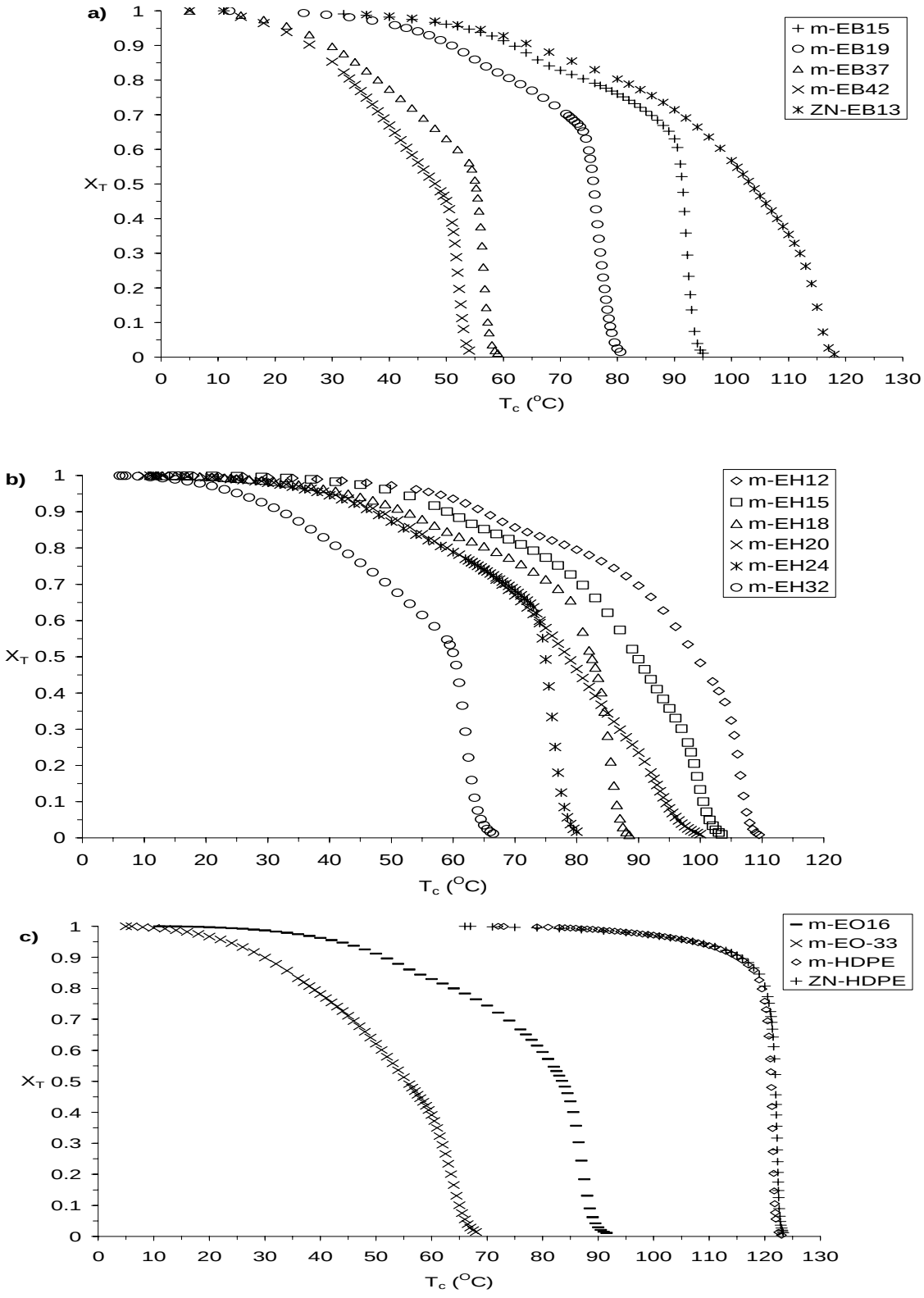

Figure 4.2.6: Relative crystallinity as a function of crystallization temperature for EB, EH, and EO LLDPE, ZN-HDPE and m-HDPE.

observed in other resins. The crystallization process was more gradual and the onset of crystallization was closer to that of m-EH15. The exotherm of m-EH20 in Figure 4.2.3 also showed a broad distribution. This anomalous behavior of m-EH20 was further investigated using Crystaf technique. In general, each sample first shows a dominant sharp exothermic peak, followed by a shallow tail at lower temperatures. This result confirms the previous report (Fu 2001) that metallocene short chain branched PEs possess both inter- and intramolecular heterogeneity.

Once X_T is obtained from Equation 4.2.3, its conversion into X_t (relative crystallinity based on time) can be carried out by transforming the temperature axis to the time axis using Equation 4.2.4, as shown in Figure 4.2.7. An 'S' shaped curve was expected which is consistent for a nucleation and growth process. But in the present work due to involvement of two consequent crystallization process with a large portion of secondary crystallization mechanism, the curve was not a uniform 'S' shaped curve. From these curves, the half-life of crystallization, $t_{1/2}$, can be directly determined as the time elapsed from the onset of crystallization to the point where the crystallization is half completed. All the $t_{1/2}$ values are summarized in Table 4.2.3.

Figures 4.2.8, 4.2.9 and 4.2.10 are the plots of ln(-ln(1-Xc)) versus lnt for EB, EH and EO LLDPEs and HDPE, respectively. Notice here that in the fitting, only the relative crystallinity data in the range 5-95% were used. From these plots it was found that almost all of the curves are divided into two linear parts, which means that there exist two crystallization processes. Similar observation was reported by Jiao et al. (2005) (see Figure 6a of ref Jiao 2005) for LLDPE. Janimak and stevens (1999) have shown similar curve in the Avrami plot (see Figure 5 of Janimak) for m-LLDPE. A line of best fit was

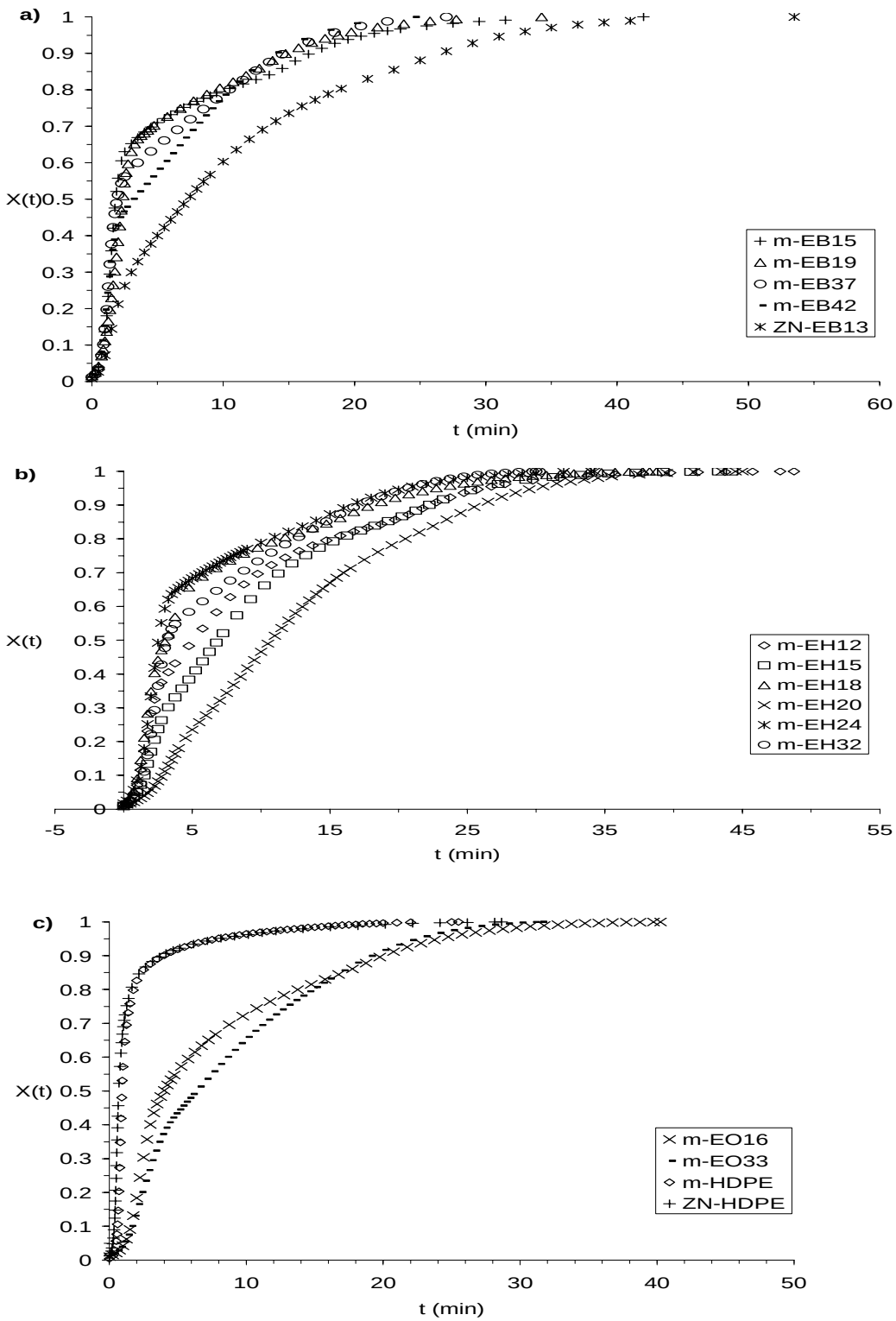

Figure 4.2.7: Relative crystallinity as a function of crystallization time for EB, EH, and EO LLDPE, ZN-HDPE and m-HDPE.

Table 4.2.3: Avrami parameters for Ethylene/α-Olefins copolymers

Resin	Primary crystallization stage				Secondary crystallization stage				Half-life, $t_{1/2}$, (min^{-1})
	n1	k_t1	k_R1	R^2	n2	k_t2	k_R2	R^2	
ZN-HDPE	2.70	1.781	1.334	0.989	0.47	1.206	1.098	0.978	0.69
m-HDPE	3.87	0.879	0.937	0.984	0.46	1.194	1.093	0.977	0.92
m-EB15	2.41	0.156	0.395	0.991	0.42	0.630	0.794	0.954	1.82
m-EB19	2.02	0.119	0.346	0.998	0.49	0.572	0.756	0.969	2.38
m-EB37	2.52	0.158	0.398	0.991	0.53	0.473	0.688	0.958	1.94
m-EB42	1.69	0.272	0.521	0.999	0.66	0.339	0.583	0.946	3
ZN-EB13	1.55	0.078	0.279	0.990	0.89	0.123	0.351	0.995	7.5
m-EH12	2.09	0.077	0.278	0.994	0.8	0.194	0.44	0.987	5.08
m-EH15	1.85	0.05	0.225	0.999	1	0.103	0.322	0.996	6.87
m-EH18	2.02	0.1	0.317	0.996	0.67	0.332	0.576	0.982	3.06
m-EH20	1.39	0.026	0.161	0.998					10.71
m-EH24	2.09	0.093	0.306	0.993	0.56	0.461	0.679	0.952	2.53
m-EH32	2.35	0.049	0.222	0.995	0.76	0.258	0.508	0.958	3.17
m-EO16	2.36	0.039	0.199	0.996	0.76	0.235	0.485	0.988	4
m-EO33	1.65	0.056	0.237	0.997	1.02	0.110	0.332	0.985	6.2

n = nucleation Index;

k_t = Crystallization rate constant;

k_R = Corrected crystallization rate constant for a specific cooling rate;

R = Coefficient of determination;

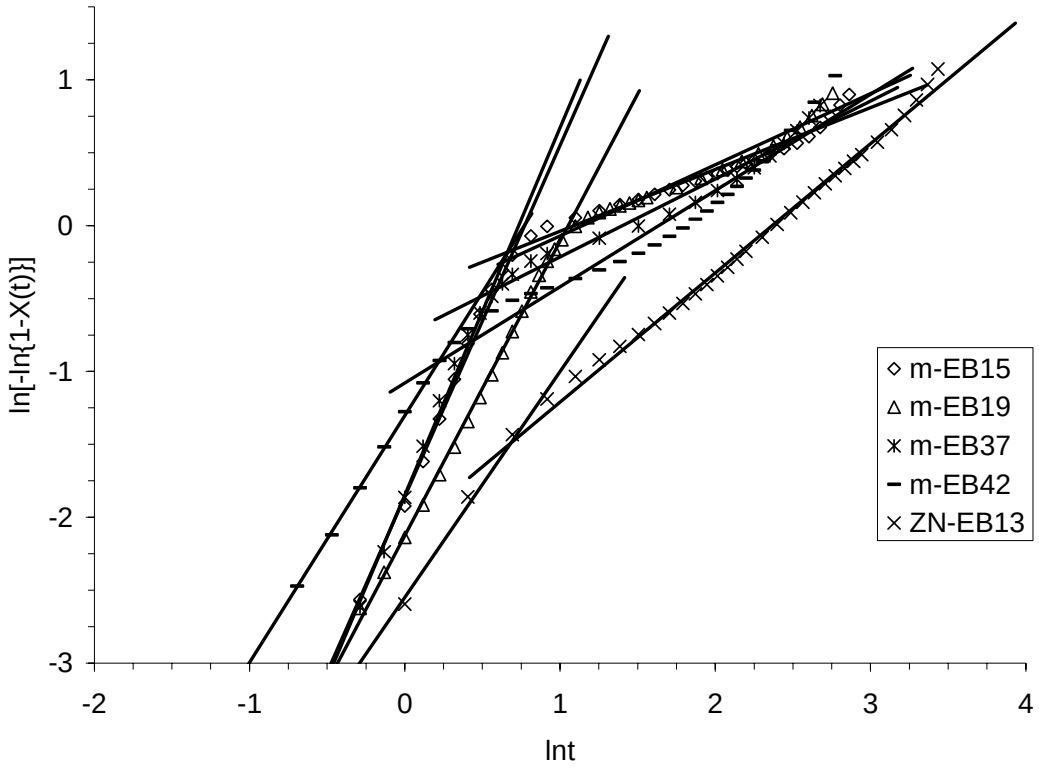

Figure 4.2.8: Avrami plots for the nonisothermal crystallization of EB LLDPEs.

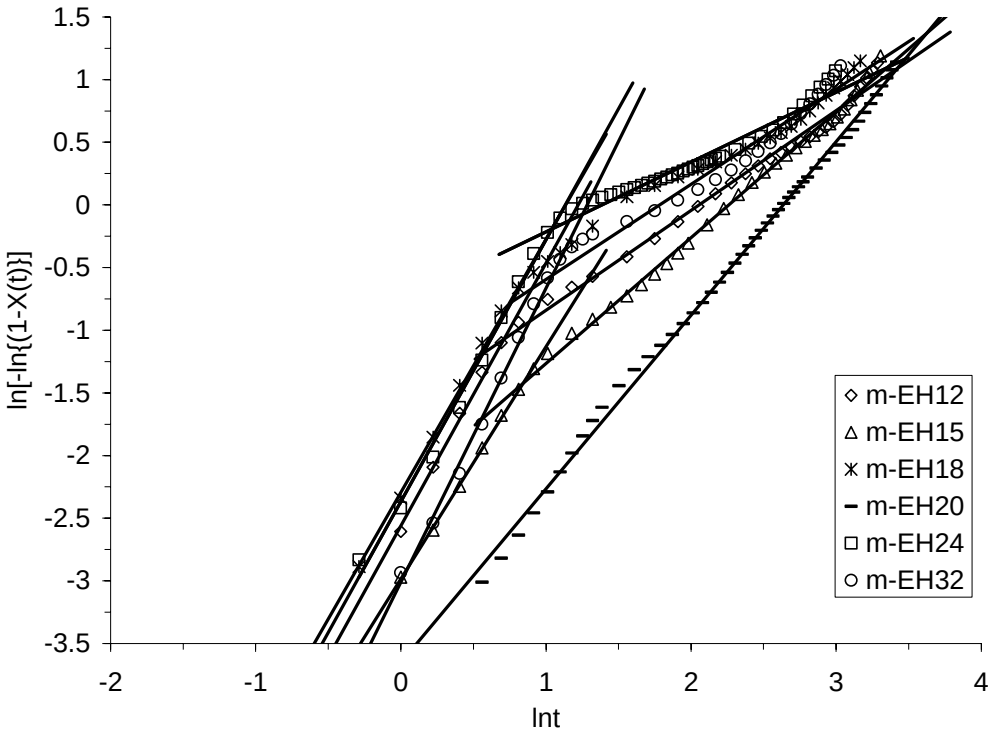

Figure 4.2.9: Avrami plots for the nonisothermal crystallization of EH LLDPEs

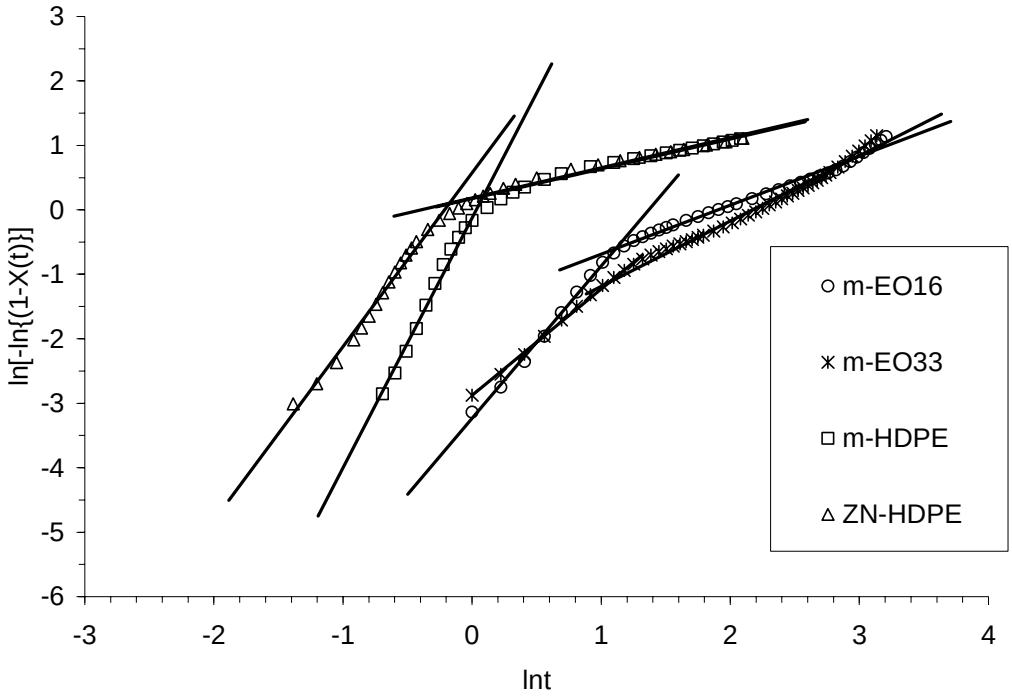

Figure 4.2.10: Avrami plots for the nonisothermal crystallization of EO LLDPEs, ZN-HDPE and m-HDPE.

presented using the least square method. It is more realistic to divide the curve into two portions and fit the data rather than poorly fit the whole data with one line. In these plots, two straight lines were observed for every BC ($R^2 > 0.98$). The Avrami parameters, n and k obtained from the slope and the intercept of the Avrami plots are summarized in Table 4.2.3. For primary crystallization process, n values were in the range of 1.7-2.5, 1.4-2.4, and 1.6-2.4 for EB, EH and EO m-LLDPE, respectively. For ZN-EB13, ZN-HDPE and m-HDPE, n values were 1.55, 2.7, and 3.87, respectively. It has been reported in the literature that linear polyethylene exhibits spherulitic growth with the n values in the range of 3-4 (Buchdahl, 1959), while branched polyethylene has rod like growth with n values between 1 and 2 (Mandrek, 1983). In the secondary crystallization process n values fall in the range of 0.4-0.7, 0.5-1.0 and 0.75-1.0 for EB, EH and EO LLDPE, respectively. For ZN-EB13, ZN-HDPE and m-HDPE, n values were 0.89, 0.47 and 0.46, respectively. The value of n is usually an integer between 1 and 4 for different crystallization mechanisms and it is a fraction due to the secondary crystallization (Chen 2004). Wunderlich (1976) suggested that the mechanism of secondary crystallization is either a crystal perfection process or a crystal thickness growth. But this was opposed by Strobl et al (1983). They suggested that BC hinder longitudinal chain diffusion through the crystals, thus suppresses crystal thickness growth. So, a very slow further lateral extension of lamellae was suggested to occur during secondary crystallization. Storbi et al. (1983) observations were confirmed by SAXS experiments.

For further investigation of the branch distribution crystaf technique was used. The results were summarized in Table 4.2.4. It was observed that resins having BC higher than 30 did not precipitate at room temperature regardless of branch types. Figure

4.2.11 shows the results for resins with similar BC. A broad branch distribution was observed for ZN-EB13. m-EH15 as well as other m-EHs (m-EH20 and m-EH24) displayed a wide distribution as given in Figure 4.2.12. Figure 4.2.13 showed the behavior of resins having same branch type of butene but different BC and different composition distribution. The peak temperature shifted to lower temperature region with the increase of BC (Figure 4.2.12 and 4.2.13). It was also noticed from Figure 4.2.11 that the peak temperature shifted to a lower temperature region as branch type changes from butene to octene.

The effect of cooling rates on the nonisothermal crystallization was also investigated in this study. Four resins were selected for this purpose. m-EB15 and ZN- EB13 were chosen to examine the influence of composition distribution at medium BC on nonisothermal crystallization kinetics. ZN-HDPE and m-HDPE were taken to investigate the molecular weight distribution.

Figure 4.2.14 and 4.2.15 are the nonisothermal crystallization exotherms for m-EB15 and ZN-EB13 and m-HDPE and ZN-HDPE at different cooling rates. It is clear from both figures that the peak crystallization temperature shifts to lower temperature regions as the cooling rate increased. Using Equation 4.2.5 Avrami exponent, n, and crystallization rate constant, k_R were calculated from Figures 4.2.16 and 4.2.17 and were listed in Table 4.2.5.

Table 4.2.4: Crystaf analysis of some selected resins

Resin	Soluble Fraction (SF)	Standard Deviation (σ)	Peak Temperature (^{O}C)	Short Chain Branching Distribution Index (SDBI)
m-EB15	0.1	3.6	57.3	7.2
m-EB19	1.7	3.9	43.0	8.1
m-EB37	97.6	-	-	-
ZN-EB13	9.3	15.1	79.6, 67.7	18.8
m-EH15	1.8	8.7	51.3	12.3
m-EH20	13.3	8.4	41.5	14.1
m-EH24	6.2	6.1	40.7	11.7
m-EH32	94.5	-	-	-
m-EO16	2.2	3.9	46.1	7.9
m-EO33	96.9	-	-	-

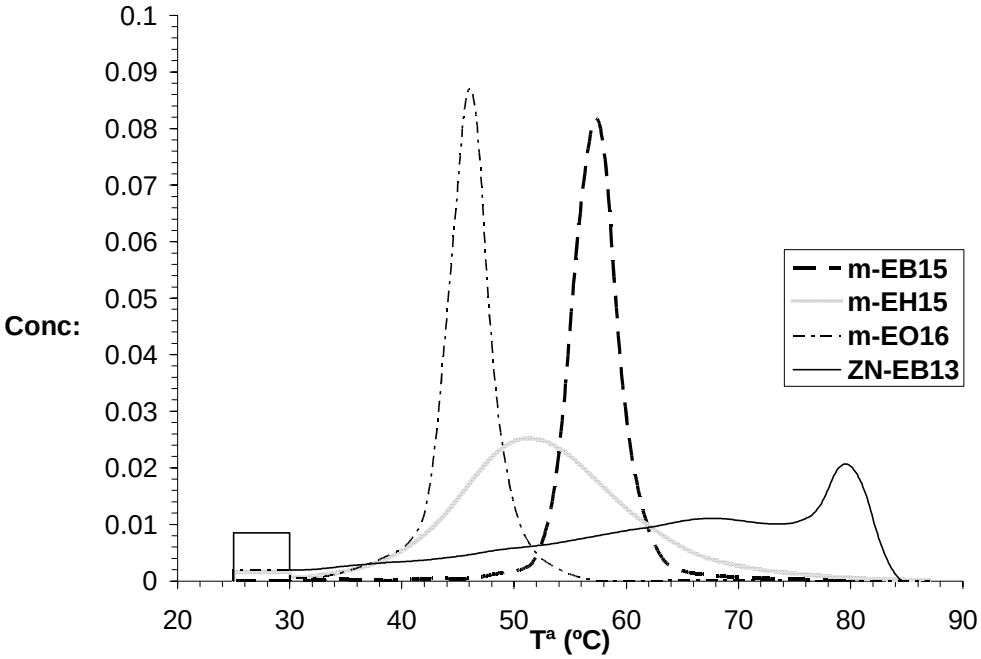

Figure 4.2.11: Resin concentrations as a function of branch type and composition distribution.

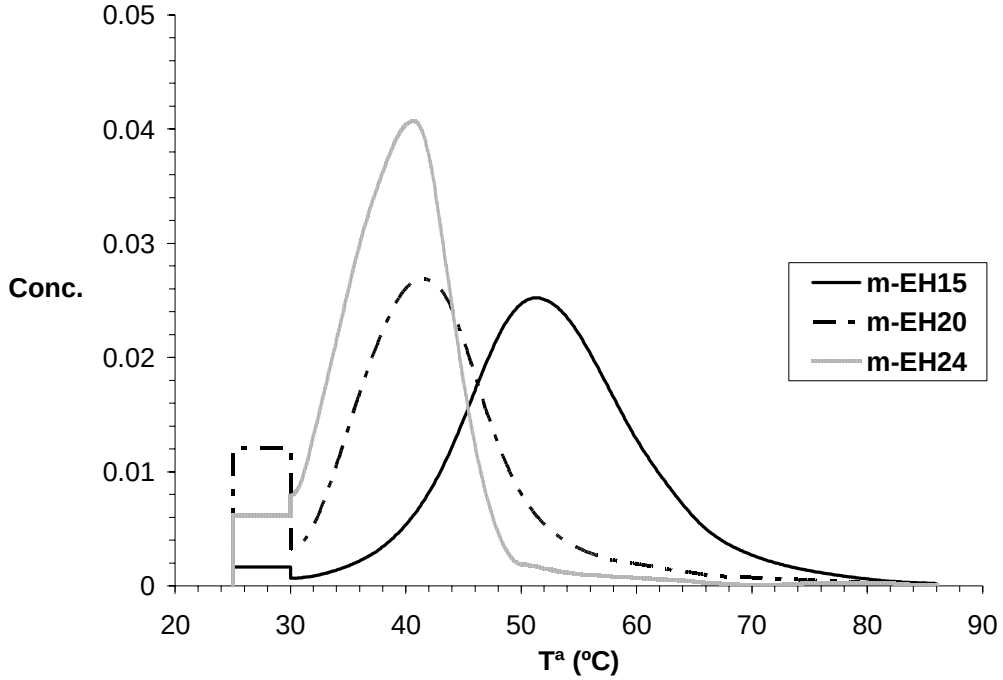

Figure 4.2.12: Concentration of EH-LLDPE as a function of BC.

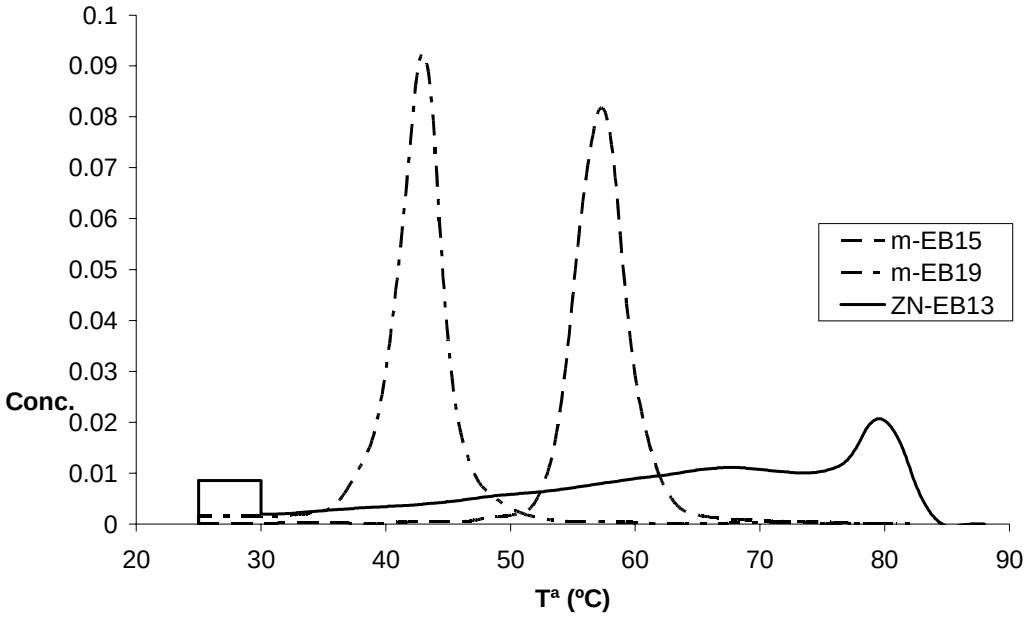

Figure 4.2.13: Concentration of EB-LLDPE as a function of BC and composition distribution.

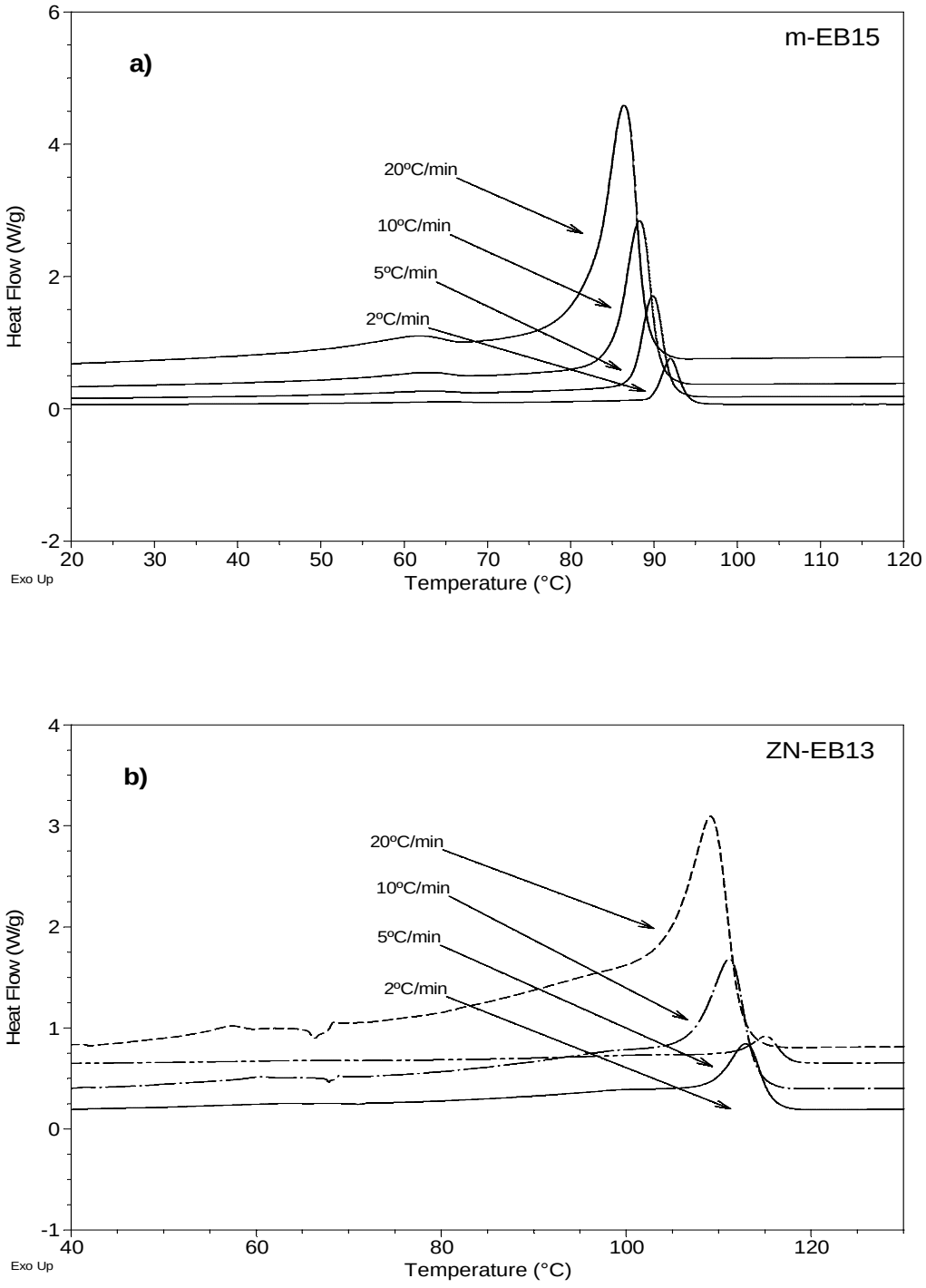

Figure 4.2.14: Conventional DSC crystallization exotherms of a) m-EB15 and b) ZN-EB13.

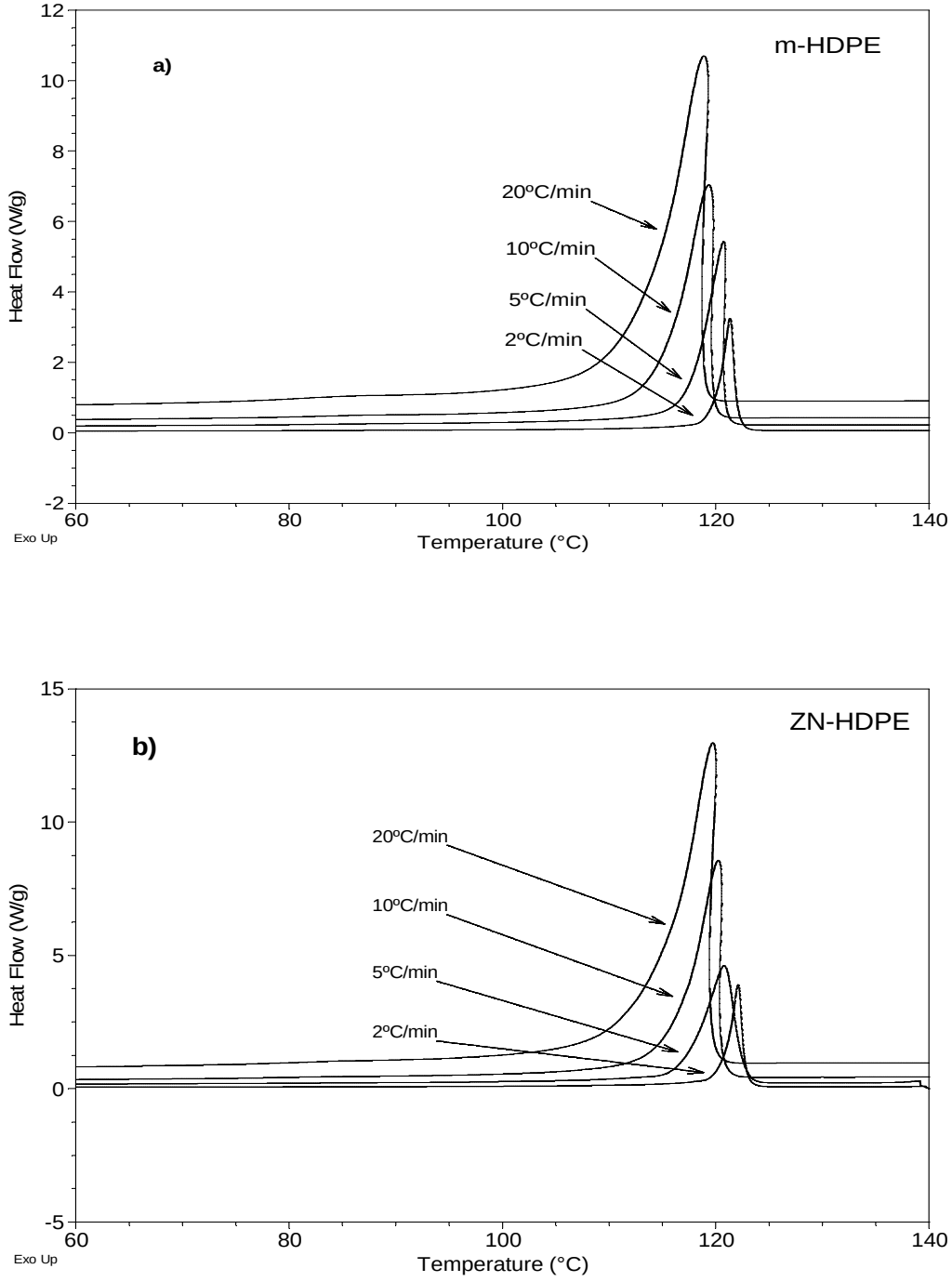

Figure 4.2.15: Conventional DSC crystallization exotherms of a) m-HDPE and b) ZN-HDPE.

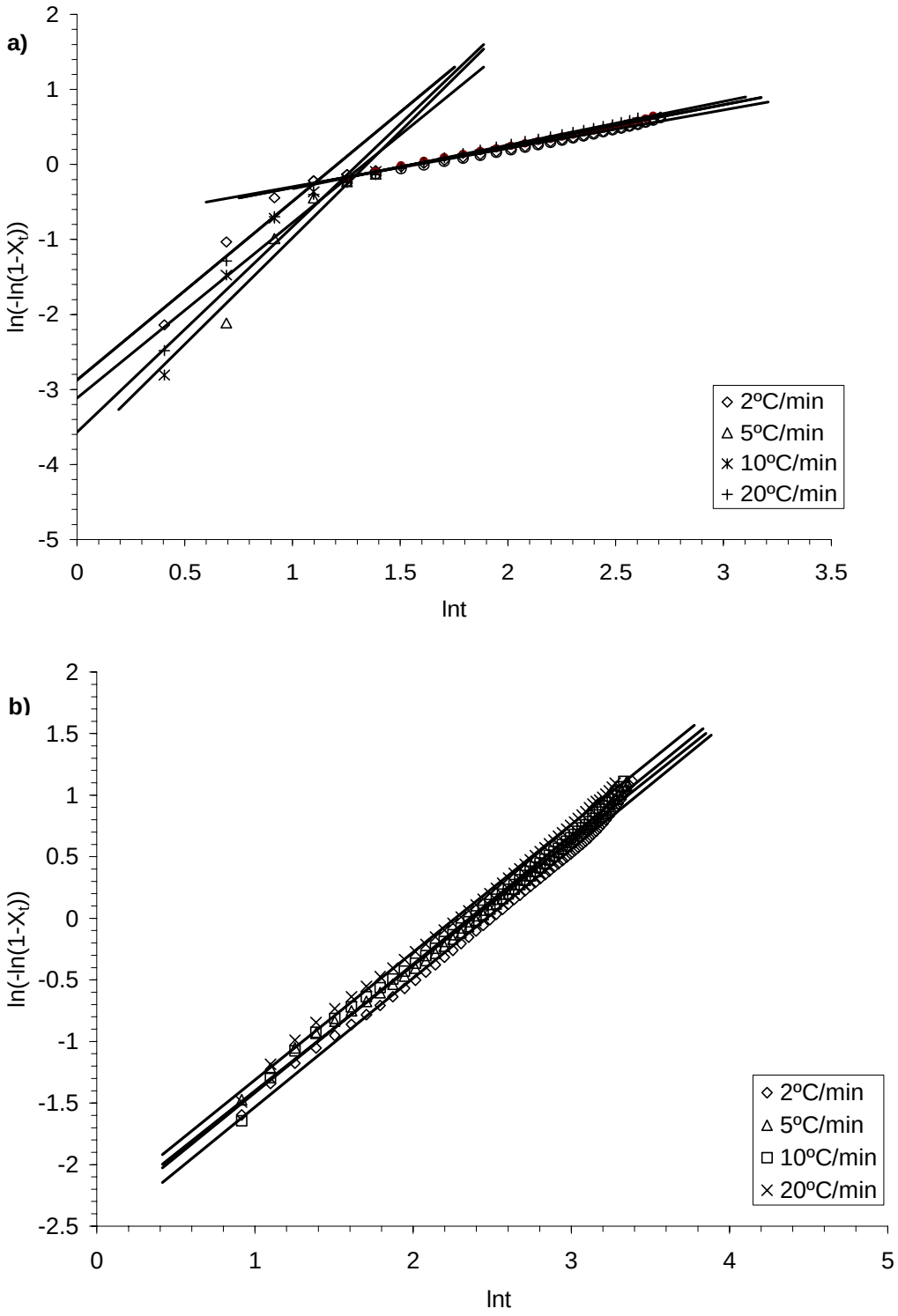

Figure 4.2.16: Avrami plots for the nonisothermal crystallization of a) m-EB15 and b) ZN-EB13 at different cooling rates.

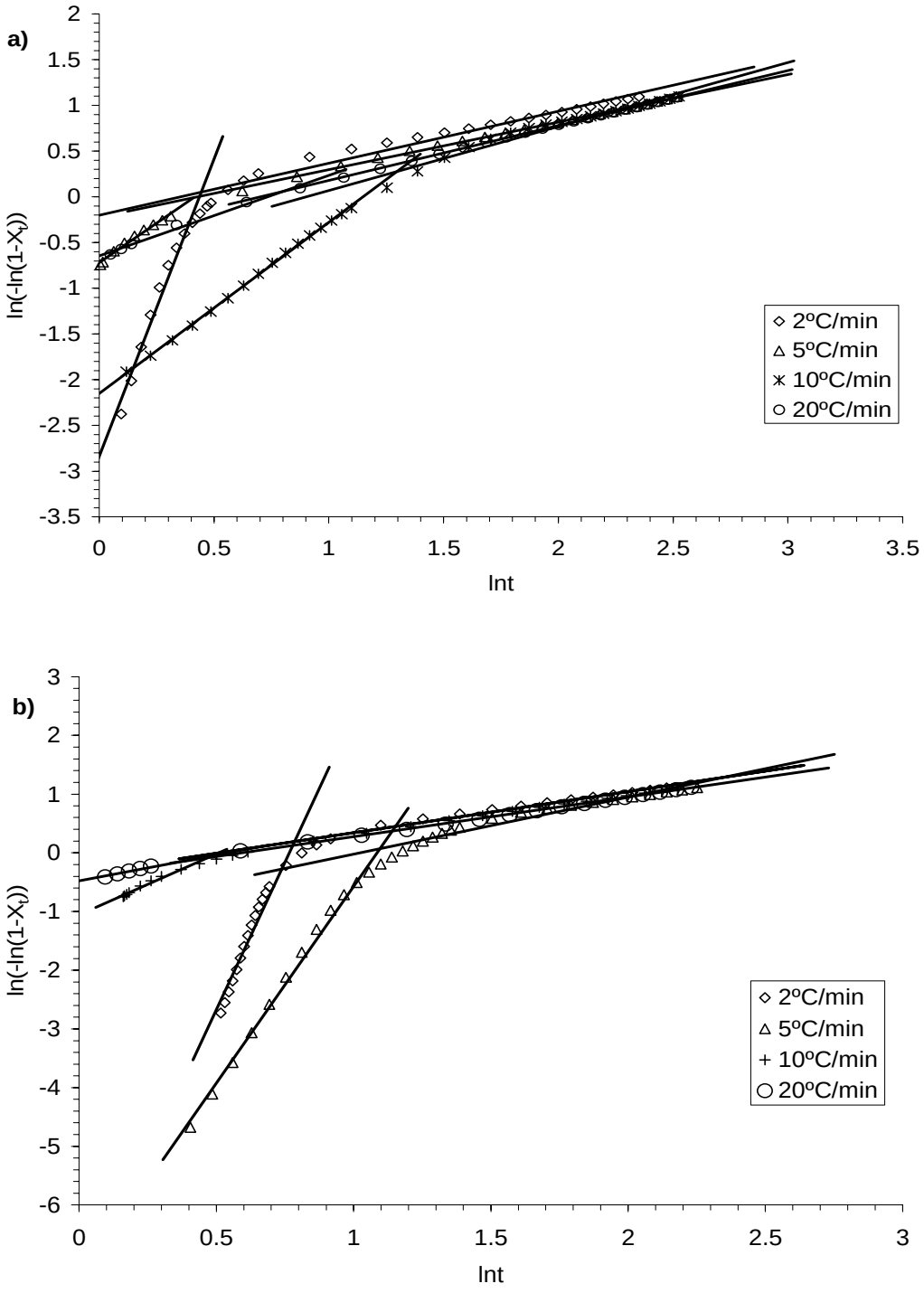

Figure 4.2.17: Avrami plots for the nonisothermal crystallization of a) m-HDPE and b) ZN-HDPE at different cooling rates.

Table 4.2.5: Avrami parameters for m-EB15, ZN-EB13, m-HDPE and ZN-HDPE at different cooling rates

Resin	Cooling rates (ºC/min)	Primary Crystallization Stage			Secondary Crystallization Stage		
		n1	k_t1	k_R1	n2	k_t2	k_R2
m-EB15	2	2.38	0.0565	0.2376	0.51	0.4456	0.6675
	5	2.84	0.0220	0.1482	0.55	0.4009	0.6332
	10	2.74	0.0282	0.1679	0.55	0.4234	0.6507
	20	2.34	0.0443	0.2106	0.58	0.4050	0.6365
ZN-EB13	2	1.05	0.0757	0.2751			
	5	1.02	0.0888	0.2980			
	10	1.04	0.0854	0.2922			
	20	1.04	0.0953	0.3088			
m-HDPE	2	6.50	0.0583	0.2416	0.57	0.8167	0.9037
	5	1.72	0.4879	0.6985	0.52	0.7999	0.8944
	10	1.87	0.1166	0.3415	0.70	0.5332	0.7302
	20	0.88	0.5251	0.7246	0.60	0.6550	0.8093
ZN-HDPE	2	10.08	0.0004	0.0210	0.7	0.6983	0.8356
	5	6.71	0.0006	0.0262	0.97	0.3703	0.6085
	10	2.07	0.3476	0.5895	0.70	0.6579	0.8111
	20	0.89	0.6203	0.7876	0.68	0.6678	0.8172

n = nucleation Index;

k_t = Crystallization rate constant;

k_R = Corrected crystallization rate constant for a specific cooling rate;

Acknowledgement

Authors are grateful to King Abdul Aziz City for Science and Technology (KASCT) for providing financial support for this research under research Grant # AT-22-16. Authors also acknowledge the support of KFUPM. We are also thankful to ExxonMobil for providing PE samples.

4.2.5. Conclusion

The following conclusions can be drawn from the above discussions:

1. The nonisothermal crystallization of LLDPEs goes through two crystallization processes. After passing the maximum heat flow in the exotherm, a large fraction of crystallinity was developed by slower, secondary kinetic process.

2. The Avrami exponent, n, for primary crystallization was in the range of 1.5 to 2.5, suggesting a rodlike growth. Usually, the Avrami exponent was expected to be an integer. Due to the association of secondary crystallization fractional values were observed (Chen 2004). The variation of BC did not affect the crystallization mechanism significantly, as seen by invariance of the Avrami exponent. However, HDPEs show a higher n value than LLDPEs. The Avrami exponent was found to be 3.9 and 2.7 for m-HDPE and ZN-HDPE, respectively. This suggests a three dimensional spherulitic growth process for linear HDPE.

3. The peak crystallization temperature, T_c, and was strongly influenced by the BC. It moved to a lower temperature region as BC increased. Comonomer type did not influence T_c strongly. However, the comonomer composition distribution affects T_c significantly. ZN-EB13 show higher T_c than m-EB15. Nevertheless, comonomer composition distribution did not affect the T_c of HDPEs.

4. The enthalpy of crystallization, ΔH_c, was influenced by BC. Increase in BC has lowered ΔH_c means absolute crystallinity. Comonomer type did not affect the ΔH_c but it was slightly influenced by comonomer composition distribution. ZN-EB13 show higher enthalpy of crystallization compared to m-EB15, even this was also observed in case of linear HDPEs.

4.2.6. References

1. Miller BG, Nally GM, Murphy WR. ANTEC 2002, 2415.
2. Peacock AJ. Handbook of Polyethylene: Structures, Properties, and Applications, 1st Ed., New York: Marcel Dekker, Inc.; 2000. p. 516
3. Evans UR. Trans Faraday Soc 1945,41,365
4. Ozawa T. Polymer 1971, 12, 150
5. Jeziorny A. Polymer 1978, 19, 1142
6. Jayakannan M., Ramakrishnan S., J Appl Polym Sci 1999, 74, 59
7. Sajkiewicz P., Carpaneto L., Wasiak A., Polymer 2001, 42, 5365
8. Qui Z., Ikehara T., Nishi T., Polymer 2003, 44, 5429
9. Hay JN, Mills PJ, Polymer 1982, 23, 1380
10. McHugh AJ, Burghardt WR, Holland DA, Polymer 1986, 27, 1585
11. Parasnis NC, Ramani K., J Thermal analysis and Calorimetry 1999, 55, 709
12. Kao YH, Phillips PJ, Polymer 1986, 27, 1669
13. Phillips PJ, Kao YH, Polymer 1986, 27, 1679
14. Nordmeier E, Lanver U., Lechner MD, Macromolecules 1990, 23, 1072
15. Sutton SJ, Vaughan AS, Bassett DC, 1996, 37 (25), 5735
16. Wagner J, Abu-Iqyas S., Monar K., Phillips PJ, Polymer 1999, 40, 4717

17. Wagner J, Phillips PJ, Polymer 2001, 42, 8999
18. Mandelkern L, Maxfield J, J Polym Sci, Part B: polym phy ed, 1979, 17, 1913
19. Strobl GR, Engelke T, Maderek E, Urban G, Polymer 1983, 24, 1585
20. Maderek E, Strobl GR, Colloid & polymer Sci, 1983, 261, 471
21. Alamo R, Domszy R, Mandelkern L, J Phys Chem, 1984, 88, 6587
22. Mandelkern L, Polym J, 1985, 17,(1), 337
23. Usami T, Gotoh Y, Takayama S, Macromolecules 1986, 19, 2722
24. Alamo RG, Mandelkern L, Macromolecules 1989, 22 (3), 1273
25. Fatou JG, Marco C, Mandelkern L, Polymer 1990, 31, 1685
26. Alamo RG, Viers BD, Manselkern L, Macromolecules 1993, 26, 5740
27. Shanks RA, Amarasinghe G, J thermal analysis and Calorimetry 2000, 59, 471
28. Wang C, Chu MC, Lin TL, Lai SM, Shih HH, Polymer 2001, 42, 1733
29. Zhang M, Lynch DT, Wanke SE, 2001, 42, 3067
30. Teng H, Shi Y, Jin X, J Polym Sci, Part B: Polym Phys 2002, 40, 2107
31. Rabiej S, Goderis B, Janicki J, Mathot VBF, Koch MHJ, Groeninckx G, Reymaers H, Gelan J, Wlochowicz A, Polymer 2004, 45, 8761
32. Jiao C, Wang Z, Liang X, Hu Y, Polymer Testing 2005, 24, 71
33. Voigt-Martin IG, Alamo R, Mandelkern L, J Polym Sci, Part B: Polym Phys 1986, 24, 1283
34. Bensason S, Minick J., Moet A, Chum S, Hiltner A, Baer E, J Polym Sci, Part B: Polym Phys 1996, 34, 1301
35. Keating MY, Lee IH J. macromol sci.- Phys 1999, B38(4), 379
36. Starck P, Lehmus P, Seppala V, Polym Eng Sci 1999, 39, 1444

37. Xu J, Xu X, Feng L Eur Polym J 1999, 36, 685

38. Janimak JJ, Stevens GC Termochimica acta 1999, 332, 125

39. Razavi-Nouri M, Hay JN Polymer 2001, 42, 8621

40. Fu Q, Chiu F, He T, Liu J, Hsieh ET Macromol Chem Phys 2001, 202, 927

41. Chiu F, Fu Q, Peng Y, Shih H J Polym Sci, Part B: Polym Phys 2002, 40, 325

42. Starck P, LÖfgren B Eur Polym J 2002,38, 97

43. Gill PS, Sauerbrunn SR, Reading M J Thermal analysis 1993,40, 931

44. Reading M, Elliott D, Hill VL J Thermal analysis 1993,40, 949

45. Qui ZB, Ikehara T, Nishi T Polymer 2003, 44, 3095

46. Okazaki I, Wunderlich B, Macromol Rapid Commun 1997, 18,313

47. Yuan ZH, Song R, Shen DY Polym Int 2000, 49, 1377

48. Hameed T, Hussein IA. Polymer 2002 ;43:6911.

49. Tobin MC. J Polym Sci, Part B: Polym Phys 1974;12:399.

50. Rychly J, Janigova I, Thermochimica acta 1993, 215, 211.

51. Herrero CH, Acosta JL. Polymer J 1994;26:786.

52. Ziabbicki A, Colloid Polym Sci 1974, 6, 252

53. Ziabbicki A, Appl Polym Symp 1967, 6, 1

54. Liu TX, Mo ZS, Wang SE, Zhang HF, Polym Eng Sci 1997, 37, 568

55. Caze C, Devaux E, Crespy A, Cavrot JP, Polymer 1997, 38, 497

56. Nakamura K, Katayama K, Amano T, J Appl Polym Sci 1973, 17, 1031.

57. Chan TW, Isayev AI, Polym Eng Sci 1994, 34, 461.

58. Avrami M, J Chem Phys 1939, 7, 1103

59. Avrami M, J Chem Phys 1940, 8, 212

60. Avrami M, J Chem Phys 1941, 9, 177

61. B. Wunderlich, Macromolecular Physics, vol 2, New York: Academic Press; 1976, p. 147.

62. Buchdahl R, Miller RL, Newman S, J Polym Sci 1959, 36, 215

63. Chen K, Tang X, Shen J, Zhou Y, Zhang B, Macromol Mat Eng, 2004, 289, 539

CHAPTER 5

CONCLUSIONS AND RECOMMENDATIONS

5.1. Conclusions

In this work, the influences of BC, branch type of metallocene LLDPEs on the mechanical and thermal properties were studied. To examine the effect of composition distribution some ZN-LLDPEs were selected (one from each branch type).

The influences of branch content (BC) and branch type on the mechanical properties of m-LLDPEs were investigated by means of stress/strain experiment at room temperature. The degree of crystallinity of these copolymers before and after the test was determined by differential scanning calorimetry. It was found that samples with low BC displayed an increase in T_m without any significant change in total crystallinity. An increase in T_m and a significant increase in total crystallinity were observed for high BC samples. The BC strongly affects the low strain properties such as Young's modulus and yield stress. A power series relationship is observed for Young's modulus due to the influence of BC. Yield stress becomes less distinct and broader with the increase of BC. In this investigation it was also found that the ultimate properties of m-LLDPEs were not strong function of BC. However, ZN-LLDPEs showed higher small strain properties but lower ultimate properties than m-LLDPEs of similar Mw and BC. In comparison with low BC resins, m-LLDPEs with high BC exhibit a stronger strain hardening during stress/strain experiments. The strain hardening was modeled by a modified Avrami

equation, and the order of the mechanically induced crystal growth is in the range of 1-2 suggesting athermal nucleation. The branch type did not affect any of the mechanical properties. In this study, the effect of strain rate was also investigated. The strain rate was varied in the range 10-500 mm/min. For low BC m-LLDPEs, a very narrow strain rate window was found, within which a maximum in modulus and ultimate properties were observed. The location of the maximum was independent of BC. The influence of the strain rate on the mechanical properties of m-LLDPEs is a strong function of BC. The strain rate has no influence on the mechanical properties of highly branched m-LLDPEs.

The influence of branch content (BC), Comonomer type and composition distribution on the crystallization kinetics of metallocene LLDPEs has been examined by nonisothermal crystallization kinetics by using modulated differential scanning Calorimetry. It was found that branch causes a significant change in the crystallization behavior. Crystallization peak temperature shifts to lower region as BC increases. Also, the enthalpy of crystallization decreased as BC increased. The secondary crystallization process strongly influences the nonisothermal crystallization of all resins. The Avrami exponent, n, was found close to 2 (between 1.5 and 2.5), suggesting a rodlike growth. The influence of comonomer type has very small/ no effect on the crystallization kinetics. A strong effect of composition distribution was found on crystallization peak and the enthalpy of crystallization. However, similar crystallization mechanism was observed both for m-LLDPEs and ZN-LLDPEs. The influence of cooling rate on the nonisothermal crystallization kinetics was also examined in this study. m-EB15 and ZN-EB13 were selected for similar BC but for different composition distribution. m-EB15 have shown involvement of two crystallization processes, whereas ZN-EB13 have shown only a

broad single crystallization process. Avrami exponent, n for m-EB15 and ZN-EB13 were found around 2.5 and 1 respectively. m-HDPE and ZN-HDPE have shown very narrow exotherm, which indicates very fast crystallization processes. Secondary crystallization process was observed for both of these resins. However, the proportion was not significant as in m-EB15.

5.2. Recommendations for Future Work

Following are some of the recommendations for any future work to be done:

1. The effect of temperature on the tensile properties can be a useful extension to the present work.
2. The effect of molecular weight on the mechanical properties of these m-LLDPEs can be investigated.
3. MDSC can be used for investigating isothermal crystallization kinetics of m-LLDPEs.

References

[1] Alamo R., Domszy R., Mandelkern L., (1984), "Thermodynamic and structural properties of copolymers of ethylene", *Journal of Physical Chemistry*, 88: 6587-6595.

[2] Alamo R. G., Mandelkern L., (1989), "Thermodynamic and structural properties of ethylene copolymers", *Macromolecules,* 22 (3): 1273-1277.

[3] Alamo R. G., Viers B. D., Mandelkern L., (1993), " Phase structure of random ethylene copolymers: a study of counit content and molecular weight as independent variables", *Macromolecules,* 26 (21): 5740-5747.

[4] Amarasinghe G., Chen F., Genovese A., Shanks R. A., (2003), "Thermal Memory of Polyethylenes Analyzed by Temperature Modulated Differential Scanning Calorimetry", *Journal of Applied Polymer Science,* 90: 681-692.

[5] Andrew J. M., Ward I.M., (1970), Journal of Material Science, 5: 411.

[6] Avrami M., (1939), *Journal of Chemical Physics*, 7 : 1103.

[7] Avrami M., (1940), *Journal of Chemical Physics*, 8 : 212.

[8] Avrami M., (1941), *Journal of Chemical Physics*, 9 : 177.

[9] Barrall E. M., Johnson J. F., (1970), "Differential scanning calorimetry theory and applications ", *Technical Methods of Polymer Evaluation*, 2: 1-39.

[10] Bensason S., Minick J., Moet A., Chum S., Hiltner A., Baer E., (1996), "Classification of Homogeneous Ethylene-Octene Copolymers Based on Comonomer Content", *Journal of Polymer Science: Part B: Polymer Physics Edition*, 34: 1301-1315.

[11] Billmeyer F. W., (1984), "*Textbook of Polymer Science*", 3rd edition, John Wiley & Sons.

[12] Brintzinger H. H., Fischer D., Mifflaupt R., Rieger B., Waymouth R., (1995), "Stereospecific olefin polymerization with chiral metallocene catalysts", *Angewandte Chemie, International Edition in English,* 34(11): 1143-1170.

[13] Brooks N. W., Unwin A. P., Duckett R. A., Ward I. M., (1997), "Temperature and Strain Rate Dependence of Yield Strain and Deformation Behavior in Polyethylene", *Journal of Polymer Science: Part B: Polymer Physics Edition,* 35: 545-552.

[14] Brooks N. W. J., Duckett R. A., Ward I.M., (1999), "Effects of crystallinity and stress state on the yield strain of polyethylene", *Polymer,* 40: 7367-7372.

[15] Buchdahl R., Miller R. L., Newman S., (1959), "Crystallization kinetics and mechanical properties of polyethylene", *Journal of Polymer Science*, 36: 215-231.

[16] Caze C., Devaux E., Crespy A., Cavrot J. P., (1997), " A new method to determine the Avrami exponent by DSC studies of non-isothermal crystallization from the molten state", *Polymer*, 38 : 497-502

[17] Chan T. W., Isayev A. I., (1994), "Quiescent polymer crystallization: modeling and measurements", *Polymer Engineering and Science*, 34: 461-471.

[18] Chen K., Tang X., Shen J., Zhou Y., Zhang B., (2004), "Non-Isothermal Crystallization Behavior of Poly(trimethylene terephthalate) Synthesized with Different Catalysts", *Macromolecular Materials and Engineering*, 289: 539-547

[19] Chiu F., Fu Q., Peng Y., Shih H., (2002), "Crystallization kinetics and Melting Behavior of Metallocene Short-Chain Branched Polyethylene Fractions", *Journal of Polymer Science: Part B: Polymer Physics Edition*, 40: 325-337.

[20] Dasari A., Duncan S. J., Misra R. D. K., (2002), "Atomic force microscopy of scratch damage in polypropylene", *Materials Science and Technology*, 18: 1227-1234.

[21] Dasari A., Misra R. D. K., (2003), "On the strain rate sensitivity of high density polyethylene and polypropylenes", *Materials Science and Engineering*, A358: 356-371.

[22] Evans U. R., (1945), "Laws of expanding circles and spheres in relation to the lateral growth of surface films and the grain size of metals" *Transactions of the Faraday Society*, 41: 365-374.

[23] Fatou J. G., Marco C., Mandelkern L., (1990), "The influence of molecular weight on the regime crystallization of linear polyethylene", *Polymer*, 31: 1685-1693

[24] Flory P. J., Yoon D. Y., (1978), *Nature*, 272: 226.

[25] Freid J. R., (2003), *Polymer Science and Technology*, vol 2, New Jersey: Prentice Hall, Inc.

[26] Fu Q., Chiu F., He T., Liu J., Hsieh E. T., (2001), "Molecular Heterogeneity of Metallocene Short-Chain Branched Polyethylenes and Their Fractions ", *Macromolecular Chemistry and Physics*, 202: 927-932.

[27] Gill P. S., Sauerbrunn S. R., Reading M., (1993), "Modulated Differential scanning calorimetry", *Journal of Thermal analysis*,40: 931-939.

[28] Graham J.T., Alamo R.G., Mandelkern L., (1997), "The Effect of Molecular Weight and Crystallite Structure on Yielding in Ethylene Copolymers", *Journal of Polymer Science: Part B: Polymer Physics Edition*, 35:213-223.

[29] Gupta V.K., (1997), "*Handbook of Engineering Polymeric Materials*", Marcel Dekker, Inc.

[30] Hameed T., Hussein I. A., (2002), "Rheological study of the influence of M_w and comonomer type on the miscibility of m-LLDPE and LDPE blends", *Polymer,* 43: 6911-6929.

[31] Hameed T., Hussein I. A., (2004), "Effect of short chain branching of LDPE on its miscibility with linear HDPE", *Macromolecular Materials and Engineering*, 289(2): 198-203.

[32] Hay J. N., Mills P. J., (1982), "The use of differential scanning calorimetry to study polymer crystallization kinetics", *Polymer,* 23: 1380-1384.

[33] Herrero CH, Acosta JL. Polymer J 1994; 26:786.

[34] Horton A. D., (1994), "Metallocene catalysis: polymers by design?", *Trends in Polymer Science*, 2(5): 158-166.

[35] Hosoda S.**,** Uemura A., (1992), "Effect of the structural distribution on the mechanical properties of linear low-density polyethylenes" *Polymer Journal*, 24 (9): 939-949.

[36] Hussein I. A., (2004), "Implications of melt compatibility/incompatibility on thermal and mechanical properties of metallocene and Ziegler-Natta linear low density polyethylene (LLDPE) blends with high density polyethylene (HDPE): Influence of composition distribution and branch content of LLDPE", *Polymer International*, 53: 1327-1335.

[37] Janimak J. J., Stevens G. C., (1999), "Structure correlated properties of metallocene catalyzed polyethylenes by modulated temperature differential scanning calorimetry", *Termochimica Acta,* 332: 125-142.

[38] Jayakannan M., Ramakrishnan S., (1999), "Effect of Branching on the Crystallization kinetics of Poly(ethylene terephthalate), *Journal of Applied Polymer Science,* 74: 59-66.

[39] Jeziorny A., (1978), "Parameters Characterizing the kinetics of the non-isothermal crystallization of poly(ethylene terephthalate) determined by d.s.c.", *Polymer*, 19: 1142-1144.

[40] Jiao C., Wang Z., Liang X., Hu Y., (2005), "Non-isothermal crystallization kinetics of silane crosslinked polyethylene", *Polymer Testing*, 24: 71-80.

[41] Jordens K., Wilkes G.L., Janzen J., Rohlfing D.C., Welch M.B., (2000), "The influence of molecular weight and thermal history on the thermal, rheological and mechanical properties of metallocene-catalyzed linear polyethylenes", *Polymer*, 41: 7175-7192.

[42] Juana R. D., Jauregui A., Calahora E., Cortazar M., (1996), « Non-isothermal crystallization of poly(hydroxy ether of bisphenol-A)/poly(ε-caprolactone), PH/PCL blends, *Polymer,* 37: 3339-3345.

[43] Kale L., Plumley T., Patel R., Redwine O., Jain P., (1995), *Journal of Plastic Film and Sheeting*, 12: 27.

[44] Kaminsky W., Miri M., Sinn H., Woldt R., (1983), "Bis(cyclopentadienyl)zirconium compounds and aluminoxane as Ziegler catalysts for the polymerization and copolymerization of olefins**"**, *Macromolecular Chemistry Rapid Communication*, 4(6): 417-421.

[45] Kaminsky W., Schauwienold A. M., Freidanck F., (1996), "Photoinduced rac/meso interconversions of bridged bis(indenyl) zirconium dichlorides", *Journal of.Molecular. Catalysis A: Chemical,* 112: 37-42.

[46] Kaminsky W., (1996), "New polymers by metallocene catalysis", *Macromolecular Chemistry and Physics*, 197(12): 3907-3945.

[47] Kaminsky W., (1998) "New polyolefins by metallocene catalysts", Pure &Applied Chemistry, 70: 1229-1233

[48] Kao Y. H., Phillips P. J., (1986), "Crystallinity in chemically crosslinked low density polyethylenes: 1. Structural and fusion studies", *Polymer* 27: 1669-1678.

[49] Keating M. Y., Lee I H. (1999), "Glass Transition, Crystallinity, Resin Stiffness, and Branch Distribution in Metallocene and Ziegler-Natta Ethylene 1-Olefins", *Journal of Macromolecular Science- Physics*, B38 (4): 379-401.

[50] Kennedy M. A., Peacock A. J., Mandelkern L., (1994), "Tensile Properties of Crystalline Polymers: Linear Polyethylene", *Macromolecules,* 27: 5297-5310.

[51] Kontou E., Niaounakis M., Spathis G., (2002), "Thermomechanical behavior of metallocene ethylene-α-olefin copolymers", *European Polymer Journal*, 38: 2477-2487.

[52] Kontou E., Spathis G., (2003), "Interrelation between long-term viscoelasticity and viscoelastic responses of semicrystalline polymers", *Journal of Applied Polymer Science,* 88: 1942-1950.

[53] Li Pi Shan C, Soares J.B.P., Pendelis A., (2002), "Mechanical properties of ethylene/1-hexene copolymers with tailored short chain branching distributions", *Polymer,* 43: 767-773.

[54] Liu T and Harrison I.R., (1988), "Effect of draw rate on the stress-strain behaviour of polymers" *Polymer,* 29: 233-239.

[55] Liu T. X., Mo Z. S., Wang S. E., Zhang H. F., (1997), "Nonisothermal melt and cold crystallization kinetics of poly(aryl ether ether ketone ketone)", *Polymer Engineering and Science*, 37(3): 568-575.

[56] Lovisi H., Tavares M. I. B., Silva N. M., Menezes S. M. C., Maria L. C. S., Coutinho F. M. B., (2001), "Influence of comonomer content and short branch length on the physical properties of metallocene propylene copolymers", *Polymer*, 42: 9791-9799.

[57] Lucas J. C., Failla M. D., Smith F. L., Mandelkern L., (1995), "The double Yield in the Tensile Deformation of the Polyethylene", Polymer Engineering and Science, 35: 1117-1123.

[58] Maderek E., Strobl G. R., (1983), "Crystallization and melting of fractions of branched polyethylene", *Colloid & polymer Science*, 261: 471-476

[59] Mandelkern L., Maxfield J., (1979), "Morphology and Properties of Low-Density (Branched) Polyethylene", *Journal of Polymer Science: Part B: Polymer Physics Edition*, 17: 1913-1927.

[60] Mandelkern L., (1985), "The Relation between Structure and Properties of Crystalline Polymers", *Polymer Journal*, 17: 337-350.

[61] Mark H. F., Bikales N. M., Overberger C. G., Menges G., (1986), *Encyclopedia of Polymer Science and Engineering*, 2nd Ed., vol 6, John Wiely & Sons.

[62] Mauler R. S., Simanke A. G., Galland G. B., Freitas L. L., Jornada J. A. H., Quijada R., (2001), "Dynamic-Mechanical Properties of Ethylene/α-Olefin Copolymers Prepared by a Metallocene Catalyst", *Macromolecular Chemistry and Physics*, 202: 172-179.

[63] McHugh A. J., Burghardt W. R., Holland D. A., (1986), "The kinetics and morphology of polyethylene solution crystallization", *Polymer,* 27: 1585-1594.

[64] Miller B. G., Nally G. M., Murphy W. R., (2002), " The effect of Extrution Processing Conditions on the Thermal and Mechanical Performance of Extrusion Cast Metallocene Polyethylene Films", Annual Technical Conference, 2415-2419.

[65] Minick J., Moel A., Hiltner A., Baer E., Chum S. P., (1995), "Crystallization of Very Low Density Copolymers of Ethylene with α-Olefins", Journal of Applied Polymer Science, 58: 1371-1384.

[66] Nakamura K., Katayama K., Amano T., (1973), "Nonisothermal crystallization of polymers. II. Consideration of the isokinetic condition" *Journal of Applied Polymer Science*, 17(4): 1031-1041.

[67] Nitta K. H., Tanaka A., (2001), "Dynamic mechanical properties of metallocene catalyzed linear polyethylenes", *Polymer*, 42: 1219-1226.

[68] Nordmeier E., Lanver U., Lechner M. D., (1990), "The Molecular Structure of Low-Density Polyethylene. 1. Long-Chain Branching and Solution Properties", *Macromolecules*, 23: 1072-1076.

[69] Okazaki I., Wunderlich B., (1997), "Reversible local melting in polymer crystals", *Macromolecular Rapid Communications*, 18: 313-318.

[70] Ozawa T., (1971), "Kinetics of non-isothermal crystallization", *Polymer*, 12: 150-158.

[71] Parasnis N. C., Ramani K., (1999), "Non-isothermal crystallization of UHMWPE", *Journal of Thermal analysis and Calorimetry*, 55: 709-719.

[72] Peacock A.J., Mandelkern L., (1990), "The Mechanical Properties of Random Copolymers of Ethylene: Force-Elongation Relations", *Journal of Polymer Science: Part B: Polymer Physics Edition*, 28: 1917-1941.

[73] Peacock A. J., (2000), "Handbook of Polyethylene: Structures, Properties, and Applications", 1st Ed., New York: Marcel Dekker, Inc.

[74] Phillips P. J., Kao Y. H., (1986), "Crystallinity in chemically crosslinked low density polyethylenes: 2. Crystallization kinetics", *Polymer,* 27: 1679-1686

[75] Popli R., Mandelkern L., (1987), "Influence of Structural and Morphological Factors on the Mechanical Properties of the Polyethylenes", *Journal of Polymer Science: Part B: Polymer Physics Edition*, 25:441-483.

[76] Qui Z., Ikehara T., Nishi T., (2003), "Crystallization behaviour of biodegradable poly(ethylene succinate) from the amorphous state", *Polymer*, 44 : 5429-5437.

[77] Qui Z., Ikehara T., Nishi T., (2003), "Melting behaviour of poly(butylene succinate) in miscible blends with poly(ethylene oxide) " *Polymer*, 44 : 3095-3099.

[78] Rabiej S., Goderis B., Janicki J., Mathot V. B. F., Koch M. H.J., Groeninckx G., Reymaers H., Gelan J., Wlochowicz A., (2004), "Characterization of the dual crystal polulation in an isothermally crystallizaed homogeneous ethylene-1-octene copolymer ", *Polymer*, 45: 8761-8778.

[79] Razavi-Nouri M., Hay J. N., (2001), "Thermal and dynamic mechanical properties of metallocene polyethylene", *Polymer*, 42: 8621-8627.

[80] Reading M., Elliott D., Hill V. L., (1993), "A new approach to the calorimetric investigation of physical and chemical transitions", Journal of Thermal analysis, 40: 949-955.

[81] Rychly J., Janigova I., (1993), "Avrami equation and nonisothermal crystallization of polyethylene investigated by DSC", *Thermochimica Acta*, 215: 211-218.

[82] Sacristan J., Benavente R., Perena J. M., Perez E., Bello A., Rojas R., Quijada R., Rabagliati F. M., (1999), " Thermal and Mechanical Properties of Polyethylene Synthesized with Metallocene Catalysts", *Journal of Thermal Analysis and Calorimetry,* 58: 559-568.

[83] Sajkiewicz P., Carpaneto L., Wasiak A., (2001), "Application of the Ozawa model to non-isothermal crystallization of poly(ethylene terephthalate)" *Polymer*, 42: 5365-5370.

[84] Seguela R., Rietsch F., (1986), "Tensile drawing behavior of ethylene/α-olefin copolymers: influence of the co-unit concentration", *Polymer,* 27: 703-708.

[85] Seguela R., Rietsch F., (1986), "Tensile drawing behavior of a linear low-density polyethylene: Change in Physical and mechanical properties", *Polymer,* 27: 532-536.

[86] Sehanobish K., Patel R. M., Croft B. A., Chum S. P., Kao C. I., (1994), "Effect of Chain Microstructure on Modulus of Ethylene-α-Olefin Copolymers", *Journal of Applied Polymer Science,* 51: 887-894.

[87] Shanks R. A., Amarasinghe G., (2000), "Comonomer distribution in polyethylenes analyzed by DSC after thermal fractionation", *Journal of Thermal Analysis and Calorimetry*, 59: 471-482.

[88] Simanke A. G., Galland G. B., Baumhardt N. R., Quijada R., Mauler R. S., (1999), "Influence of the Type and the Comonomer Contents on the Mechanical

Behavior of Ethylene/α-Olefin Copolymers", *Journal of Applied Polymer Science*, 74: 1194-1200.

[89] Sinn H., Kaminsky W., Adv. Organomet Chem 18, 99, 1980.

[90] Slade Jr. P. E. & Jenkins L. T., (1970), "*Techniques and methods of Polymer Evaluation*", Vol 02, Marcel Dekker, Inc. New York.

[91] Soares J. B. P., Shan C. L. P., Penlidis A., (2002), "Mechanical properties of ethylene/1-hexene copolymers with tailored short chain branching distributions.", *Polymer*, 43: 767-773.

[92] Starck P., (1997), "Dynamic Mechanical Thermal Analysis on Ziegler-Natta and Metallocene type ethylene copolymers, *European Polymer Journal*, 33: 339-348.

[93] Starck P., Lehmus P., Seppala V., (1999), "Thermal Characterization of Ethylene Polymers Prepared with Metallocene Catalysts", *Polymer Engineering and Science*, 39: 1444-11454.

[94] Starck P., LÖfgren B., (2002), „Thermal properties of ethylene/long chain α-olefin copolymers produced by metallocenes", *European Polymer Journal*, 38: 97-107.

[95] Stevens J. C., (1996), "Constrained geometry and other single site metallocene polyolefin catalysts: A revolution in olefin polymerization", *Studies in Surface Science & Catalysis*, 101: 11-20.

[96] Strobl G. R., Engelke T., Maderek E., Urban G., (1983), "On the kinetics of isothermal crystallization of branched polyethylene", *Polymer*, 24: 1585-1589

[97] Sumita M., Miyasaka K., Ishikawa K., (1977), "Effect of Drawing on the Melting Point and Heat of Fusion of Polyethylene", *Journal of Polymer Science: Part B: Polymer Physics Edition*, 15:837-846.

[98] Sutton S. J., Vaughan A. S., Bassett D. C., (1996), "On the morphology and crystallization kinetics of monodisperse polyethylene oligomers crystallizaed from the melt", *Polymer,* 37(25): 5735-5738.

[99] Swallowe G. M., (1999) "Mechanical Properties and Testing of Polymers: An A-Z Reference", *Polymer Science and Technology*.

[100] Tanem B.S., Stori A., (2001), "Blends of single-site linear and branched polyethylene. I. Thermal characterization", *Polymer*, 42:5389-5399.

[101] Teng H., Shi Y., Jin X., (2002), "Novel Characterization of the Crystalline Segment Distribution and Its Effect on the Crystallization of Branched Polyethylene by Differential Scanning Calorimetry", *Journal of Polymer Science: Part B: Polymer Physics Edition*, 40: 2107-2118.

[102] Termonia Y., Allen S. R., Smith P., (1988), "Kinetic Model for Tensile Deformation of Polymers. 3. Effects of Deformation Rate and Temperature", *Macromolecules* 21: 3485-3489.

[103] Thayer A. M., Chemical & Engineering News, Washington, 11 Sept. 1995, p. 15

[104] Thomas L. C., "Characterization of melting phenomena in linear low density polyethylene by Modulated DSC", *Thermal Analysis and Rheology*.

[105] Tobin M. C., (1974), "Theory of phase transition kinetics with growth site impingement. I. Homogeneous nucleation" *Journal of Polymer Science: Part B: Polymer Physics Edition,* 12: 399-406.

[106] Turi edith A., (1997), "*Thermal characterization of polymeric materials*", 2nd edition, Vol 1, Academic Press, New York.

[107] Usami T., Gotoh Y., Takayama S., (1986), "Generation Mechanism of Short-Chain Branching Distribution in Linear Low-Density Polyethylenes", *Macromolecules,* 19: 2722-2726.

[108] Van der Wal A., Mulder J. J., Gaymans R. J., (1998), "Fracture of polypropylene: 2. The effect of crystallinity", *Polymer,* 39: 5477-5481..

[109] Vernyi B., Plastic News, Sept 18, pp 1, 1995

[110] Voigt-Martin I. G., Alamo R., Mandelkern L., (1986), "A quantitative electron microscopic study of the crystalline structure of ethylene copolymers ", *Journal of Polymer Science: Part B: Polymer Physics Edition*, 24(6): 1283-1302

[111] Wagner J., Abu-Iqyas S., Monar K., Phillips P. J., (1999), "Crystallization of ethylene-octene copolymers at high cooling rates", *Polymer,* 40: 4717-4721.

[112] Wagner J., Phillips P. J., (2001), "The mechanism of crystallization of linear polyethylene, and its copolymers with octane, over a wide range of supercoolings", *Polymer,* 42: 8999-9013.

[113] Walker S., Nally G. M., Martin P.J., (2003a), "Effect of material properties on the mechanical and thermal performance of metallocene catalyzed LLDPEs", *Annual Technical Conference paper*, pp 3638-3642.

[114] Walker S., Nally G. M., Martin P.J., (2003b)"The influence of mould temperature and polymer structure on the mechanical and thermal properties of metallocene catalyzed LLDPEs", *Annual Technical Conference paper*, pp 671-675.

[115] Wang C., Chu M. C., Lin T. L., Lai S. M., Shih H. H., Yang J. C., (2001), "Microstructure of a highly short-chain branched polyethylene", *Polymer*, 42: 1733-1741.

[116] Ward I. M., Hadley D. W., (2000), *An Introduction to the Mechanical Properties of Solid Polymers*, 3rd Ed., John Wiley & Sons, New York.

[117] Welch M. B., Palackal S. J., Geerts R. L., Fahey D. R., (1995) "Polyethylene produced in Phillips slurry loop reactors with metallocene catalysts", MetCon 95 Proceedings, USA.

[118] Woo L., Ling M. T. K., Westphal S. P., (1996), "Dynamic mechanical analysis (DMA) and low temperature impact properties of metallocene polyethylenes", *Thermochimica Acta*, 272: 171-179.

[119] Wunderlich B., In: Turi EA, editor. (1997), *Thermal characterization of Polymeric Materials*, vol. 1, Academic Press, New York.

[120] Wunderlich B., (1976), *Macromolecular Physics*, Vol 2, Academic Press, New York.

[121] Xu X., Xu J., Feng L., Chen W., (2000), "Effect of Short Chain-Branching Distribution on Crystallinity and Modulus of Metallocene-Based Ethylene-Butene Copolymers", *Journal of Applied Polymer Science,* 77: 1709-1715.

[122] Xu J., Xu X., Feng L., (1999), "Short chain branching distribution of metallocene-based ethylene copolymers", European Polymer Journal, 36: 685-693.

[123] Yuan Z., Song R., Shen D., (2000), "Study of multiple melting behavior of syndiotactic polystyrene in □-crystalline form", *Polymer International*, 49(11): 1377-1382

[124] Zhang M., Lynch D. T., Wanke S. E., (2001), „Effect of molecular structure distribution on melting and crystallization behavior of 1-butene/ethylene copolymers", *Polymer*, 42: 3067-3075.

[125] Ziabbicki A., (1974), "Network structure, kinematics of deformation, and constitutive equations of rubber elasticity", *Colloid and Polymer Science*, 252(10): 767-783.

[126] Ziabbicki A., (1967), "Kinetics of polymer crystallization and molecular orientation in the course of melt spinning", *Applied Polymer Symposia*, 6: 1-18.

VITA

Name:	**Md. Ashraful Islam**
Faher's Name:	**Md. Abdul Wahed**
Place of Birth:	**Natore, Bangladesh**
E-mail:	**ashraful@kfupm.edu.sa**
	Ashraf_masum@yahoo.com
Education:	**B.S. in Chemical Engineering from Bangladesh University of Engineering & Technology (BUET), Dhaka, Bangladesh. August, 2001.**
	M.S. in Chemical Engineering from King Fahd University of Petroleum & Minerals (KFUPM), Dhahran, Saudi Arabia. January, 2005.